INTEGRATED HYDROLOGIC MODEL FOR THE ASSESSMENT OF SURFACE-GROUNDWATER INTERACTIONS

The case of Ziębice Basin (Poland)

BAKAR, OMAR MSHINDO

February, 2015

SUPERVISORS:
Dr. M.W. Lubczynski (Maciek)
Ir. G.N. Parodi (Gabriel)

INTEGRATED HYDROLOGIC MODEL FOR THE ASSESSMENT OF SURFACE-GROUNDWATER INTERACTIONS

The case of Ziębice Basin (Poland)

BAKAR, OMAR MSHINDO
Enschede, The Netherlands, February, 2015

Thesis submitted to the Faculty of Geo-Information Science and Earth Observation of the University of Twente in partial fulfilment of the requirements for the degree of Master of Science in Geo-information Science and Earth Observation.
Specialization: Water Resources and Environmental Management

THESIS ASSESSMENT BOARD:
Dr. Ir. C. van der Tol (Chair)
Dr. P. Gurwin (External Examiner, University of Wroclaw)
Dr. M.W. Lubczynski
Ir. G.N. Parodi

This work is dedicated to my wife and my children

ABSTRACT

Integrated management of surface and groundwater systems is important, especially, when there is high interaction between surface and groundwater flows. It can be carried out optimally by using integrated hydrologic models (IHM). The aim of this study was to assess the surface-groundwater interaction of Ziębice Basin using IHM. A quasi-3D model was created with two aquifers separated by an aquitard. The simulation period was five hydrologic years. The steady-state model was calibrated with abstraction wells and its solution was used as initial condition for transient calibration. The natural state of the Basin was simulated by removing abstraction wells from the calibrated transient model.

It was observed that fluxes of the steady-state model did not differ substantially from maximum fluxes of the transient model. The fluxes varied between 0 and 967 $mm.yr^{-1}$ for the steady-state model while for the transient model varied between 11 and 1070 $mm.yr^{-1}$. Moreover, the results showed no difference of flux exchange between the streams and aquifers under natural and groundwater abstraction conditions. The aquifers received more fluxes (20% of precipitation) than what it supplied to the stream (8%). The effects of groundwater abstraction on groundwater heads was observed in the Quaternary and Tertiary aquifers where the heads declined by about 5 m. However, the decline did not result in changes of flow direction and pattern of groundwater heads in the Basin. Moreover, groundwater abstraction showed insignificant effects on streams such that the interactions were more or less in natural condition.

The water balance components of the transient model as a percent of precipitation showed that groundwater recharge was a major component that contributed about 58% followed by 20% of stream leakage into the aquifer. The outflow components was dominated by 39% of surface leakage and 28% of groundwater evapotranspiration. Stream leakage from the aquifer accounted for about 8% and the lateral flow through the drain and groundwater abstraction accounted for 2%, each. The change of storage of the aquifer accounted for about 3%.

The IHM method used to study surface-groundwater interaction worked well in the study case of Ziębice Basin as the method is particularly suitable for areas with large surface-groundwater interactions. However, calibration of IHM is a data and time demanding.

Key words: Surface-groundwater interaction; Integrated hydrologic model; Ziębice Basin

ACKNOWLEDGEMENTS

First and foremost, I am grateful to the Government of the Kingdom of The Netherlands through the Netherlands Fellowship Programme for granting me the scholarship to support my study at ITC. Furthermore, I extend my gratitude to my organisation, Zanzibar Water Authority, which complied with the terms and conditions of the scholarship and allowed me to attend the study programme.

I am heartily thankful for my first supervisor, Dr Maciek Lubczynski, whose encouragement, guidance and support from the initial to the final level enabled me to develop an understanding of the subject to reach the success. I am also indebted to my second supervisor, Ir. Gabriel Parodi, for his invaluable guidance and comments throughout the course of this research.

My sincere and special appreciation goes to the followings: Dr Jaciek Gurwin of the Department of Applied Hydrogeology, Faculty of Natural Sciences, University of Wroclaw (Poland), who organised the field visits to the case study and facilitated data acquisition for my research; Mr. Richard Winston of the United States Geological Survey for his technical support and advice on the use of Modflow-NWT and Modflow ModelMuse software, his prompt response to the questions and on fixing the bugs ensured timely completion of my modelling works; Ir. V. Retsios (Bas) of the Department of Geo-Information Processing (ITC) who helped to convert the earlier versions of ILWIS files into the latest version; and Ir. Amr El-Zehairy of the Faculty of Engineering, Mansoura University (Egypt) who helped to set the UZF package and other technical aspects of Moflow-NWT.

I am grateful to Mr Arno van Lieshout, the Course Director of the Department of Water Resources and Environmental Management (ITC) and all Department members of staff for their kind collaboration for the entire period of 18 months. I extend my thanks to all ITC academic and non-academic staffs and to all of those who supported me in any respect during my study in ITC. Also, my kind and special regards go to my companions Mr Hezron Timothy, Mr Damas Kalokola and Mrs Paskalia Bazil for their wise advice and encouragements in the course of the whole study period in ITC.

Lastly, but not least in any way, I offer my regards and blessings to my wife and my children who accepted my absence in the family for the period of 18 months and for their moral support for the whole period of my study.

TABLE OF CONTENTS

LIST OF FIGURES

LIST OF TABLES

1. INTRODUCTION

1.1. Background of the study

The study of surface-groundwater interactions has gained special attention in the field of water resources management in recent decades. This is due to the fact that surface and groundwater flow systems, in many cases, interact with each other. For instance, groundwater abstraction can reduce base flow and adversely affect river hydrology. Conversely, surface water abstraction can reduce groundwater recharge and reduce groundwater potentials of aquifer system. Moreover, surface water can gain solute from groundwater while the quality of groundwater can be impaired by surface waters. From these facts, the management of surface and groundwater are hardly separable. Krause et al. (2007) pointed out that interactions between surface and groundwater and the exchange of fluxes between them have high spatial and temporal variability. In that regard, the type of interaction is determined by the direction of flux exchange. For example, a surface water source experiences influent condition when it loses water into an aquifer and experiences effluent condition when it gains water from the aquifer system.

Formerly, the surface and groundwater flow systems were analysed separately because the flows take place at different temporal scales (Gupta, 2010) and, thus, its representation was a very difficult undertaking. This approach allowed surface and groundwater flow regimes to be analysed in separation using the uncoupled or stand-alone models. For instance, the HBV, PRMS and SWAT codes focus more on modelling surface water and simplify groundwater flow processes. Likewise, the codes like standard MODFLOW and AQUIFEM-1 emphasise more on groundwater flow processes and simplify surface water flow processes. However, the ever increasing developments in computing facilities have enabled the flow systems to be analysed together in both spatial and temporal domains. The conjunctive analysis of surface and groundwater flows is performed through the integrated or coupled models. The typical examples of such models include, among others, MODFLOW-2005, MODFLOW-NWT and GSFLOW. It should be pointed out that selection of an appropriate code to deal with a particular problem in hand is of paramount importance. For example, an uncoupled groundwater model can perform better in a particular environment where a coupled model cannot do the same.

The ever increasing demands of water are largely fulfilled by groundwater or surface water resources to satisfy cultural, societal and economic needs in many parts of the world. Ziębice Township is no exceptional as the wellfields at Henrykow, Nieszkow and Starczowek play a great role in groundwater abstraction. The hydrology of the Ziębice Basin involves precipitation and melt of snow cover which results in groundwater infiltration and surface runoff into the streams. Part of the infiltrating water recharges groundwater and the rest leaves the system by evapotranspiration. Moreover, groundwater discharge into streams, as a base flow, sustains continuous flow of Olawa River augmented by surface runoff. However, groundwater abstraction affects groundwater storage which consequently interferes the linkage between the surface and groundwater systems.

The ultimate aim of this research is to improve understanding of the surface-groundwater interactions to influence effective decision making in water resource management in Ziębice Basin. Moreover, it aims to improve more societal benefits by ensuring availability of water for drinking, agricultural activities, recreational and sustenance of ecological systems in the study area. In order to be able to model the interactions in the Basin, this research uses the MODFLOW-NWT codes running under ModelMuse as the graphic user interphase. The model codes, among others, employ the Unsaturated Zone Flow (UZF) and Stream Flow Pouting (SFR) Packages to facilitate the study of surface-groundwater interactions. The model is calibrated in steady-state followed by transient state calibration to simulate the surface-groundwater interactions in the Basin.

1.2. Problem definition

Ziębice Basin has a high abundance of surface and groundwater resources. Comparing the two resources, groundwater is highly preferred to meet the daily water demands in the study area. Moreover, there is a good documentation of water resources in various data banks such as Bank Hydro. However, despite the good documentation of water resources in the Basin, little has been done to investigate the interaction between the surface and groundwater flow systems and its imposed effects in the hydrogeological regime of the Basin. On one hand, the existing studies in the area focused more on the steady-state models, on the other hand, no transient model was implemented.

1.3. Research Objectives

1.3.1. Main objective

To assess the surface-groundwater interactions in Ziębice Basin.

1.3.2. Specific objectives

i) To calibrate transient integrated hydrologic model of Ziębice Basin.

ii) To investigate the surface-groundwater interactions in Ziębice Basin.

iii) To improve the water balance estimates of Ziębice Basin.

1.4. Research questions

1.4.1. Main research questions

What are the effects of surface-groundwater interactions on the hydrologic system of Ziębice Basin?

1.4.2. Specific research questions

i) Which parametric distribution does optimally fulfil the model calibration?

ii) What are the spatial and temporal variability of water fluxes in Ziębice Basin?

iii) What are the estimates of water balance of Ziębice Basin?

1.5. Study area

1.5.1. Location

The Ziębice Basin is in Ziębice Township of the Dolnoslaskie Province in the Southern part of Poland (Figure 1-1). It lies between the latitudes 50^{o} 32' 00" to 50^{o} 42' 25" North and the longitudes 16^{o} 54' 00" to 17^{o} 06' 00" East. The Basin covers an area of about 214 km^2.

1.5.2. Climate

The climate of the study area is a mild-moderate with an average annual temperature of 8 ^{o}C. In addition, the annual average minimum and maximum temperatures of 0 and 18 ^{o}C, respectively, are experienced in February and July. The study area receives minimum precipitation in February and maximum in July (Figure 1-2). Furthermore, precipitation in the Basin has high spatial variability with some areas receiving low precipitation and others receiving high precipitation with an increasing trend from north to south-west. This phenomenon is likely influenced by high altitude of about 374 m above the mean sea level (m-asl). Moreover, the evaporation demand of the study area is estimated using the FAO Penman-Monteith Method in Section 2.4.3 from meteorological data of temperature, relative humidity, wind speed and extra-terrestrial solar radiation as recorded at ADAS station (Figure 1-3).

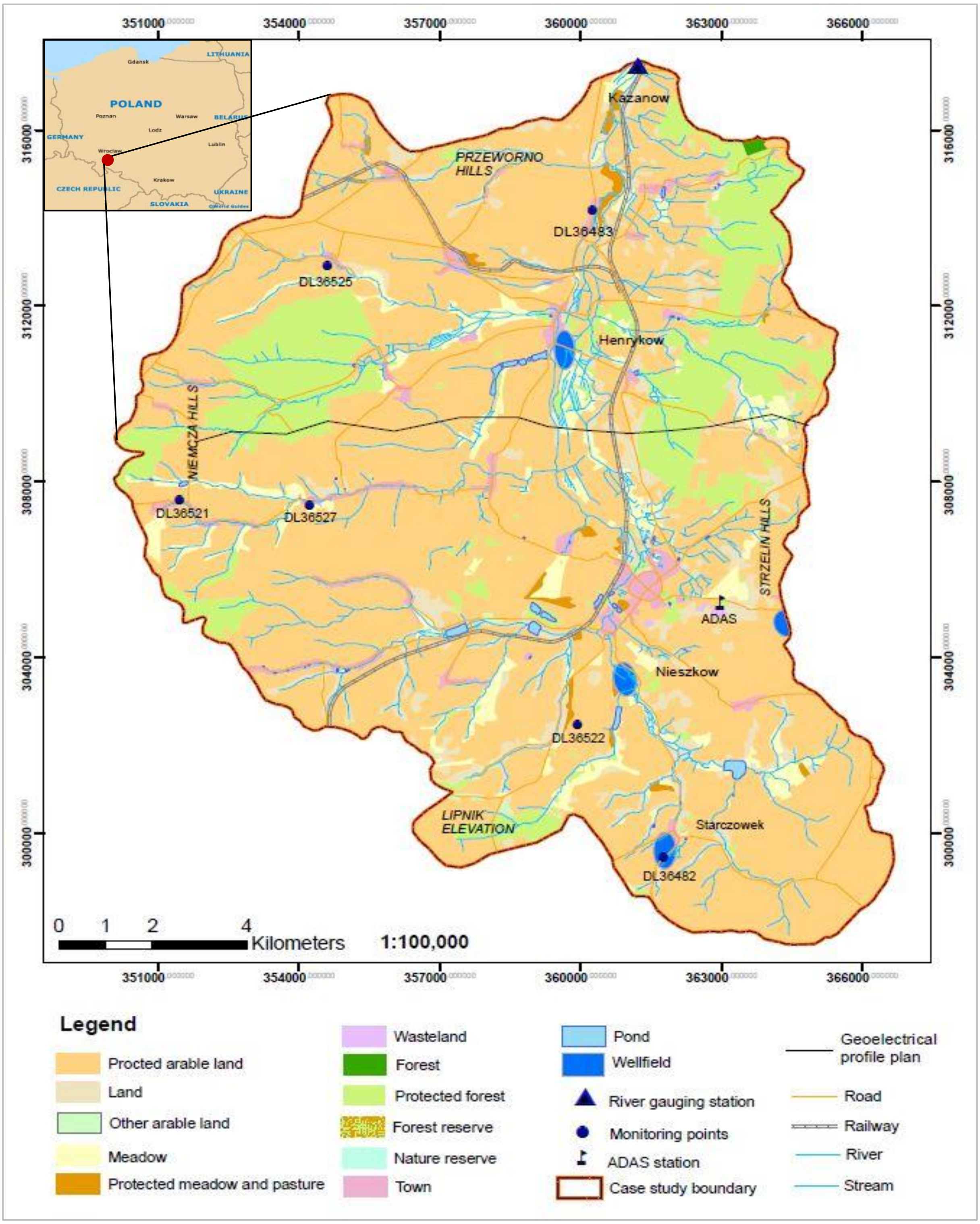

Figure 1-1: Study area, location and land use

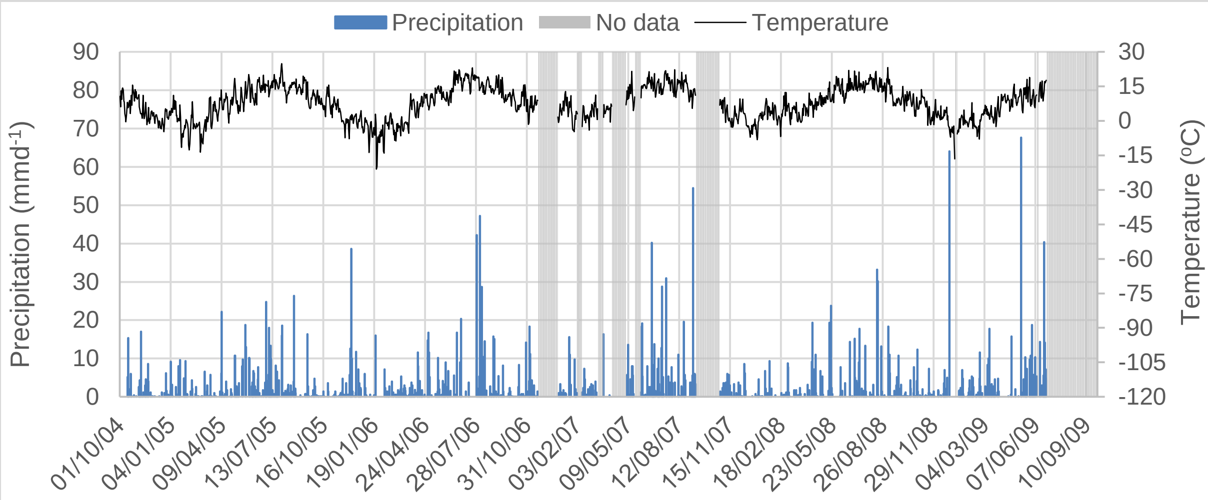

Figure 1-2: Precipitation and temperature measurements at Ziębice ADAS station

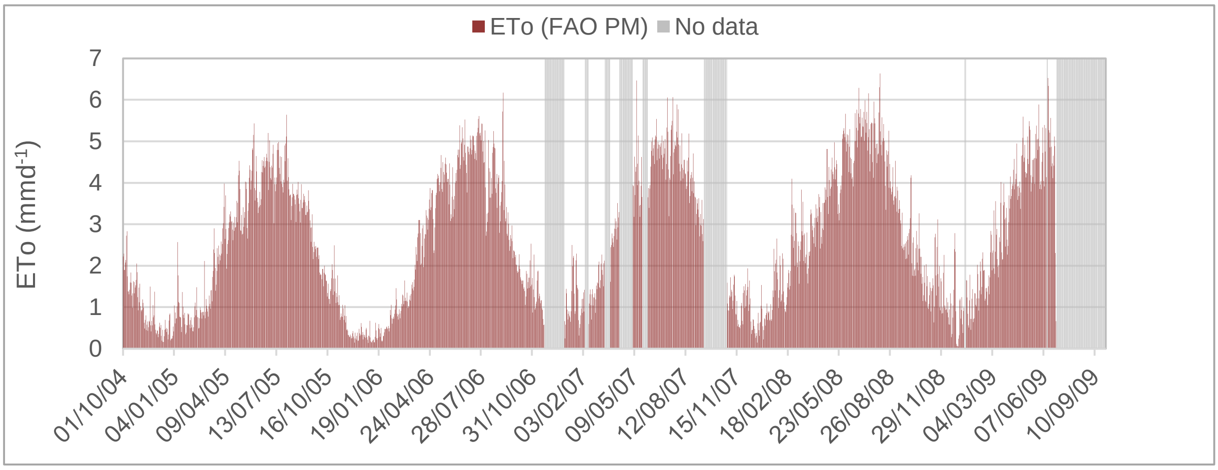

Figure 1-3: Potential evapotranspiration

1.5.3. Physiography

The study area is bounded by the Hills of Strzelin from the east and Niemcza from the west (Figure 1-4) with an altitude of about 375 m-asl. While the Przeworno elevations (300 to 225 m-asl) bound the Basin from the north, the Lipnik elevations (about 300 m-asl) bound from the south (Figure 1-1). The northern part of the basin is called Lowland of Henrykow and the southern part is called the Highland of Ziębice. The lowest altitude is about 174 m-asl at Kazanow, the place where Olawa River exits the Ziębice Basin. Moreover, the highest point is about 389 m-asl at the Strzelin Hills on the south-east of Kazanow. The relief of the Basin is of moderate category with the stream gradient of 5.2 mkm^{-1} from its tail to the discharge point at Kazanow (Shah, 1995).

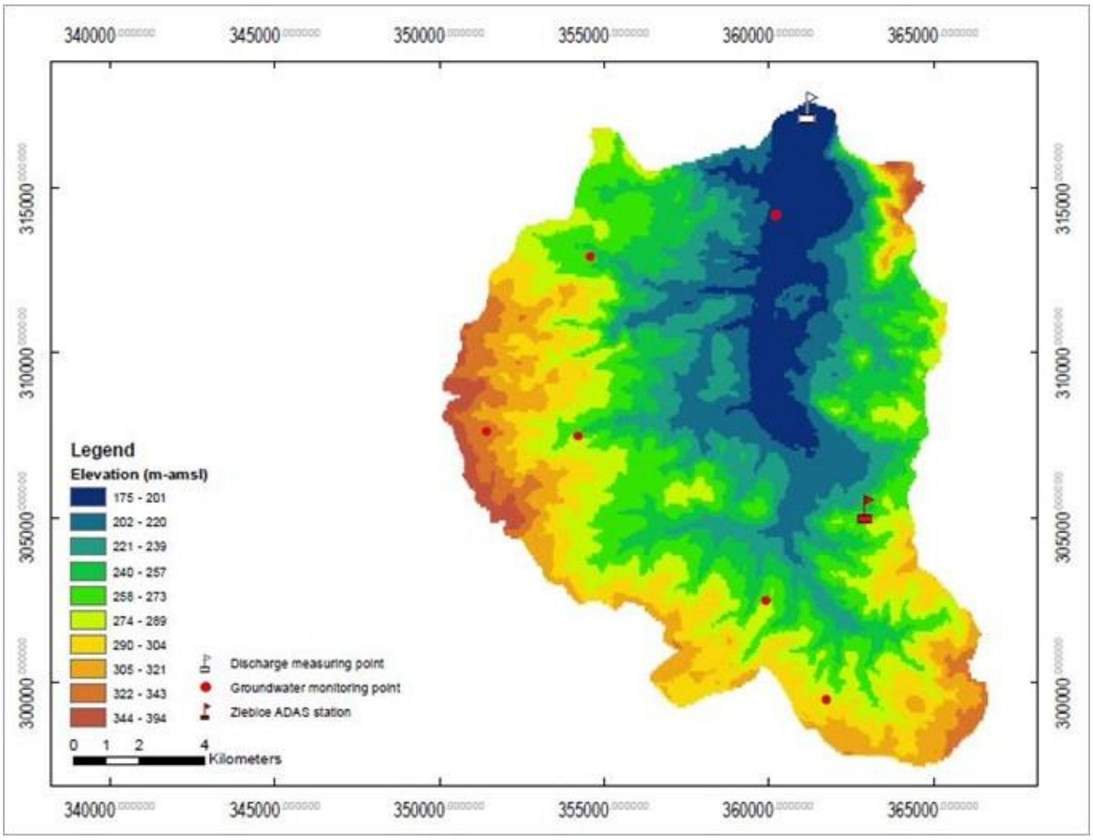

Figure 1-4: Digital elevation model (DEM) of the study area

1.5.4. Land-use

In the study area, there are different land use practices (Figure 1-1). These include residential settlements, wellfields, arable land, protected and unprotected meadows, forests, forest reserves, protected forests, etc. Moreover, the large part is occupied by arable land which covers about 67 % of the total area followed by about 13 % of protected forest. Land and meadow occupy about 7 and 6 %, respectively, while the residential settlements and other arable lands occupy about 3 % each. The rest of the land uses, each, occupy less than 1 % (Figure 1-5).

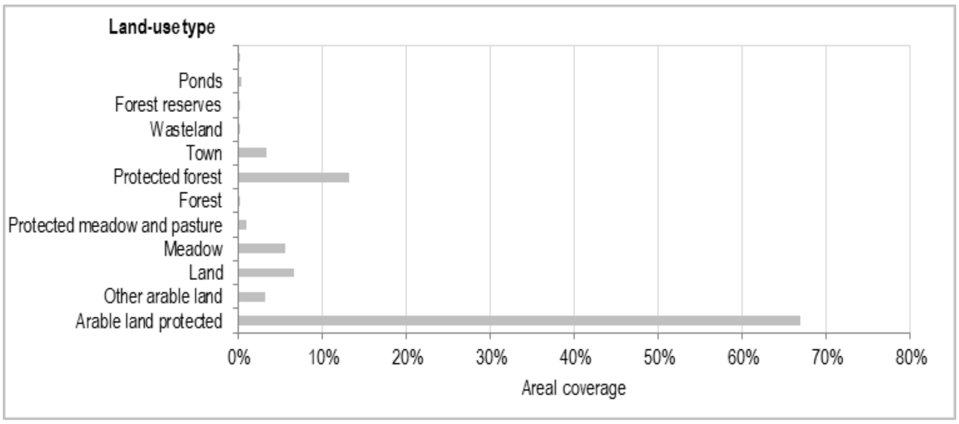

Figure 1-5: Land use distribution in the study area

1.5.5. Geology

Ziębice Basin forms part of the Sudeta Foreland which is a regional structural unit (Shah 1995; Gurwin 2010). The Basin is marked by occurrence of Quaternary, Tertiary, Carboniferous and Precambrian ages of geologic units with different rock types and diverse spatial distribution. The Quaternary layer overlays the Tertiary layer in most of the Basin area. Both are comprised largely of sand, clay and gravels. The Carboniferous rock outcrops made up of granite and pegmatite are found on the eastern part of the Basin. The outcrops of the Precambrian rock types with gneisses, schist and quartzite are also found on the western side of the Basin. The crystalline Carboniferous and Precambrian rocks form the crystalline bedrock of the Basin.

The study conducted by Shah (1995) revealed that Ziębice Basin is composed of two stratigraphic layers and three hydrostratigraphic layers, namely; Quaternary and Tertiary composed of sediments underlain by impervious crystalline bedrock. These layers form the main stratigraphic formations of the Basin despite the presence of minor layers within the major ones. For instance, the Tertiary layer is further comprised of sub layers of upper, middle and lower Tertiary. Moreover, two valleys of the Pliocene and Oligocene ages are respectively buried and incised in the upper Tertiary clays and within the crystalline bedrock.

The structural changes of Ziębice Basin was governed by tectonic activities and glaciation processes. The bedrock of the Basin was affected by complex tectonic deformations that occurred in the regional scale. For example, the regional discontinuity crosses the Basin along the deepest part of the bedrock and approximately in the North-South direction. Consequently, the Basin was divided into Eastern block called Metamorphic Wzgorz Strzelinskich and the Western block called Synclinorium Wzgorz Niemczanskich (Shah, 1995). Moreover, the bedrock developed a rugged surface with structures like faults, horsts and grabbens which are also a result of tectonic activities. The process of glaciation took place during the Pleistocene age under two Glaciation epochs. While in the first epoch, i.e. the South-Poland Glaciation, glaciation reached the Southern boundary, the second epoch, i.e. the Mid-Poland Glaciation, the effects of glaciation was marked by several recessions and advances that resulted into deposits of boulders and build-up of the Southern water divide of the Basin.

1.5.6. Hydrology

The Ziębice Basin has a main water stream flowing from South to North direction. The stream forms part of Olawa River. The drainage system of the Basin is of a dendritic configuration in which small streams flow from west and east to the main stream. Since the topographic boundary of the Ziębice Basin forms the surface water divide, all precipitation falling within the Basin contribute the stream flow. The outflow of the stream is at Kazanow (Figure 1-1); a point where stream discharge measurements were recorded as shown in Figure 1-6. The stream flow originates from baseflow, precipitation and snow melt water.

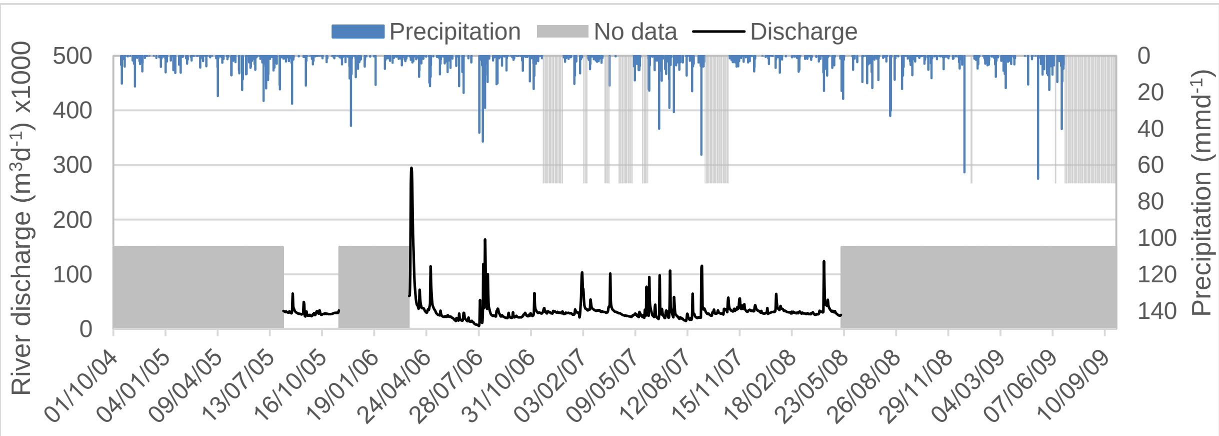

Figure 1-6: Stream discharge at Kazanow gaging station and precipitation at ADAS station

1.5.7. Hydrogeology

1.5.7.1. Groundwater flow

The Hills surrounding Ziębice Basin form the surface water divide that coincides with the groundwater divide (Shah, 1995). As a result, there is no flow contribution from outside of the Basin and the outflow is only through the river discharge point at Kazanow. There is a hydraulic contact between Quaternary and Tertiary aquifers. This contact is influenced by interbedded depositional materials of sand layers within the upper clay layer separating the Quaternary and middle littoral layer, on one hand, and the lower clay layer separating the middle littoral layer from the bedrock buried valleys, on the other hand. As a result, a vertical flow (seepage) is observed between the aquifer layers with its direction determined by hydrostatic pressure in the respective layers. Moreover, the pumping test results revealed that there is no seepage losses from the crystalline bedrock.

1.5.7.2. Pumping tests

Pumping tests were conducted to evaluate characteristics of the aquifer systems in Ziębice Basin. The pumping tests were conducted only around Henrykow and Ziębice sites (Shah, 1995). Despite the low spatial coverage of the pumping tests in the study area, sufficient number of tests (43 tests) were carried out at Henrykow and Ziębice sites. Out of the 43 tests, 26 tests were conducted in the Quaternary aquifer, 16 tests in the Tertiary aquifer and 3 tests were conducted in the wells that jointly tap both Quaternary and Tertiary aquifers. Moreover, Koziol (2006) extended pumping tests on the far south of the Basin at Nieszkow and Starczowek and on the north at Henrykow. A total of 5 tests were conducted at Nieszkow in Tertiary aquifer and 2 tests in Quaternary at Starczowek site. While 3 tests at Henrykow were conducted in Tertiary, only 1 test was conducted in Quaternary at the same area. The pumping tests revealed different aquifer properties as mentioned in Subsections (1.5.7.3) and (1.5.7.4). Furthermore, the short pumping tests carried out in the wells drilled up to the bedrock revealed that the bedrock is impervious (Shah, 1995) due to very large drawdown observed of about 80 m.

The pumping test conducted at Nieszkow, Starczowek and Henrykow by Koziol (2006) was used to evaluate groundwater potentials of Ziębice Basin. Hydraulic characteristics such as well discharge, drawdown and radius of influence were determined for each well. For instance, the Tertiary aquifer of Nieszkow wellfield was realized to be more promising with an acceptable discharge of 420 m^3h^{-1} of water resources with a drawdown of about 15 m. This wellfield was followed by Starczowek (Quaternary) with a discharge of 128 m^3h^{-1} and a drawdown of about 4.8 m. Lastly, Henrykow wellfield has a least discharge of 34 m^3h^{-1} in Tertiary with a drawdown of 29 m and 22 m^3h^{-1} in Quaternary with a drawdown of about 6 m. Moreover, the largest radius of depression cone (950 m) was observed at Nieszkow wellfield while a radius of 400 m and 252 m were respectively observed at Henrykow and Starczowek wellfields.

1.5.7.3. Hydraulic conductivity

The upper part of the shallow Quaternary layer is not considered as the groundwater reserve (Figure 1-7); its lower part has varying hydraulic conductivities ranging between 0.5 to 7.0 $md^{-1.}$ However, there also exist outwash fans within the Quaternary layer with good hydraulic conductivities ranging up to 100 md^{-1}. This layer forms an unconfined aquifer with a thickness of not more than 20 m and covers almost the entire Basin. The Tertiary layer has lower and upper sub layers which are considered as aquitards separated by a middle sub layer which is a confined aquifer with low hydraulic conductivity ranging between 0.1 to 0.5 md^{-1}. Moreover, the depth of the upper sub layer ranges between 20 to 60 m and the bottom of the sub layer ranges between 20 to more than 100 m. Also, the depth of the middle sub layer ranges between 0 to 60 m. The buried valleys within the bedrock have hydraulic conductivities between 12 to 20 md^{-1} and in some areas even higher than 100 md^{-1}, therefore they represent high groundwater prospects.

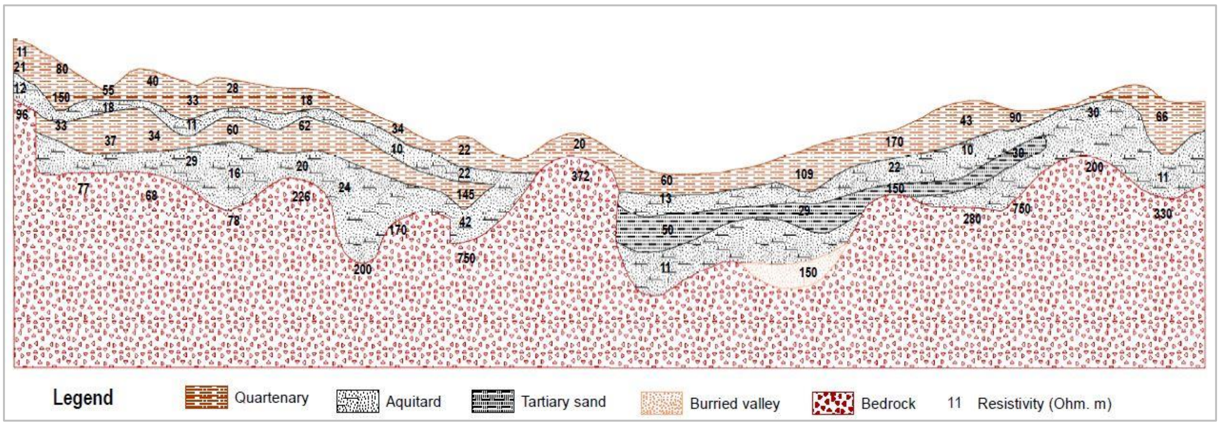

Figure 1-7: Geoelectrical cross-section of Ziębice Basin, Shah (1995); location map Figure1-1

1.5.7.4. Heads distribution

Fluctuations of water table may be caused by different processes but can be generally classified into natural and man-made. The natural processes include recharge, evapotranspiration, bank storage near steams, atmospheric pressure changes and aquifer deformations due to tectonic forces. The man-made processes include mainly groundwater abstraction for irrigation and municipal water supply. Moreover, it is common that more than one process take place simultaneously. Thus, it is very important to make a thorough investigation on the involvement of each process before coming to the conclusion.

The groundwater heads in the Quaternary and Tertiary aquifers are higher from the east and the west of the Basin and decrease towards the centre (Figure 1-8 (a) and (b)). Also, the heads decrease from the south to the north of the Basin. This phenomenon justifies that groundwater flows to the north of the Basin.

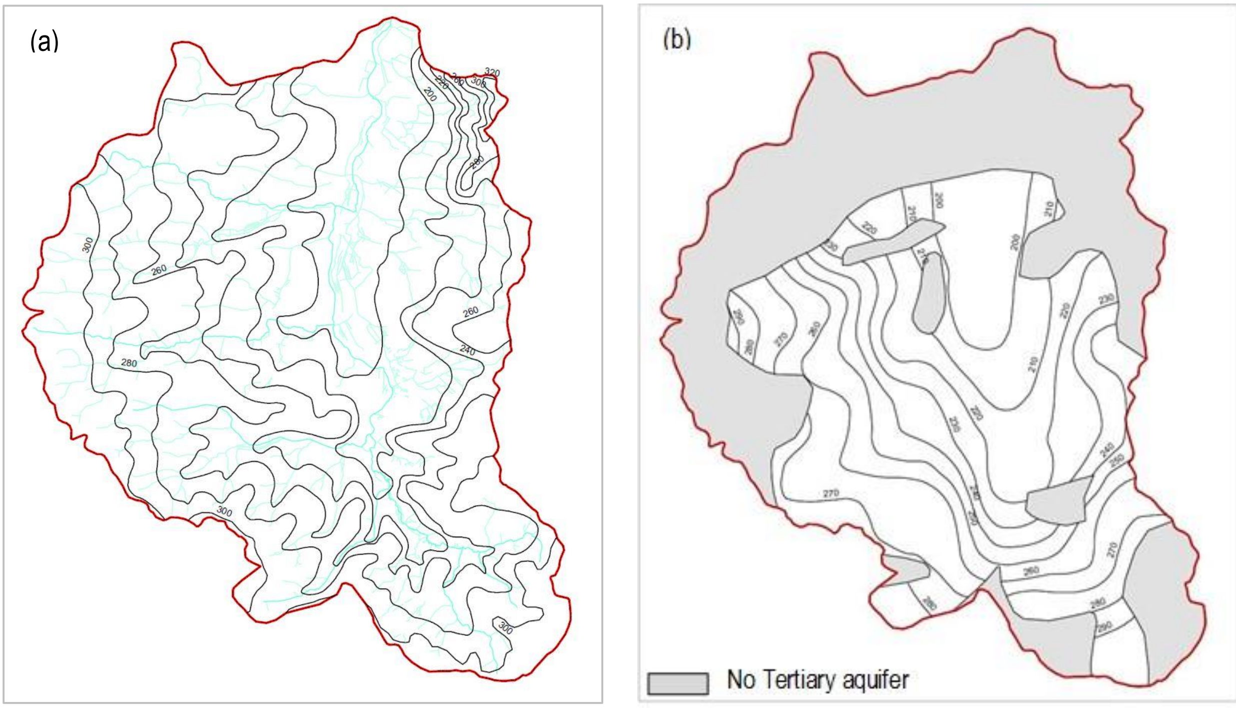

Figure 1-8: Groundwater heads in the (a) Quaternary and (b) Tertiary aquifers after (Lubczynski, 1991)

1.5.7.5. Water quality

The groundwater of Ziębice Basin is largely used for domestic purposes. Therefore, evaluation of its quality is inevitable. In general, the water is considered of calcium carbonate type especially around Ziębice area with a mineral content ranging between 250 to 350 mgl^{-1}. The same water mineralisation is found in groundwater in Henrykow wellfield but the water is of sodium carbonate type. However, despite the same mineralization as the water around Ziębice area, the water in Henrykow wellfield has high fluorine content of about 5 to 6 mgl^{-1}. This water is entirely allotted for industrial supply.

1.6. Thesis organization

This report is divided into four Chapters. The first Chapter introduces the background knowledge of the research topic, problem definition of the study area, the objectives and the research questions and an in-depth introduction to the study area. It covers, among others, location of the study area and its climatic, physiographic, geologic, hydrologic and hydrogeologic aspects. The second Chapter refers to research methodology of the study. It explains state-of-the-art of the research topic and points out previous studies conducted in the study area to identify the gaps that need to be covered in the new research. Moreover, it explains each component of the research methodology in a sequential manner with emphasis on how it contributes to achieving the research objectives. The critical analysis and discussion of the research results are in Chapter three. Finally, the fourth Chapter is reserved for conclusion and recommendations.

2. RESEARCH METHOD

2.1. Introduction

The methods used to achieve the research objectives and answering the research questions are summarized in Figure 2-1. In a nutshell, the method is composed of 5 basic steps, namely: reconnaissance survey and data collection, literature review, model selection, modelling of surface-groundwater interactions and analysis of model results.

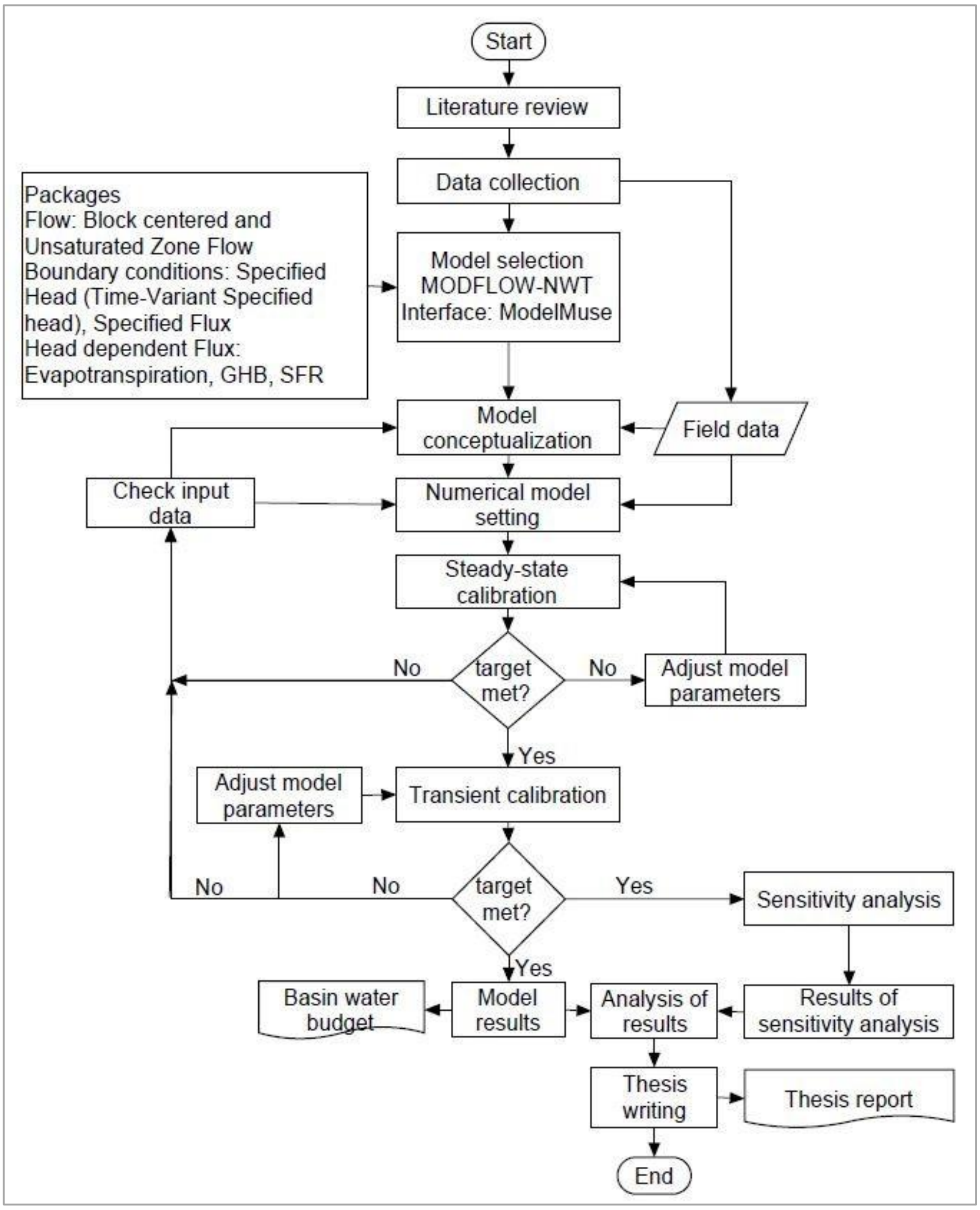

Figure 2-1: The adopted research methodology

2.2. Reconnaissance survey and data collection

This step aimed at acquiring a thorough knowledge of the study area by paying field visits. It enabled understanding of the hydrologic and hydrogeological environment and features of the area and any other significant aspects that could not be easily recognized in different map sources. In addition, the field visits aimed at collecting data regarding the study area. Apart from the digital elevation model (DEM), the data sets were collected from the Department of Geology of the WROCLAW University (Poland).

The data sets for the study covered the period from October 2004 to September 2009. Meteorological data were collected from the Automatic Data Acquisition System (ADAS) station with hourly piezometric heights covering the period from June 2005 to July 2009. Moreover, the station included records of hourly precipitation covering the period from June 2004 to June 2009, wind speed, temperature, relative humidity and solar radiation. The stream discharge measurements contained measurements covering the period from June 2006 to May 2008 with 30 minutes interval. Hydrogeological data included hourly piezometric heights from seven groundwater monitoring stations covering the period from November 2004 to June 2009 (Figure 1-1). The average groundwater abstraction data were collected from three wellfields (number of wells in brackets), namely: for Nieszkow (5), Henrykow (3) and Starczowek (2). The maps of the Ziębice Basin including land use, geologic and hydrogeological features were also collected and the DEM of three arc second (90 m) was downloaded from CGIAR-CSI SRTM.

2.3. Literature review

Surface-groundwater interactions

Surface-groundwater interaction is a hydrologic process that occurs through vertical and lateral exchange of fluxes between surface water and groundwater systems through unsaturated zone and infiltration to or exfiltration from saturated zone. The interactions can also occur through flows in fractures or solution channels in the case of fractured rocks or karst (Sophocleous, 2002). The flux direction is governed by head differences between the water sources (McCallum et al., 2013). That is to say, when aquifer head is greater than surface water stage the flux would be towards the surface water and when it is less, the flux would be towards the aquifer. Under those circumstances, an aquifer can be continuously losing water while a surface water source gaining the same or vice versa. However, the flux exchange can sometimes have spatial and temporal behaviours (McCallum et al., 2013). For instance, the gaining or losing trend in an entire surface water source can alternate depending on the hydrologic characteristics of the basin. Moreover, in the same surface water source the losing reach at particular times can be a gaining one at other times and its reverse may also be true. In conclusion, the surface water and groundwater sources hardly ever exist in disconnection and their management has to consider an integrated approach.

In the past few decades, there has been rapid advancement in computing tools in terms of hardware and software. Henceforth, these developments have tremendously eased and saved time on numerical computations, which is an underlying principle in numerical modelling. While many modelling software have been developed to fulfil different needs, stand-alone and integrated hydrologic models (IHM) are widely used in the studies of surface-groundwater interactions. However, these two types of models use different approaches to study the interactions. The stand-alone models, in most cases, explain better individual system and considers adjacent system as a boundary condition (Furman, 2008) and thus, may not be useful for studying surface-groundwater interactions. In contrast, the IHMs simulate simultaneously surface water and groundwater systems; which is a good approach to study the surface-groundwater interactions and have shown good performance in many studies (Hassan et al., 2014; Guay et al., 2013; Ely and Kahle, 2012). While the IHMs integrates precipitation, temperature and boundary conditions to simulate evapotranspiration, runoff, recharge and discharges (Hassan et al., 2014), in stand-alone models, that possibility does not exist.

MODFLOW-NWT is an example of IHM running under the MODFLOW ModelMuse as the graphic user interphase (GUI). Among other things, the model was designed to link the surface water and groundwater flow systems through the unsaturated zone. It simulates flows and storage in the unsaturated zone using the Unsaturated Zone Flow (UZF) and Streamflow Routing (SFR) packages. As a result, the interactions of these hydrologic flow regimes can be modelled.

In Ziębice Basin, five different researchers conducted studies between the years 1991 and 2010. At first, Lubczynski (1991) prepared a groundwater flow model of the Basin. The author did not deal with surface-groundwater interactions in his research. He used stand-alone steady-state finite element model. The second research by Shah (1995) intended to evaluate groundwater potential in the Basin. The author managed to develop a conceptual model of the Basin for implementation in numerical MODFLOW model. In the third research, Koziol (2006) analysed water production of the four groundwater intakes in the Basin. The author also analysed physical and chemical changes of groundwater compositions in the four intakes. The fourth research was conducted by Pawalec (2006) who studied groundwater flow in Ziębice Basin. The author used hydrologic, hydrodynamic and water balance methods to achieve the study objectives. In the fifth and the final research, Gurwin (2010) conducted MODFLOW-based modelling study to find out the best way to evaluate groundwater recharge in a complex multi-layered aquifer system of the Sudetic Foreland in which Ziębice Basin is a part. The author developed and calibrated the steady-state MODFLOW model under the Groundwater Modelling System (GMS) environment. However, according to Palma and Bentley (2007), steady-state models cannot detect critical hydrologic stress periods that are well described by transient models. As none of the studies conducted in Zebiece Basin used transient simulations, therefore this study was invented to improve understanding of the study of surface-groundwater interactions in Ziebice Basin.

2.4. Data processing

Hydrologic parameters form the basic inputs to any hydrological model. The parameters may be derived from a single meteorological variable such as rainfall intensity or sometimes may be derived from many variables such as potential evapotranspiration. The source of meteorological data was the Ziębice ADAS station. In this study, four hydrologic parameters were considered and are explained in the following Subsections.

2.4.1. Precipitation estimation

Daily precipitation is most important input of the integrated model applied in this study. Precipitation data were collected from Ziębice ADAS station. The daily precipitation of the Ziębice Basin was estimated from the ADAS time series data sets. Moreover, there were gaps in the precipitation data that were necessary to be filled. Generally, the gaps filling was done by correlating the ADAS precipitation data sets with those from weather stations in vicinity of the study area. However, in the case of this study, the gaps were filled using precipitation data from Klodzko station downloaded from NNDC climate database.

2.4.2. River flow estimation

Olawa river discharge as the catchment outlet was applied in this study as transient model calibration control. The discharge of Olawa River out of Ziębice Basin was measured at Kazanow gaging station. The discharge was measured at an interval of 30 minutes (Figure 1-6). The average daily discharge was calculated from the 30 minutes measurements.

2.4.3. Potential evapotranspiration estimation

Evapotranspiration (ET) is among the major components of a hydrologic system and affects deeply availability of both surface and groundwater resources. With regard to groundwater management, it affects unsaturated and saturated zones. The amount of ET removed from the groundwater depends, among other things, on the amount of soil moisture and depth to a water table. In the context of MODFLOW-NWT, ET is simulated through the Unsaturated Zone Flow Package using estimated potential evapotranspiration (PET).

The ET rate that would occur from a reference surface, not short of water, under specified conditions is termed as a reference evapotranspiration denoted by ETo. Conventionally, the reference surface used is a hypothetical reference crop such that its height is 0.12 m, has a fixed surface resistance of 70 sm^{-1} and has an albedo of 0.23 (Allen et al., 1998). The sole standard method for computation of the ETo is the FAO Penman-Monteith (FAO P-M) Method. The method is recommended by the World's Food and Agricultural Organisation (FAO) because of its high likelihood of predicting correct ETo at different geographical settings and climatic conditions and allows its application in a data short situations (Allen et al., 1998).

The daily ETo was calculated from the FAO P-M Method. In this method, different meteorological data collected from the Ziębice ADAS station and atmospheric parameters were used. While the used meteorological data included solar radiation, air temperature, air humidity and the wind speed, the atmospheric parameters included atmospheric pressure, latent heat of vaporisation and psychrometric constant. Moreover, due to missing data in temperature time series of the ADAS station it was necessary to fill the gaps. The gaps were filled by correlating the temperature data sets of the ADAS and Opole stations. The obtained temperatures after correlation were used to calculate ETo from the Hargreaves Method using the formulas described in Appendix 1. Finally, the ETo estimated by the Hargreaves Method was correlated with that estimated from FAO P-M Method to enable gaps filling. In this study, the PET was assumed to be equal to the estimated ETo. This assumption was important due to the fact that ETo is the maximum evapotranspiration rate possible with a given set of meteorological and physical parameters (Burba, 2010).

The general equation of the FAO P-M Method is shown in Equation (2.2) and the detailed explanation of the quantities in the Equation are found in Appendix 1.

$$ETo = \frac{0.408\Delta(R_n - G) + \gamma\frac{900}{T_{mean}+273}u_2(e_s - e_a)}{\Delta + \gamma(1 + 0.34u_2)} \tag{2.1}$$

where: ETo is the reference evapotranspiration ($mmday^{-1}$), Δ is the slope of the saturation vapour pressure curve ($kPa°C^{-1}$), R_n is the net radiation at the crop surface ($MJm^{-2}day^{-1}$), G is the soil heat flux density ($MJm^{-2}day^{-1}$), γ is the psychrometric constant ($kPa°C^{-1}$), T_{mean} is the mean daily air temperature at a height of 2m (°C), u_2 is the wind speed at a height of 2 m (ms^{-1}), e_s is the mean saturation vapour pressure (kPa), and e_a is the actual vapour pressure (kPa).

2.4.4. Interception

Interception is the amount of precipitation retained by the plant canopy which is eventually lost by evaporation. It is affected by different factors such as: the type of vegetation, the time of year, the type of storm, canopy density and meteorological conditions (Fleming et al., 2004; Wang et al., 2007). It is used to estimate the amount of infiltrating water into groundwater system. Different studies have come out with different ranges of canopy interception. For instance, Fleming et al. (2004) estimated interception to account between 10 and 20% of precipitation while Wang et al. (2007) accounted interception between 10 to 48% of precipitation in different forests. Leuning et al. (1994) accounted 33% of precipitation as an estimate of interception rate on a wheat canopy.

In this study, the rate of intercepted precipitation was estimated using the land covers of the study area as shown in Figure 1-1 and Figure 1-5. In order to facilitate estimation of the intercepted precipitation, the land cover classes were further subdivided into two major categories namely; forests and general vegetation. While the first category included forests, forest reserves and protected forests, the second category included the rest of the land covers mentioned in Figure 1-1 except Pond and Town. In addition, the forests land cover were represented by *Pinus silvestris* canopy and the general vegetation was represented by wheat canopy. The adopted interception rates were 27.3% for the forest from Wang et al. (2007) and 33% for the general vegetation from Leuning et al. (1994).

2.4.5. Infiltration and runoff

In the context of the Unsaturated Zone Flow (UZF) Package, infiltration rate is estimated from the difference between precipitation and interception rates. According to Niswonger et al. (2006), the infiltrating water is converted to water content. Moreover, the authors mentioned that the water content is set to the saturated water content when the specified infiltration rate in the UZF package exceeds the saturated hydraulic conductivity. The infiltration rate into the unsaturated zone was calculated from the precipitation and interception rates estimated in Sections 2.4.1 and 2.4.4, respectively.

In Ziębice Basin, runoff is a result of precipitation and snow cover melt in the form of excess infiltration runoff and saturation excess runoff (Equation 2.14) that flow into the streams. In MODFLOW-NWT, runoff is an input to the Stream Flow Routing Package (SFR) where stream flow is simulated.

2.4.6. Piezometric heads

In the study area there were seven groundwater monitoring points with transient data collected by Wroclaw University (Poland) of which one was an ADAS station (Figure 1-1). Despite the gaps in the time series of the observations, the monitoring points had hourly heads for the intended period of simulation as shown in Figure 2-2(a) through (g). There is no regular pattern of water level fluctuations within and between the observation points. For instance, in Figure 2-2(c), (d) and (f) there are large variations in water table with a range of about 1.5 to 3.0 m. Moreover, the monitoring points show small variations in range of fluctuations of about 0.60 to 0.70 m. However, the monitoring point in Figure 2-2(e) shows the least fluctuation range of about 0.50 m with an interesting trend of gradual increasing in head. The behaviour of water table fluctuations is influenced by various factors such as spatial variability of rainfall, water table depth, amplitude of fluctuation, geology and physiography of the area.

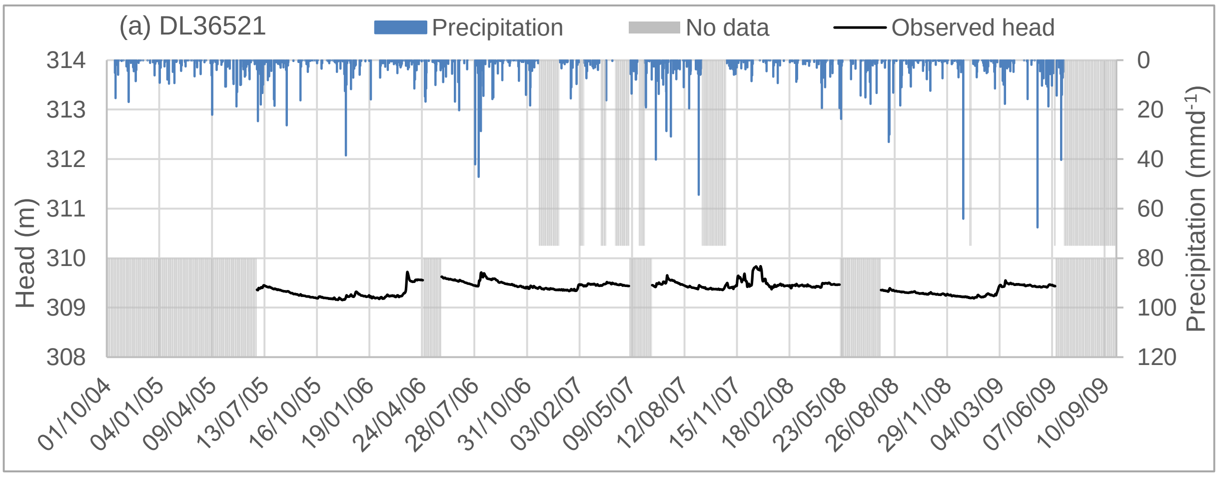

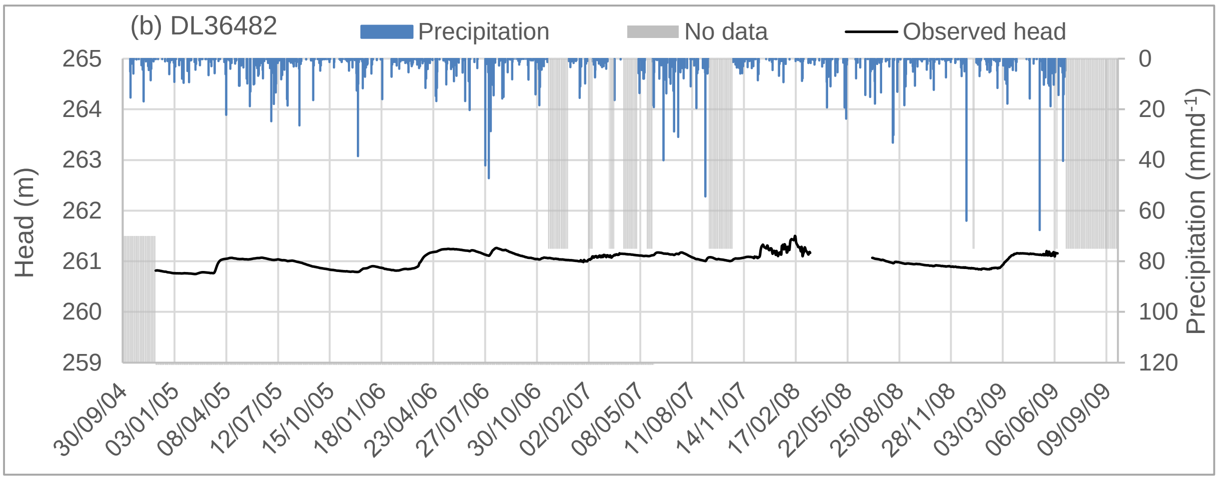
(b) DL36482
Precipitation
No data
Observed head
Head (m)
Precipitation (mmd-1)
265
264
263
262
261
260
259
0
20
40
60
80
100
120
30/09/04
03/01/05
08/04/05
12/07/05
15/10/05
18/01/06
23/04/06
27/07/06
30/10/06
02/02/07
08/05/07
11/08/07
14/11/07
17/02/08
22/05/08
25/08/08
28/11/08
03/03/09
06/06/09
09/09/09

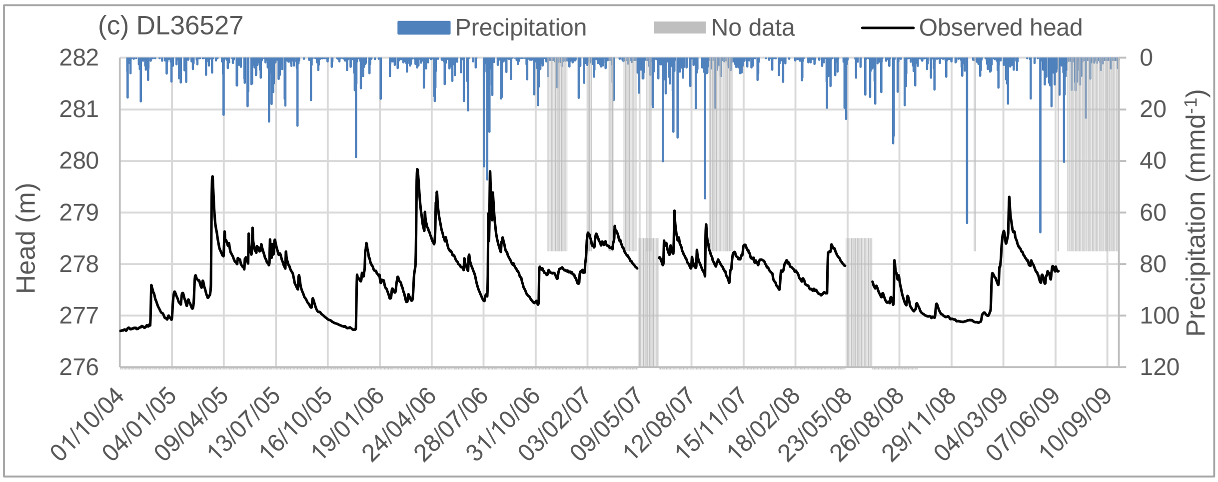
(c) DL36527
Precipitation
No data
Observed head
Head (m)
Precipitation (mmd-1)
282
281
280
279
278
277
276
0
20
40
60
80
100
120
01/10/04
04/01/05
09/04/05
13/07/05
16/10/05
19/01/06
24/04/06
28/07/06
31/10/06
03/02/07
09/05/07
12/08/07
15/11/07
18/02/08
23/05/08
26/08/08
29/11/08
04/03/09
07/06/09
10/09/09

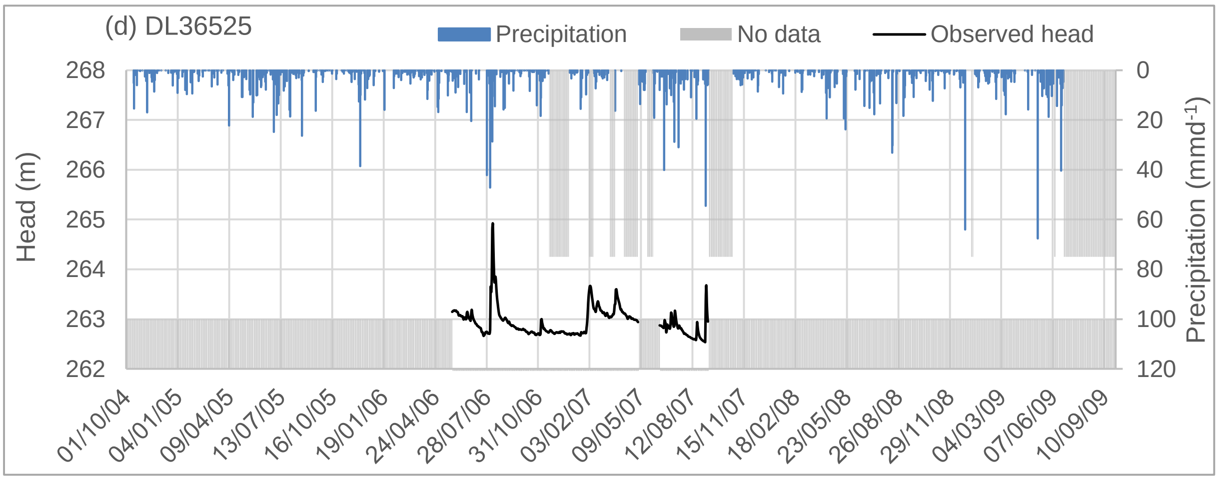
(d) DL36525
Precipitation
No data
Observed head
Head (m)
Precipitation (mmd-1)
268
267
266
265
264
263
262
0
20
40
60
80
100
120
01/10/04
04/01/05
09/04/05
13/07/05
16/10/05
19/01/06
24/04/06
28/07/06
31/10/06
03/02/07
09/05/07
12/08/07
15/11/07
18/02/08
23/05/08
26/08/08
29/11/08
04/03/09
07/06/09
10/09/09

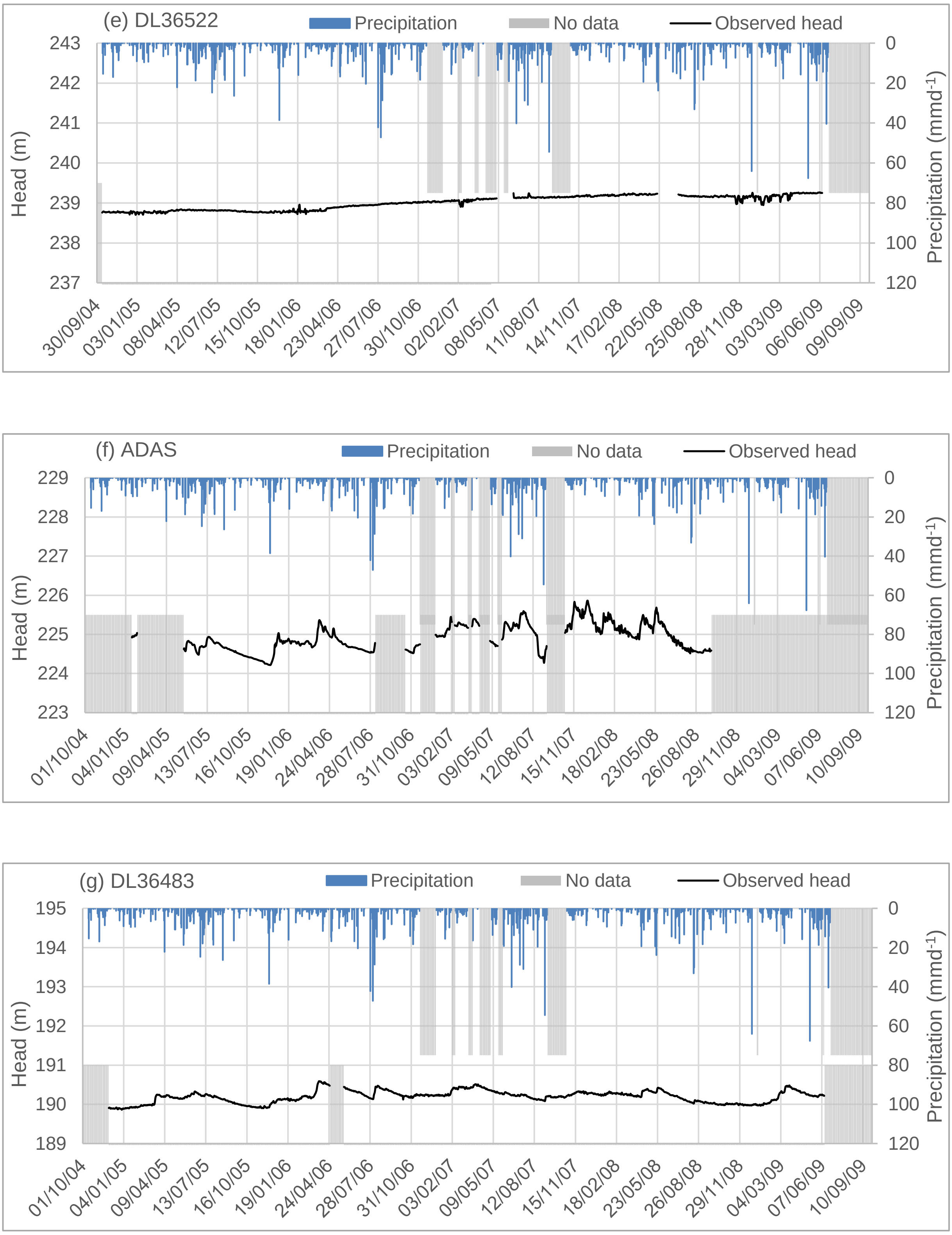

Figure 2-2: Time series of head observations at monitoring points; Locations map Figure 1-1

2.5. Conceptual model

Anderson and Woessner (1992) defined conceptual model in the context of groundwater studies as a pictorial representation of the groundwater flow system. Its ultimate objective is to configure the field problem in a simple but meaningful schema to ease analysis procedures and the field data organization. The representation could be in the form of a block diagram or a cross section of the model area. Moreover, it is an important tool that determines the numerical model dimensions and design of grids. To sum up, the conceptual model is a foundation of a numerical model and its closer representation to the field situation influences accuracy of numerical model results. In order to build a conceptual model, the authors mentioned three important steps to be followed, namely; defining hydrostratigraphic units, preparing water budget and defining the flow system. These steps are more elaborated in the following Subsections.

2.5.1. Hydrostratigraphic units

A conceptual model is constructed from hydrostratigraphic units. These are units with similar hydrogeological properties that may be combined into a single unit or a geologic formation may be subdivided into aquifers and confining units depending on the hydrogeological characteristics (Anderson and Woessner 1992). The conceptual model of Ziębice Basin was adopted from Shah (1995). The author assumed a three layered aquifer model, i.e. two aquifers separated by an aquitard. While the upper layer (Quaternary) is a shallow unconfined aquifer covering the entire Basin (Figure 1-8(a)), the lowest layer (Tertiary) is a deep confined with a limited areal extent (Figure 1-8(b)) bounded at bottom by an impervious crystalline bedrock.

2.5.2. Flow system pattern, flow direction and flow rates

The shallow aquifer system of the Basin is recharged by precipitation and leakages along the stream banks. Moreover, the deep unconfined aquifer system is recharged by the leakage from the shallow aquifer system. The Olawa River penetrates fully the unconfined aquifer and drains water from the basin through Kazanow gaging station. There is a horizontal flow in the unconfined layer and vertical flow due to leakage in the confined layer. The leakage is bidirectional by which in some areas the flow is downward and in other areas the flow is upward (Shah, 1995). Moreover, the crystalline bedrock under the Basin is impervious.

2.5.3. Preliminary water balance

Part of water that falls as precipitation on the Basin evaporates, some drains to the stream as overland flow and some infiltrates into the aquifer system. Since the bedrock of the Basin is impervious and there is no flow across the Basin boundaries except at the river outlet, the percolating water is drained into the stream as a base flow. In addition, groundwater abstraction at the wellfields and groundwater evapotranspiration are the major sinks to the water balance of the Basin.

2.5.4. External and internal model physical boundaries

There is an external no-flow boundary all around the Quaternary aquifer except where the Olawa River outlet exits at Kazanow location on the northern side of the Basin (Figure 2-5). At this point, the groundwater outflow from the basin takes place but only within the shallow unconfined aquifer. Moreover, the no-flow boundary surrounds completely the confining layer and the Tertiary aquifer (Figure 2-5). The abstraction wells at Henrykow, Nieszkow, and Starczowek wellfields and Olawa River within the Basin form the internal model boundaries.

2.6. Numerical model

2.6.1. General concepts

In numerical modelling, the groundwater flow can be simulated in two methods, namely: steady-state and transient flows. In the steady-state condition, there is no change in aquifer storage with time while in the transient condition the aquifer storage changes with time in response to the prevailing stresses in the hydrological system. The flow of an incompressible three-dimensional groundwater system through a porous medium under a confined environment is governed by Equation (2.2). In addition, Equations (2.3) and (2.4) justify application of the Equation (2.2) under steady-state and transient conditions.

$$\frac{\partial}{\partial x}\left(K_x\frac{\partial h}{\partial x}\right)+\frac{\partial}{\partial y}\left(K_y\frac{\partial h}{\partial y}\right)+\frac{\partial}{\partial z}\left(K_z\frac{\partial h}{\partial z}\right)+W=S_s\frac{\partial h}{\partial t} \qquad (2.2)$$

For the steady-state flow, $\frac{\partial h}{\partial t}=0$ (2.3)

For the transient flow, $\frac{\partial h}{\partial t}>0$ (2.4)

where:

K is hydraulic conductivity in x, y and z directions [LT^{-1}]; x, y, z are orthogonal Cartesian coordinates [L]; h is a piezometric head [L]; W is a source or sink [T^{-1}]; S_s is a specific storage [L^{-1}] and t is time [T]. The same equation could also be used to represent unconfined environment if the specific storage (S_y) is replaced by specific yield (S_y) [-].

Anderson and Woessner (1992) pointed out that transient flow simulations compute different sets of heads at each time step of a given stress period. For that reason, a transient model enables identification of the critical stresses in the flow systems. In addition, Gurwin and Lubczynski (2004) pointed out that the transient flow is characterized by unique solutions which is not the case in the steady-state flow.

2.6.2. Software selection

The MODFLOW-NWT model under ModelMuse environment was applied to simulate the interactions between surface water and groundwater systems. The main advantage of this model is that it is of an integrated hydrologic type utilizing the UZF and SFR packages which are the cores for studying the surface-groundwater interactions. Since these two packages are very important for the research methodology adopted in this study, they are independently explained in the following two Subsections.

2.6.2.1. The Unsaturated Zone Flow (UZF) Package

The unsaturated zone is a transitional boundary of flux exchange between surface water and groundwater systems. The water flow through and the storage within the zone is governed by a nonlinear relationship (Ely and Kahle, 2012) which makes flow calculation more complicated. However, rapid developments in computing technology in terms of hardware and software have eased computational problems. Nowadays, the UZF package handles the computations with remarkable speed and efficiency.

The UZF package in MODFLOW-NWT performs the main task of simulating water flow and storage within an unsaturated zone (Figure 2-3). In doing so, the package segregates groundwater recharge and evapotranspiration from surface infiltrating water and accounts for land-surface runoff to streams and lakes (Ely and Kahle, 2012). Since the flow in the unsaturated zone is nonlinear, Ely and Kahle (2012) used the method of characteristics to solve the unsaturated kinematic wave equation. However, in order to achieve the solution the authors defined some assumptions. Firstly, they assumed that the only driving force for unsaturated flow is the gradient of gravity potential; in other words, the negative potential is neglected. Secondly, the authors assumed that in each vertical column of the model cell the hydraulic properties is uniform between the base of soil and water table.

The input data to the package involve evapotranspiration demand, infiltration rate, extinction depth and extinction water content at a specified stress period. The evapotranspiration (ET) demand and infiltration rate are, respectively, estimated in Sections 2.4.3 and 2.4.5. The extinction depth, i.e. the depth below which ET cannot be removed, was assumed to be 2 m. This assumption considered the maximum root depth of vegetation within the study area. Also, the extinction water content, i.e. water content below which ET cannot be removed from the unsaturated zone, was fixed to 0.05. The rest of the parameters in the Package were accepted as default.

2.6.2.2. The Stream Flow Routing (SFR) Package

The SFR Package simulates flow routing through a network of channels and computes the flow between stream network and aquifer systems (Figure 2-3). The Package computes stream depth of each stream reach at the stream midpoint in order to allow for streamflow simulation. As a result, the user can add and subtract the water from runoff, precipitation and evapotranspiration within each reach (Prudic et al., 2004). Moreover, Prudic et al. (2004) listed five methods that can be implemented in different segments in a network of streams to compute stream depth in the SFR Package as a specified value; Manning's equation using a wide rectangular channel; Manning's equation using an eight-point cross section; a power equation; and a table of values that relates flow to depth and width. With regard to simulation of flow diversion, Prudic et al. (2004) listed four options to implement as: diversion of all available flow at the end of the last reach of a segment up to the rate specified; diversion of the specified flow only if flow in the stream is greater than that of the diversion; diversion of a specified fraction of the available flow; and diversion of all excess flow away from the main channel during peak discharge. Moreover, the package uses Darcy's equation (2.5) to compute the flow between streams and aquifer system (Prudic et al., 2004).

$$Q_L = \frac{KwL}{m}(h_s - h_a) \tag{2.5}$$

where: Q_L is a volumetric flow between a given section of stream and volume of aquifer [L^3T^{-1}]; K is a hydraulic conductivity of streambed sediments [LT^{-1}]; w is a representative width of stream [L]; L is a length of stream corresponding to a volume of aquifer [L]; m is a thickness of the streambed deposits extending from the top to the bottom of the streambed [L]; h_s is a head in the stream determined by adding stream depth to the elevation of the streambed [L]; and h_a is a head in the aquifer beneath the streambed [L].

From the Equation (2.5) it can be explained that the flow into or out of a stream depends on the head difference between an aquifer and stream stage. That is, when an aquifer head is greater than a stream stage, water would flow into a stream. Conversely, when a stream stage is greater than an aquifer head, stream water would flow into an aquifer system. However, when an aquifer head is below the bottom elevation of a riverbed, the stream leakage is no longer dependent on the aquifer head (Prudic et al., 2004). In that situation, the authors estimated stream leakage flow by calculating head gradient between stream head and elevation of streambed bottom. The assumptions made in the calculation are: head at the bottom of streambed is equal to elevation of streambed; unit hydraulic gradient at the interval between streambed bottom and water table; and streambed leakage rate does not exceed saturated hydraulic conductivity.

Prior to data input, stream ordering map was created and used as a basis of data input into the SFR Package. The input data into the Package include: stream width of a rectangular channel, flows into upstream ends of the stream segments, the volumes of precipitation, evapotranspiration and runoff into the stream segments, hydraulic conductivity, channel roughness, streambed thickness and streambed elevation. Moreover, stream gage was only established at the place of flow measurement to enable stream flow calibration.

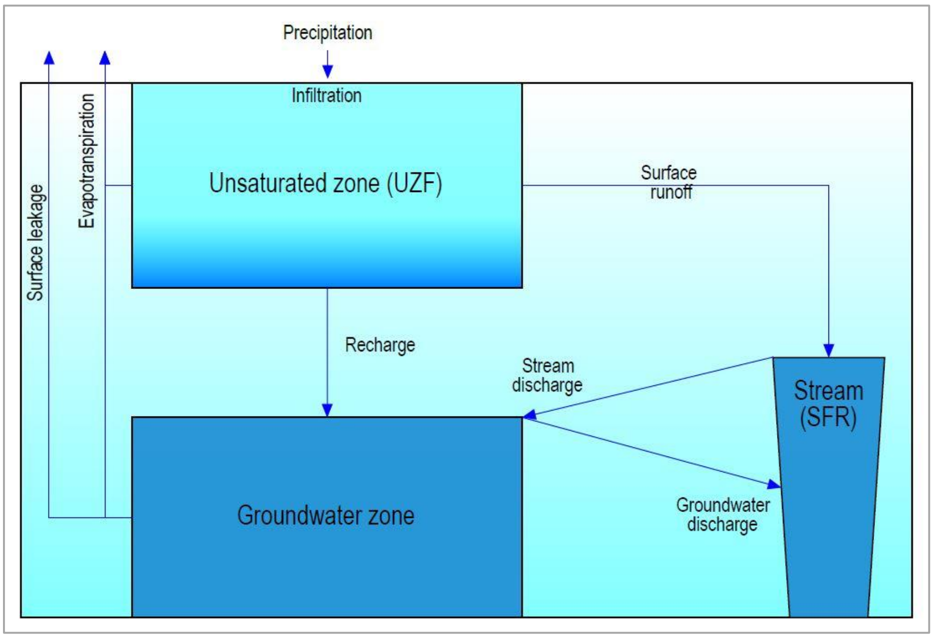

Figure 2-3: Schematic presentation of the connections between the UZF and SFR packages

2.6.3. Grid design

The model was constructed using a uniform grid cells of 350 m by 350 m. The grid network has 59 rows and 50 columns with a total of 2950 grid cells. It was aligned with the Polish coordinate system.

2.6.4. Structural model setting

2.6.4.1. Construction of structural model

Structural model involved input from model layers to resemble physical stratigraphy of the aquifer system. Since the model is made up of three layers, the surfaces of the model top and model bottoms of the aquifers and an aquitard were exactly defined and imported into the Modflow ModelMuse. The model top of the study area is the digital elevation model (DEM) which was obtained from the Wroclaw University. The contoured maps of bottoms of the Quaternary and Tertiary aquifers and geoelectrical cross-sections of the aquitard were obtained from Lubczynski (1991). The contoured maps were digitised and interpolated in ILWIS to create bottom surfaces of the aquifers. Moreover, the bottom surface of the aquitard was obtained by scaling the aquitard thickness from geoelectrical cross-sections of the study area. As a result, the scaled values of the aquitard thickness were subtracted from elevations of the bottom surface of the Quaternary aquifer followed by interpolation in ILWIS. Finally, the interpolated bottom surface of the three layers, i.e. Quaternary, aquitard and Tertiary were imported into Modflow ModelMuse as ASCII files. The schematic presentation of the conceptual model is shown in Figure 2-4.

2.6.4.2. Layer groups

The layer groups are defined by three types of layer structures when the UZF and Upstream Weighting (UPW) Packages are activated. The first structure is the convertible layer in which the heads in the model cells determine status of the cells. The cells are considered to be in confined or unconfined states when the heads are, respectively, above or below the cell tops. In the confined layer structure, the heads are always above the cell tops. The third layer structure is a non-simulated confining layer which separates the top and bottom model layers. This layer exists only in Quasi-3D models of which the model of this research belongs. In the non-simulated layer, the vertical hydraulic conductivity of the confining bed (VKCB) was used to calculate the conductance between the model layers. The layer structures are defined in the MODFLOW Layer Groups dialog box and all three layer groups mentioned above were used in this study in order to comply with the conceptual model.

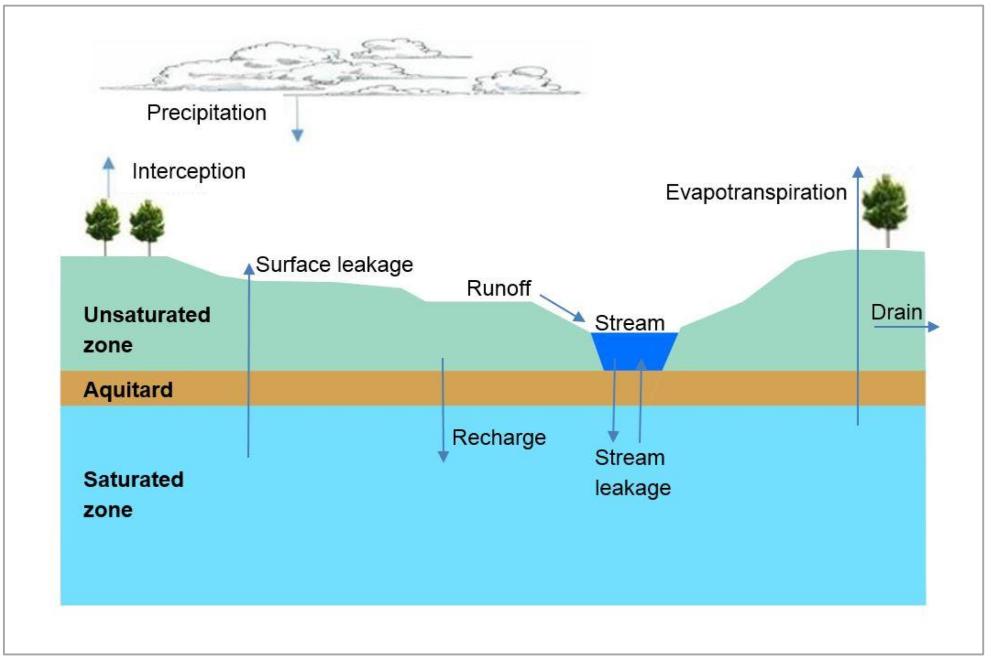

Figure 2-4: Conceptual model of the study area

2.6.5. Driving forces

When parameterisation of a model is fixed, its output will still be affected by changes on, let say, the amount of precipitation (Nossent et al., 2014). Therefore, precipitation is termed as a driving force of the model and determines the model output. The number and type of mode driving forces may differ from one type of model to the other depending on the intended purposes. In this study, the model driving forces are precipitation, interception, infiltration and potential evapotranspiration (PET) and are estimated in Section 2.4.

2.6.6. System parameterization

Aquifers have different properties that describe their capacities to transfer water to or release from storage. These properties are explained by specific yield and specific storage. For instance, specific yield, which is also called drainable porosity, is an important parameter when dealing with flows in an unsaturated zone such as modelling of drawdown in an unconfined aquifer and drainage of agricultural land. It is defined by Bear and Cheng (2010) as the volume of water drained from a soil column of a unit horizontal cross-sectional area, extending from the soil surface down to the underlying phreatic surface, per unit lowering of the phreatic surface's elevation. Moreover, it is a time dependent parameter due to the fact that it takes some times to complete drainage process after decline of a phreatic surface and reaching new equilibrium of soil moisture distribution. Specific storage is the volume of water released from storage with a unit volume of porous material per unit decline in head (Anderson and Woessner, 1992). When this quantity is used it refers to a confined aquifer. The values of specific yield are normally larger of several orders of magnitude than those of specific storage. In this study, the values used are based on previous studies in the study area and literature findings.

In the steady-state calibration, the parameter zones of hydraulic conductivities for the unconfined, confined and confining layers were established. Each zone was associated with its corresponding parameter value for steady-state calibration. Moreover, the zones for specific yield and specific storage were defined for unconfined and confined layers, respectively, during transient calibration.

2.6.7. Boundary conditions

Selection of types of flow package to be used in the model is a fundamental step in groundwater modelling. The selected packages for simulating flows in the unsaturated zone are the Upstream Weighting (UPW) and UZF Packages. In the steady-state condition, the zone parameters of horizontal and vertical hydraulic conductivities (HK and VK) of the aquifer layers and the vertical hydraulic conductivity of the confining bed (VKCB) are defined in the UPW Package. Moreover, the specific yield for the convertible layer and specific storage for the confined layer are defined in the transient condition. In the UZF Package, the recharge and discharge location (NUZTOP) were set in the top layer while the VK source (IUZFOPT) was specified. Furthermore, the UZF was set to route the discharge to the streams, to simulate evapotranspiration (IETFLG), to print summary of the UZF budget terms (IFTUNIT) and to calculate surface leakage. Also, the number of trailing waves (NTRAIL2) and the number of wave sets (NSETS2) were accepted by default as 15 and 20, respectively.

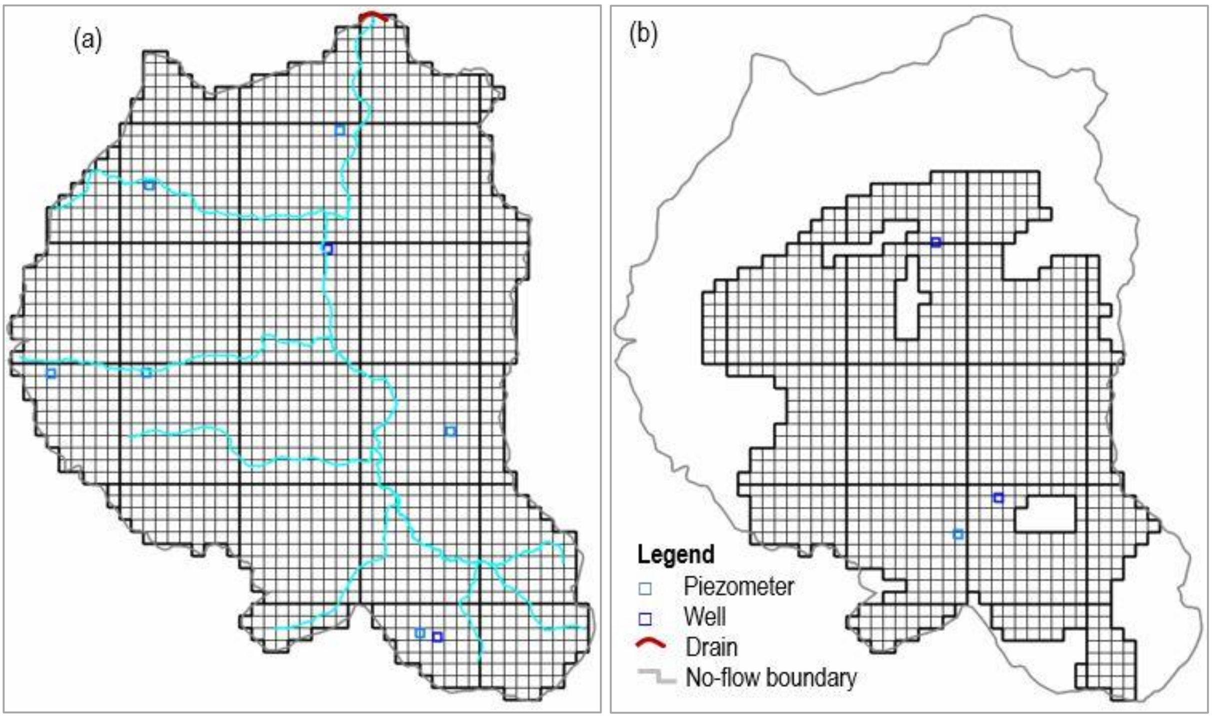

Figure 2-5: Boundary conditions in (a) Quaternary and (b) Tertiary aquifers, location Figure 1-1

The boundary conditions for the model are the no-flow, specified flux and head-dependent flux boundaries (Figure 2-5(a) and (b)). The boundaries are categorised into internal and external model boundary conditions. The external model boundary conditions are simulated through the no-flow and head-dependent flux through drain. The no-flow boundary is assigned by deactivating cells representing area outside model domains using the IBOUND condition for all 3 layers of the model. At the outlet of the Olawa the lateral groundwater outflow in the first, shallow aquifer is simulated through the head-dependent flux boundary using Drain Package. The model internal boundary conditions are the specified flux and head-dependent flux boundaries. The specified flux boundary condition, which is simulated through Well Package is applied to the Quaternary and Tertiary aquifers. This is due to the fact that one well at Henrykow and two wells at Starczowek wellfields are in Quaternary aquifer. In addition, the remaining two wells at Henrykow and all five wells at Nieszkow wellfields are in Tertiary aquifer. The stream flow of the river network is simulated by head-dependent flux boundary condition and is applied only to the Quaternary aquifer.

2.6.8. State variables

State variables are system characteristics that can have different values at different times in the system. They may include groundwater heads from piezometers, well discharges, stream discharges and soil moisture of an unsaturated zone. Normally, the state variables are simulated by the model. In this study, the state variables are groundwater heads, stream discharges at the outlet and well abstraction. In the first case, the same initial hydraulic heads as used by Gurwin (2010) are used in this model. The initial heads were obtained by interpolating water table measurements of the different piezometers and wells within the study area. Moreover, calibration of the model is based on the head observations (Figure 2-2(a) through (g)) recorded from seven monitoring wells spatially distributed in the study area as shown in Figure 1-1. Out of the seven piezometers, six are located in the Quaternary aquifer (Figure 2-5(a)) and one in the Tertiary aquifer (Figure 2-5(b)). In the second case, transient data of stream discharge measurements (Figure 1-6) were recorded only at one point in Ziębice Basin (Figure 1-1). In the last case, i.e. well abstraction, the used well discharge data were from pumping test results from Koziol (2006) and are presented in Annex 2. Generally, the calibration process is a very challenging exercise due to many data and parameters required by, both, the UZF and SFR packages. However, less number of stream gaging stations made the calibration to concentrate more on groundwater head calibration.

2.6.9. Time discretization and initial condition of transient model

Throughout the model, the units of measurements are set to meters for length and days for time. The time frame of the model simulation is five hydrologic years from 1st October 2004 to 30th September 2009. This period is comprised of one time step and a total of 1826 stress periods, each, with a length of one day, which are implemented in the calibration of the transient model. However, the steady-state solution is used as the first stress period in the transient model calibration and thus making a total of 1827 stress periods. The achieved solution of groundwater heads and streamflow of the calibrated steady-state model afsre used as the initial condition of the transient model. In MODFLOW-NWT, initialisation of transient model is done in MODFLOW Time dialog box by assigning the first stress period as a steady-state and the rest stress periods assigned as transient. This is the requirement of MODFLOW-NWT for the purposes of initialising transient calibration using the steady-state solution.

2.6.10. Numerical model calibration

2.6.10.1. General concepts of numerical model calibration

The Newton Solver (NWT), which is solely found in MODFLOW-NWT, is selected and used in model computations. It is automatically selected whenever the Upstream Weighting (UPW) Package is activated. In the beginning, all basic options of the solver are accepted by default. However, later the maximum number of iterations were set to 1000 and model complexity was set to complex.

The purpose of model calibration is to find a good match between observed and measured values of heads and flows. This is normally done by adjusting model parameters such as horizontal hydraulic conductivity, specific yield, specific storage, leakance, lake or streambed conductance, etc. Before calibration process, the steady-state model is created by calculating average stresses of the long-term measurements for the specified time frame. The stresses may include precipitation, stream discharges, recharge, groundwater abstraction and evapotranspiration. The process of calibration can be effected by using either a trial-and-error adjustment or an automated parameters estimation codes such as PEST (Anderson and Woessner, 1992). When comparing the two approaches, the trial-and-error method is preferred and is adopted in this study because it incorporates site specific knowledge and ensures gained insight of model behaviour during calibration (Hassan et al., 2014).

The transient calibration follows after the steady-state calibration. The model solutions achieved after the steady-state calibration is used as the initial conditions for the transient calibration. However, if the model fails to converge, some data may be sacrificed for model warming-up. Since the transient flow is time dependent, the parameters like specific yield, specific storage, stress periods with corresponding stresses and time discretization have to be well defined. Furthermore, the calibration parameters involve horizontal and vertical hydraulic conductivity of the different model layers, vertical leakance of the confining layer, specific yield and specific storage.

In the calibration process, it is difficult to obtain exact model parameter values due to different sources of model uncertainties. The sources of uncertainties in a groundwater model are categorized differently by different scholars. For instance, Wu and Zeng (2013) described model parameters, a conceptual model, observation data and boundary conditions as the four inherent categories of model uncertainties. Anderson and Woessner (1992) and Bear and Cheng (2010) pointed out that the effects of uncertainties on calibrated model can be studied using sensitivity analysis. During sensitivity analysis, the parameters realized to be more sensitive than others are carefully treated during model calibration or prediction scenarios. Furthermore, Bear and Cheng (2010) emphasised that more resources have to be invested on accurate determination of the most sensitive parameters. In both cases, i.e. steady-state and transient groundwater head calibrations, reliability of calibrated parameters is assessed using mean error (ME), mean absolute error (MAE) and root mean square error (RMSE) which are given in Equations (2.6), (2.7) and (2.8), respectively. According to Anderson and Woessner (1992), the magnitude of changes in heads in a model domain decides the maximum acceptable value of calibration criterion. The authors emphasised that if the ratio of the RMSE to the total head loss in the system is small, i.e. less than 10%, the errors are only a small part of the overall model system response. For water balance, the measure of calibration is assessed by discrepancy between total inflow and outflow. The water balance closure error is calculated as a ratio of the difference between total inflow and outflow to the total inflow or outflow. In most cases, an error of 0.1% is recommended, however, Anderson and Woessner (1992) considered an error of 1% acceptable and is applied in this study.

$$ME = \frac{1}{\mathrm{N}}\sum(H_{obs} - H_{sim}) \tag{2.6}$$

$$MAE = \frac{1}{\mathrm{N}}\sum|H_{obs} - H_{sim}| \tag{2.7}$$

$$RMSE = \sqrt{\frac{1}{N}\sum(H_{obs} - H_{sim})^2} \tag{2.8}$$

where:

N is the number of observations, H_{obs} and H_{sim} are the observed and simulated heads, respectively, in the unit of length.

2.6.10.2. Steady state model calibration

The steady-state model uses long-term averages of observations, on one side, and parameters, on the other side. The long-term averages are calculated from observed values of piezometric heights and stream discharges. Moreover, the average of calculated wellfield abstraction, infiltration rates and potential evapotranspiration are used. In all streams, a rectangular section was selected with the Manning's roughness coefficient of 0.035 and streambed thickness of 0.5 m. The width of the main stream was fixed to 3.0 m on the upstream and downstream ends while the width of other streams were fixed to 1.0 m on both ends. Moreover, the most upstream ends of all streams were assumed to be headwater streams at which flows were defined. Due to the existence of many small streams contributing flows to the main stream, diffuse overland runoff that enter the stream segments were also defined. The extinction depth was set to 2.0 m and extinction water content of 0.05 m^3m^{-3}. The conductance of the drain boundary condition was assigned a value of 50 md^{-1}. The parameters involved in the calibration are horizontal and vertical hydraulic conductivities of the unconfined and confined aquifers assigned at different zones. Assignment of hydraulic conductivity values in different zones was basically guided by the previous researches conducted in the study area and literature. Hydraulic conductivity values were also assigned to the upstream and downstream ends of each stream. Furthermore, vertical hydraulic conductivity of the confining bed was assigned in the confining layer. The flow into the upstream ends of the streams and diffuse overland runoff were assigned arbitrarily into stream segments to ensure that the gage at the outflow reads more or less the measured flow. Despite the many parameters involved in the model, the trial-and-error method was used in the calibration process.

As mentioned in Section 2.6.10.1 that error assessment of a calibrated model is expressed using average errors that are explained in Equations (2.6), (2.7) and (2.8). In the calibration process, the main objective is to minimise the RMSE which is also called calibration criterion. Since the parameters used in model calibration are associated with some uncertainties, the response of the model is examined on the changes of each parameter value. In general, when the model responds highly to a small change in parameter values, the model is considered sensitive to that particular parameter. In contrary, the model is considered less sensitive if its response to the changes in parameter values is very minimal. The assessment of a system response with changes in various factors on which such response depends on is called sensitivity analysis (Bear and Cheng, 2010). The response of the model in this study is examined with respect to changes in piezometric heads by varying model parameters such as horizontal and vertical hydraulic conductivities (HK and VK) and vertical leakance (VKCB), etc. The changes are measured through RMSE.

2.6.10.3. Transient model calibration

The transient calibration involved horizontal and vertical hydraulic conductivities, leakance of the confining layer, specific yield and specific storage. The transient model was initialised as explained in Section 2.6.9 and calibration process was implemented in the same manner as in steady-state calibration.

The assessment of errors and sensitivity analysis of the model were performed in the similar fashion as in the case of the steady-state calibration explained in Section (2.6.10.2). However, more parameters (specific yield and specific storage) were involved in the sensitivity analysis.

The goodness of fit and acceptability of calibration results between the observed and simulated streamflow are judged by volumetric efficiency (VE) as recommended by Ely and Kahle (2012) which is defined by Equation (2.9). The VE represents the volumetric mismatch between the observed and simulated streamflow.

$$\mathrm{V}E = 1 - \frac{\sum |Q_{sim} - Q_{obs}|}{\sum Q_{obs}} \tag{2.9}$$

where: VE is the volumetric efficiency and the subscripted Q_{sim} and Q_{obs} are the simulated and observed stream flows. The VE ranges between 0 and 1 and for an unbiased model it is equal to 1 which indicates that the predicted streamflow delivered matches the actual streamflow for a particular period (Ely and Kahle, 2012).

2.6.10.4. Zone budget

In the Modflow ModelMuse, there are two possibilities of getting the water budget of the model. In the first option, i.e. using the Listing file, the overall water budget of the model composite is automatically listed in the Listing file after each model run. The Listing file contains volumetric rates of the water budget components for the entire model. However, this option does neither give the budget of the individual model layers nor of a specified area within the model. The second option, i.e. using the Zone budget, it overcomes the shortfalls of the Listing file and calculates the water budget of the individual layers, the specified model area and the overall water budget of the model on daily basis and cumulative from the start to the end of simulation period. Implementation of the second option is through ZONEBUDGET which is under Post processors in the MODFLOW Packages and Programs main window. The ZONEBUDGET tool was used to calculate and retrieve the water budgets of the Quaternary and Tertiary aquifers and for the model composite.

The general water balances of the Basin are schematically presented in Figure 3-11 and Figure 3-12 for steady-state and Figure 3-26 and Figure 3-25 for transient models and generally explained in Equation (2.10) where the daily fluxes of the three compartments (surface, unsaturated and saturated zones) are estimated.

$$P = ET + Q_{out} + Q_D + Q_w + \Delta S \tag{2.10}$$

where: P is the precipitation rate, ET is the total evapotranspiration, Q_{out} is the stream outflow at the outlet of the model area, Q_D is the lateral outflow through drain, Q_w is well discharge and ΔS is the change in total storage.

The ET and ΔS terms of Equation (2.10) are expressed in Equations (2.11) and (2.12)

$$ET = ET_g + ET_{uz} + I \tag{2.11}$$

$$\Delta S = \Delta S_g + \Delta S_{uz} \tag{2.12}$$

Where I is the canopy interception, ET_{uz} is the unsaturated evapotranspiration, ET_g is the groundwater evapotranspiration, ΔS_g is the change of storage in the saturated zone and ΔS_{uz} is the change of storage of the unsaturated zone.

The water balance of the land surface and the unsaturated zone is expressed in Equation (2.13)

$$P + Exf_{gw} = I + Ro + R_g + ET_{uz} \pm \Delta S_{uz} \tag{2.13}$$

where: Ro is the total runoff into the streams which is a summation of the excess infiltration runoff or Hortonian runoff (Ro_{ei}) and the saturation excess runoff or Dunian runoff (Ro_{sat}) expressed in Equation (2.14).

$$Ro = Ro_{ei} + Ro_{sat} \tag{2.14}$$

Equation (2.11) can be further simplified to include the actual infiltration rate (P_e) in the unsaturated zone and the gross recharge (R_g) as shown in Equations (2.15) and (2.16).

$$P + Exf_{gw} = I + Ro + P_e \tag{2.15}$$

$$P_e = R_g + ET_{uz} \pm \Delta S_{uz} \tag{2.16}$$

The water balance of the saturated zone is expressed in Equation (2.17)

$$R_g + Q_{SLin} = ET_g + Exf_{gw} + Q_w + Q_D + Q_{SLout} \pm \Delta S_g \tag{2.17}$$

where: Q_{SLin} is the stream leakage into the groundwater, Q_{SLout} is the groundwater leakage into the streams and ΔS_g is the change in the groundwater storage.

Together with considering gross recharge, Hassan et al. (2014) recommended assessment of net recharge of a groundwater model as a good practice. The authors defined the net groundwater recharge as the water that reaches the aquifer and flows down-gradient to a groundwater discharge area. The authors were on the opinion that the concept of net recharge imitates the behaviour of changes in groundwater storage better than merely using recharge. They estimated net recharge using Equation (2.18).

$$R_n = R_g - E_{xfgw} - ET_g \qquad (2.18)$$

where: R_n is the net recharge, R_g is the gross recharge, E_{xfgw} is a groundwater exfiltration and ET_g is groundwater evapotranspiration, all in millimetres per day. It should be noted that from this Section onwards the term surface leakage denoted by Slk_{gw} is going to replace the groundwater exfiltration term to ensure consistency with the terminologies used in MODFLOW-NWT.

2.6.11. Simulating the natural surface-groundwater interactions

Transient calibration of the model involved three wellfields which are situated from the north to the south of the study area (Figure 1-1) with a total of ten abstraction wells. The wells tap groundwater from Quaternary and Tertiary aquifers. In order to predict the natural state of the aquifer system in the Basin, the abstraction wells were removed from the calibrated transient model without altering model parameters. The flow systems were analysed to identify their natural interactions such as direction of flow and influent and effluent conditions of both stream and groundwater systems. Finally, the comparison between the situation with and without abstraction wells was made to examine the extent of the effects of surface-groundwater interactions in the Basin.

3. RESULTS AND DISCUSSION

3.1. Hydrologic calculations

3.1.1. Precipitation, interception and infiltration rate

In order to fill the gaps in the time series data of precipitation from the ADAS station, the nearby precipitation data set from Klodzko station was used. The correlation between precipitation data sets was established as shown in Figure 3-1 and the equation in the Figure was used to fill the gaps in time series precipitation data of the ADAS station that finally resulted in precipitation time series data as shown in Figure 3-2. The maximum precipitation after filling the gaps was about 68 mm with a daily average value of about 1.9 mm.

The precipitation data sets of the two stations showed low correlation of about 0.3 as shown in Figure 3-1. Despite the low correlation between the data sets, the filling of gaps was done with the same data sets due to lack of other data that could give a best correlation results instead of that from Klodzko. Moreover, the filled gaps were only about 10 % of the total available data which was considered to have little effect on the model output.

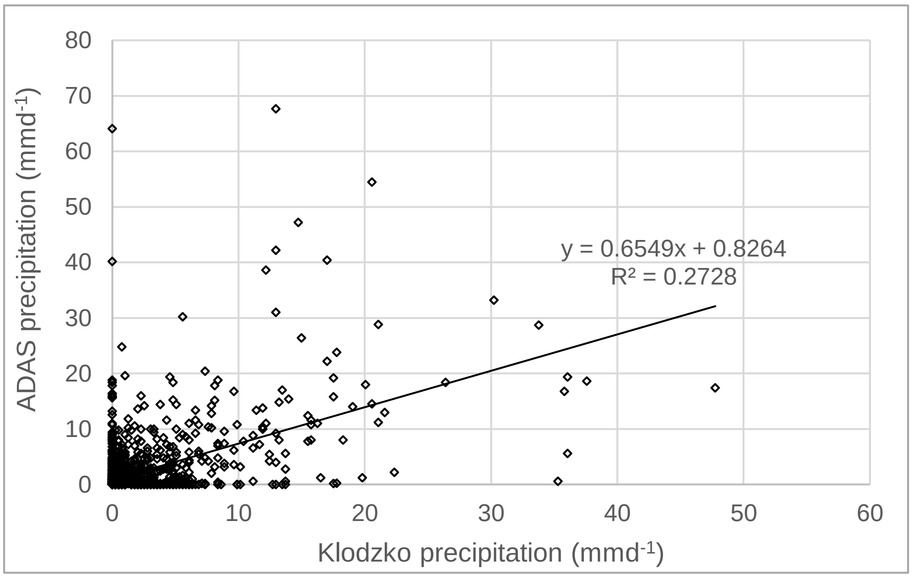

Figure 3-1: Correlation of precipitation measurements

The difference between the estimated precipitation and interception rates resulted to the estimate of infiltration rate. The average daily interception rate of about 0.58 mm was estimated and was largely contributed by the agricultural land. The final estimated daily infiltration rate was about 1.3 mm and was applied in the steady-state model and the calculated time series infiltration rates are shown in Figure 3-2.

3.1.2. Streamflow

The daily average of 32566 m^3d^{-1} was estimated from the time series of 30 minutes discharge measurements. The recorded minimum and maximum flows were 5228 and 294810 m^3d^{-1}, respectively with a standard deviation of 22420 m^3d^{-1}. The high standard deviation implies high temporal variation of streamflow which might be influenced by variable precipitation and snow cove melt. The gap in the time series measurement (Figure 1-6) was due to the recording failure of the gaging system caused by snow cover in the streams. This is also observed in Figure 1-2 due to very low temperature, about -20 ^{o}C, recorded during that period. Moreover, the peaks in the streamflow were observed during high precipitation (Figure 1-6) and snowmelt (Figure 1-2). The sudden peaks in the streamflow after rainfall events implied high relief in the Basin which results in fast concentration of runoff that lasts for a short period in the streams. Despite the short period of available discharge data, the stream discharge does not show any trend of decline with time. This situation envisages that the stream baseflow has paramount contribution to the stream discharge which signifies good groundwater reservoir in the Basin.

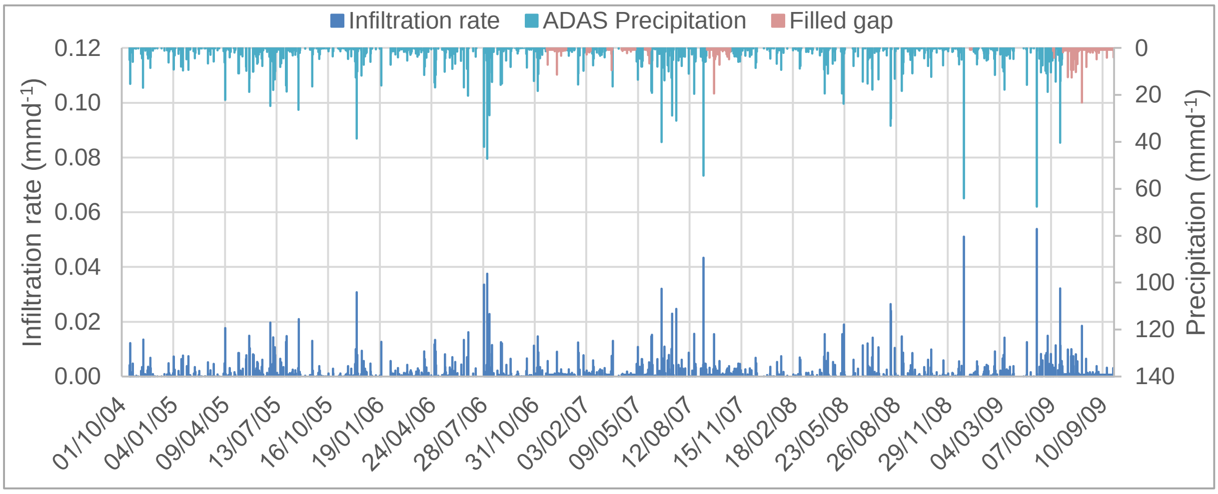

Figure 3-2: Gaps filled precipitation data of ADAS station

3.1.3. Potential evapotranspiration

Evaporation demand was calculated using the FAO Penman-Monteith (FAO P-M) formula as explained in Section 2.4.3. The correlation of temperatures between the ADAS and Opole stations was reasonable for use, i.e. more than 0.7 (Figure 3-3(a) through (c)), in order to fill the temperature gaps. The equations shown in Figure 3-3 were used to calculate the mean, maximum and minimum temperatures and fill the gaps in the time series of ADAS temperature data sets.

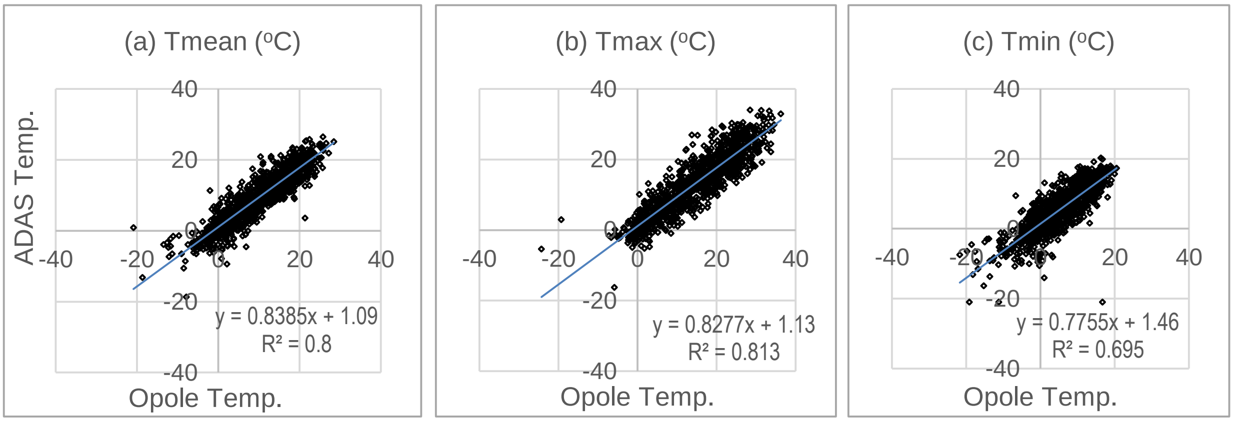

Figure 3-3: Temperature correlation between Opole and ADAS stations

The correlation between the ETo estimated from FAO P-M and Hargreaves Methods is shown in Figure 3-4 and the equation in the Figure was used to fill the gaps in ETo values. Finally, after filling the gaps, the estimated potential evapotranspiration, in millimetres per day, was found to have a minimum value of about 0.1 and a maximum of 6.6 with an average value of about 2.6 (Figure 3-5).

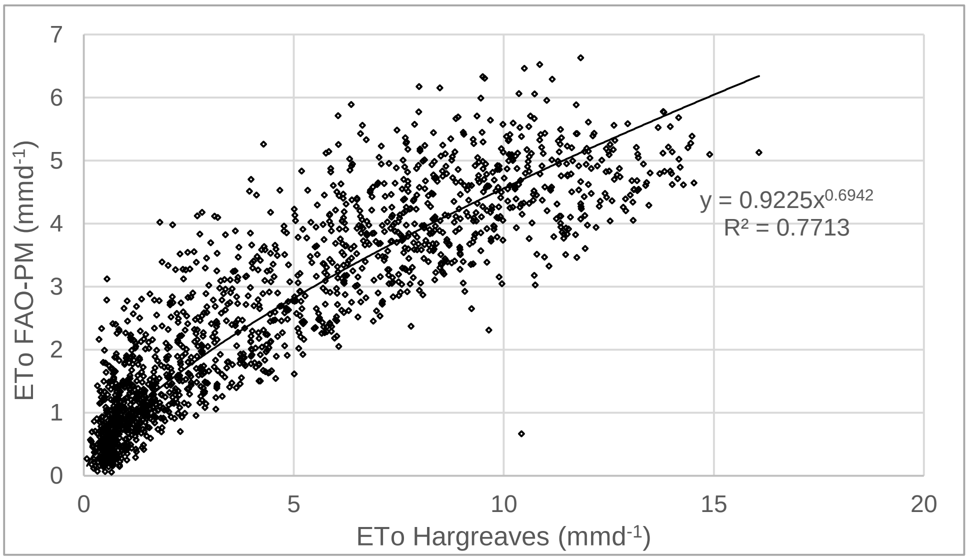

Figure 3-4: Correlation of ETo calculated from FAO P-M and Hargreaves Methods

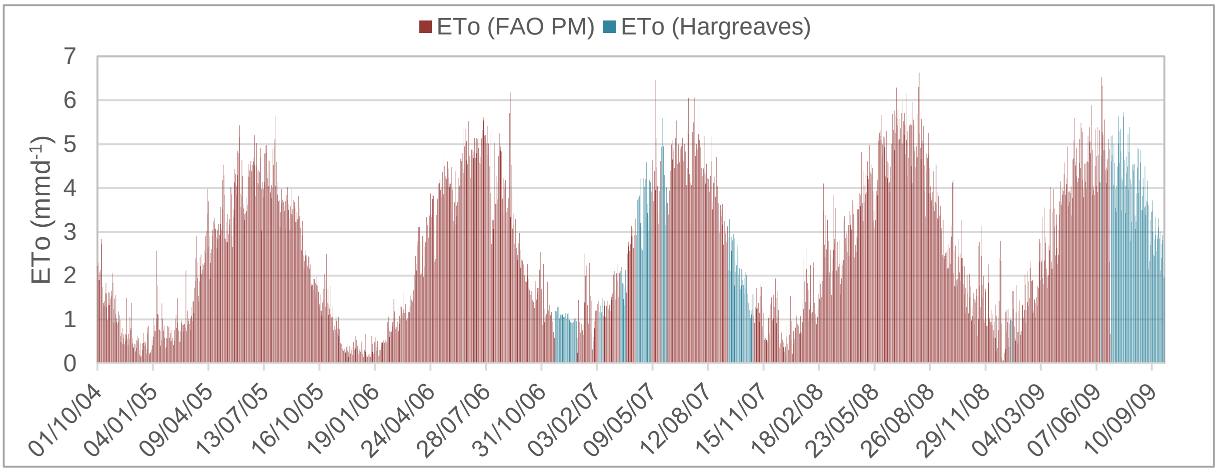

Figure 3-5: ETo from FAO P-M Method with filled gaps

3.2. Steady state model calibration

3.2.1. Calibration parameters under steady-state

Calibration of the model involved horizontal and vertical hydraulic conductivities (HK and VK) of unconfined and confined aquifers. The values of HK varied from 0.1 to 50 md^{-1} in the unconfined aquifer (Figure 3-6) while in the confined aquifer it was 25 md^{-1} (Figure 3-8). In the unconfined aquifer (Figure 3-6), the values were very small especially on the northern and western parts of the Basin. The vertical hydraulic conductivity of the confining bed (VKCB) ranged between $10x10^{-6}$ to $0.6x10^{-3}$ md^{-1}(Figure 3-7).

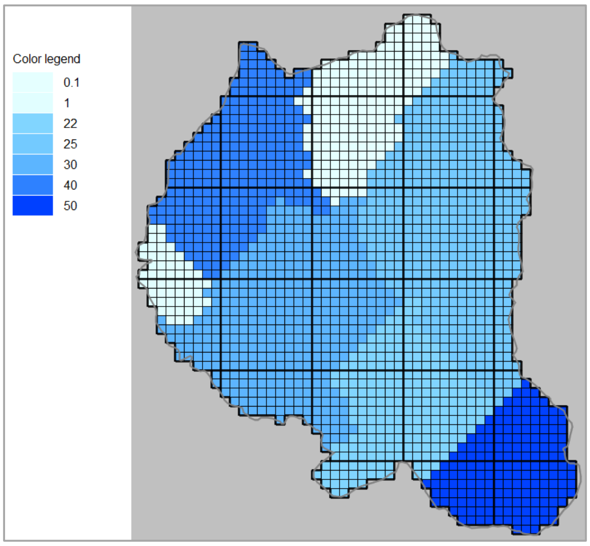

Figure 3-6: Horizontal hydraulic conductivity (md^{-1}) of the Quaternary aquifer

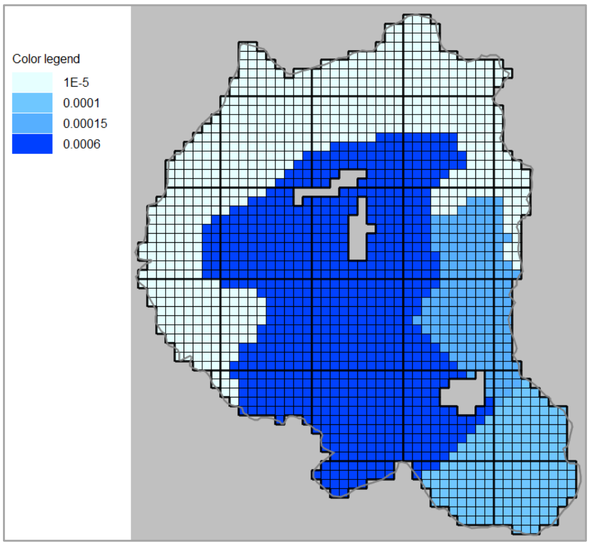

Figure 3-7: Vertical hydraulic conductivity (md^{-1}) of the aquitard

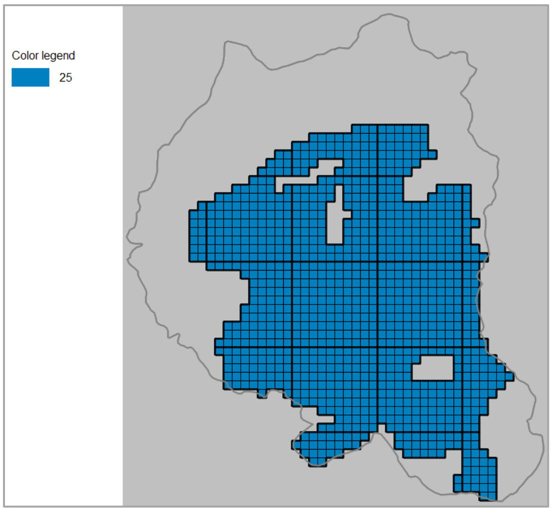

Figure 3-8: Horizontal hydraulic conductivity (md^{-1}) of the Tertiary aquifer

3.2.2. Error assessment and sensitivity analysis of the steady-state model results

3.2.2.1. Error assessment

Assessment of errors was based on the mean error (ME), mean absolute error (MAE) and root mean square error (RMSE) calculated from Equations (2.6), (2.7) and (2.8), respectively. The values of ME, MAE and RMSE are respectively equal to -0.341 m, 0.697 m and 0.829 m with the associated errors shown in Table 3-1. The decision on the acceptability of the errors was based on comparing the total head loss in the Basin and the RMSE. The water table in the Basin varies between 179.7 to 310.5 m-asl which makes a total head loss of 130.9 m in the model area. The ratio of RMSE to the total head loss was 0.6% which is smaller than the maximum acceptable error of 10%. The scatter plot of the observed versus simulated heads is shown in Figure 3-9. The Figure shows a random distribution of deviation of the points from both sides of the straight line. Finally, the results of steady-state were considered good for the initial condition of transient calibration.

Table 3-1: Error assessment of heads after steady-state calibration

Piezometer name	Aquifer	X (m)	Y (m)	Observed head (m)	Simulated head (m)	Error (m)	Absolute error (m)	Squared error (m^2)
DL36482	Q	3645123	5603761	260.423	259.406	1.017	1.017	1.034
DL36521	Q	3634376	5611318	309.394	310.356	-0.962	0.962	0.925
DL36525	Q	3637239	5616802	262.436	263.575	-1.139	1.139	1.297
ADAS	Q	3646020	5609617	224.906	225.386	-0.480	0.480	0.230
DL36483	Q	3642802	5618379	190.191	190.9564	-0.765	0.765	0.586
DL36527	Q	3637151	5611340	277.770	278.522	-0.752	0.752	0.565
DL36522	Tr	3643116	5606652	239.003	238.312	0.691	0.691	0.478

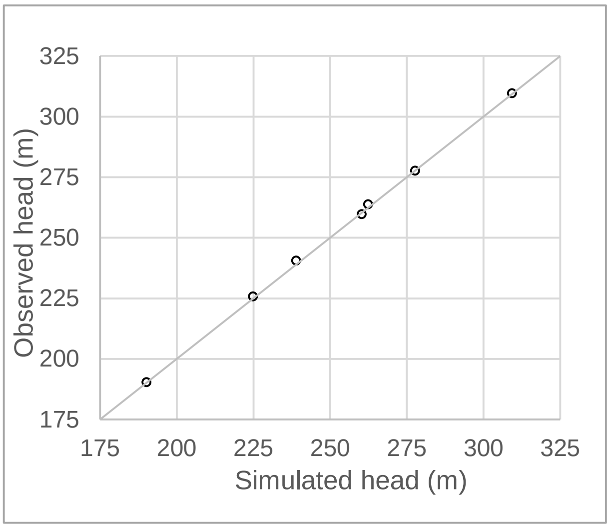

Figure 3-9: Scatter plot of observed and simulated heads after steady-state calibration

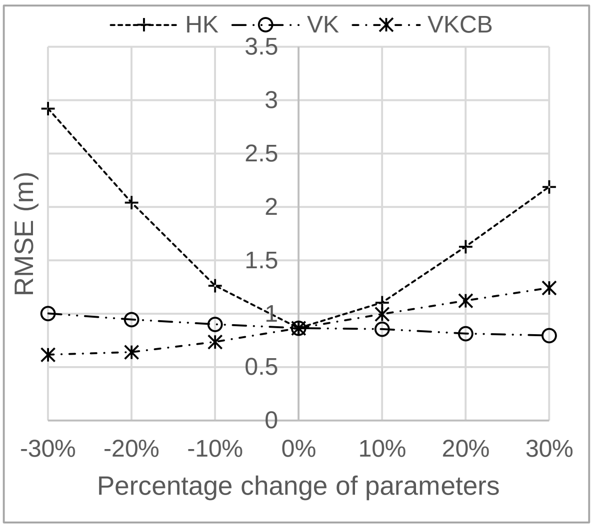

Figure 3-10: Sensitivity of model parameters under steady-state calibration

3.2.2.2. Sensitivity analysis

Sensitivity of the model was judged with respect to its response to changes in hydraulic heads and was measured using the RMSE (Figure 3-10). The Figure shows that the model heads are very responsive to increase and decrease of HK values. The HK affects the model on, both, increase and decrease of the parameter values. However, its sensitivity is higher on decreasing the parameter values when compared with increasing the parameter. The VKCB has low sensitivity to smaller values of the parameter and increases at a low rate of increasing the parameter values of VKCB. With regard to VK, the model showed little response, in general. However, the response was decreasing by increasing the parameter value. On comparing the three parameters in Figure 3-10, the reliability and quality of HK can be considered good because small changes in the parameter values produced large changes in residual error (Bear and Cheng, 2010). However, reliability and quality of VKCB and VK parameter can be considered good because it showed smaller response to the model. This implies that more investigations need to be done on these parameters in order to improve the results of model calibration.

3.2.3. Water budget of the steady-state model

The water budget of the steady-state model are presented in Table 3-2 for the individual aquifers and Table 3-3 for the model composite and their respective compartmental schematic flux diagrams are shown in Figure 3-11 and Figure 3-12. The Tables summarise the annual average flows of each component of the water budget for the Quaternary and Tertiary aquifers. The percent of water budget components is calculated with respect to the total amount of precipitation. Table 3-2 reveals that groundwater recharge is the main inflow component in the Quaternary aquifer, which constituted about 67% of the water budget of the aquifer. The stream leakage, which constituted 16% of the water budget, was in the second position on contributing the water budget and the flow from the Tertiary to the Quaternary aquifer was very small about 5%. The outflow components from the Quaternary constituted 47% of surface leakages, 26% of groundwater evapotranspiration, 11% of stream leakage, 6% of flow from Tertiary to Quaternary aquifer and 1% each for well abstraction and lateral flow through drain.

Table 3-2: Water budget of the Quaternary and Tertiary aquifer after steady-state calibration

FLOW BUDGET COMPONENTS	QUATERNARY (m^3d^{-1})		TERTIARY (m^3d^{-1})	
	IN	OUT	IN	OUT
WELLS	0	2904	0	8225
DRAINS	0	3994		
STREAM LEAKAGE	63789	37399		
GW ET	0	89823		
UZF RECHARGE	269100	0		
SURFACE LEAKAGE	0	190540		
EXCHANGE BETWEEN AQUIFERS	13904	22129	22129	13904
Total	346790	346789	22129	22129
IN - OUT		1		0
Percent Discrepancy		0.00		0.00

The inflow to the Tertiary aquifer was only from the exchange with the Quaternary aquifer (100%). The major outflow components in the Tertiary aquifer constituted about 55% of wells abstraction and 45% of the exchange from the Tertiary aquifer to the Quaternary. The water budget closure error, which was measured using the percentage of discrepancy, was within the limits of acceptable error ±1%. The flow budget envisages that the aquifer system is mostly influent since it gains much water than what it loses to the streams.

Table 3-3: Water budget components of the model composite after steady-state model calibration

FLOW BUDGET COMPONENTS	FLOW (m^3d^{-1})	
	IN	OUT
WELLS	0	11129
DRAINS	0	3994
STREAM LEAKAGE	63786	37399
GW ET	0	89823
UZF RECHARGE	269100	0
SURFACE LEAKAGE	0	190540
Total	332886	332885
IN - OUT		1
Percent Discrepancy		0.00

The water budget of the model composite (Table 3-3), as percent of precipitation, was comprised of groundwater recharge and stream leakage into the aquifer system which accounted for about 67 and 16% of precipitation as the inflows to the model. The outflows were dominated by surface leakage (47%), groundwater evapotranspiration (22%), stream leakages (9%), groundwater abstraction (3%) and the lateral flow through the drain (1%).

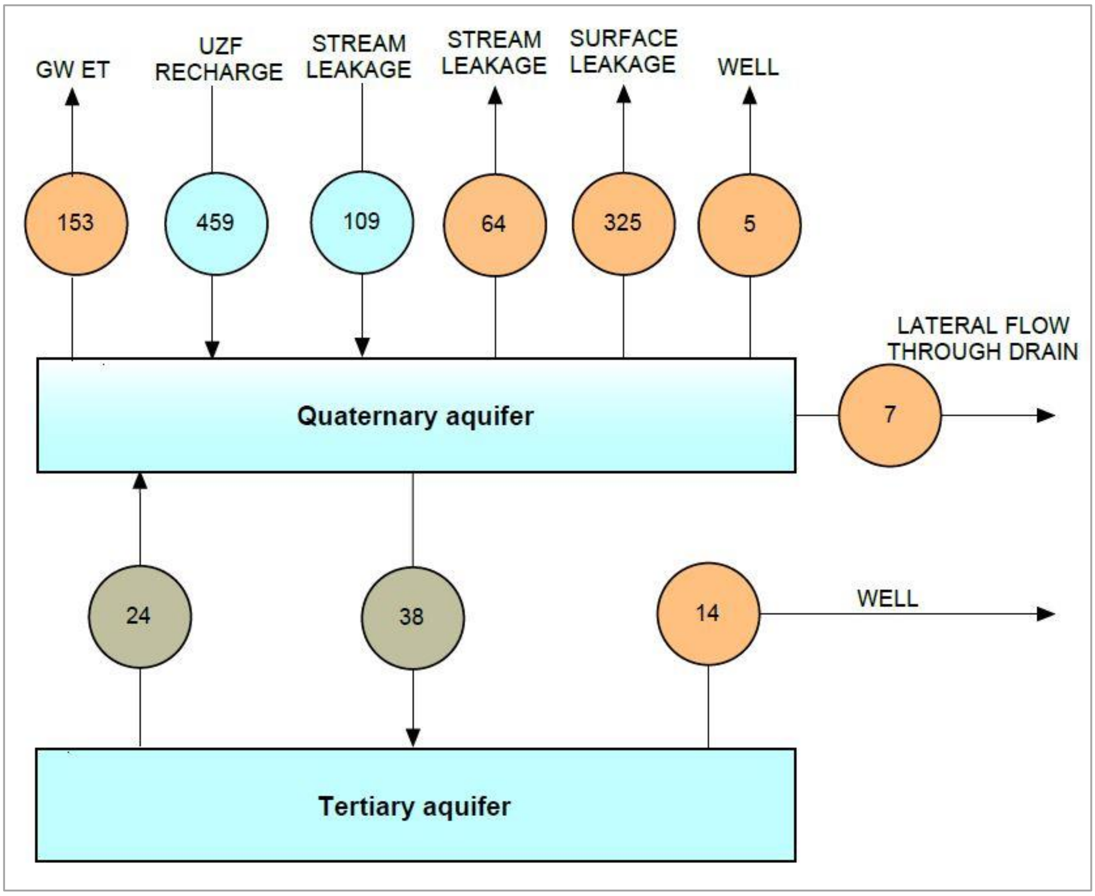

Figure 3-11: Water budget (mm.yr^{-1}) of the individual aquifers after steady-state calibration

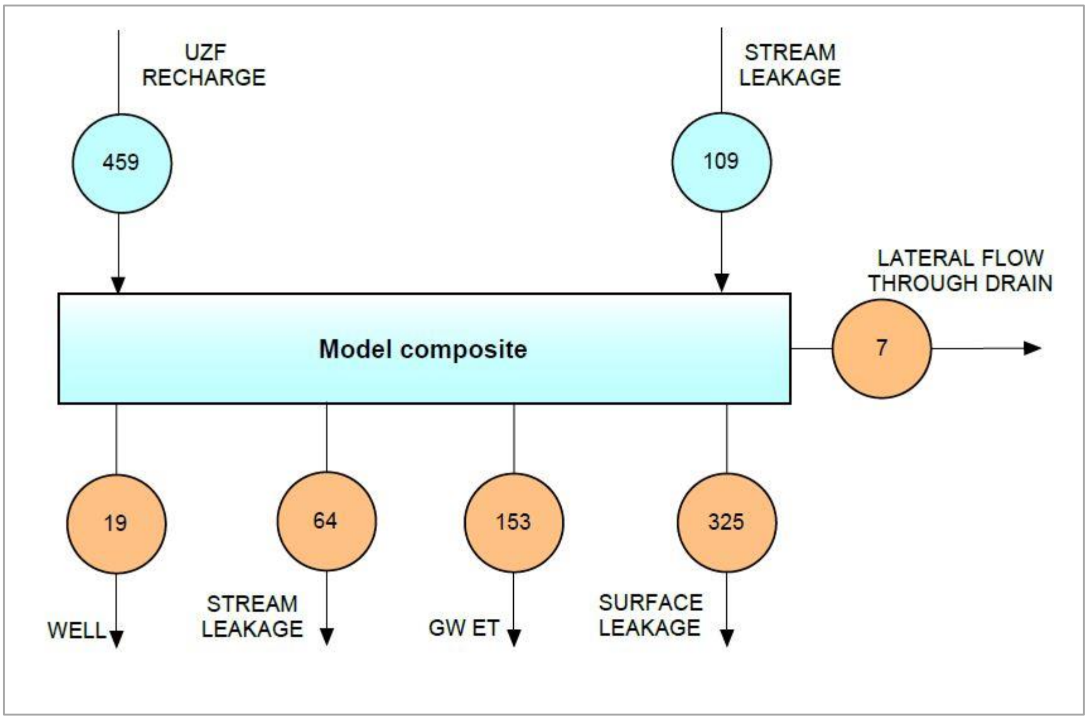

Figure 3-12: Water budget (mm.yr^{-1}) of the model composite after steady-state calibration

3.3. Transient state model calibration

Calibration of the transient model involved adjustment of model parameters to simultaneously match simulated groundwater heads and stream discharges with their respective time series measurements. The speed of the calibration process in the model runs was slower due to large volumes of data and involvement of many hydrogeological parameters in the model. As a result, the length of each model run took more or less 45 minutes.

3.3.1. Calibration parameters under transient state

The calibration task was a repetitive process, i.e. trial-and-error method, to find a good match between observed and simulated state variables (groundwater heads and river discharges) explained in Subsection 2.6.10. Since the model was constrained by surface and groundwater flows, the calibration process was time demanding. Besides constraining the model with the surface and groundwater flows at a time, the involvement of many parameters increased complexity of calibration which resulted in long times of model runs.

Transient calibration of the model involved all parameters used in the steady-state calibration explained in Section 3.2 and storage parameters (specific yield and specific storage) assigned respectively in the Quaternary and Tertiary aquifers. The parameters used to attain the solution of the steady-state model were further adjusted together with the new parameters to calibrate the state variables.

3.3.1.1. Hydraulic conductivities

Generally, there were changes of horizontal hydraulic conductivities (HK) in the different zones in the Quaternary aquifer after transient calibration (Figure 3-13 Figure 3-15) when compared with the steady-state results in Figure 3-6 and almost no changes in the Tertiary aquifer (Figure 3-8 and Figure 3-15). In the western side of the model, the HK was very low (1 md^{-1}) while the remaining areas varied between 0.1 to 80 md^{-1}. In the Tertiary aquifer that is at the central part of the Basin, the HK after calibration was 24 md^{-1} (Figure 3-15).

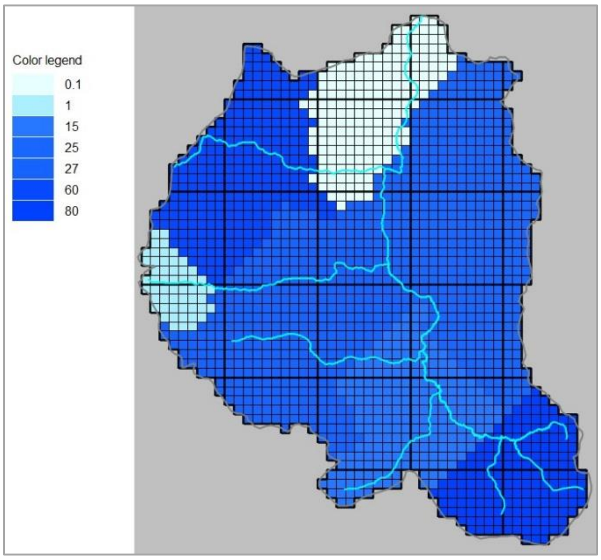

Figure 3-13: HK (md^{-1}) of the Quaternary aquifer after transient calibration

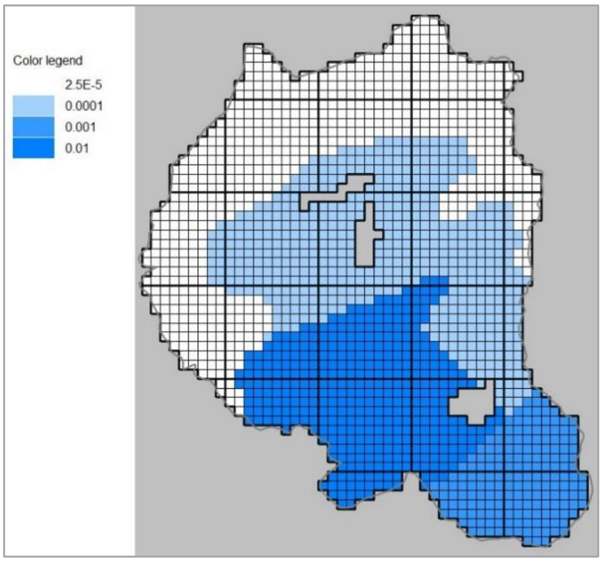

Figure 3-14: VKCB (md^{-1}) of the confining bed

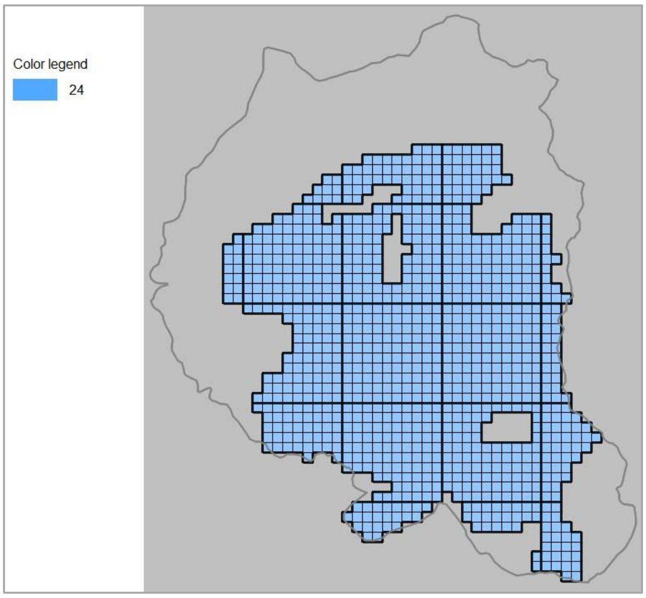

Figure 3-15: HK (md^{-1}) of the Tertiary aquifer

3.3.1.2. Specific yield and specific storage

At the onset of calibration, the model was divided into six zones with different specific yield values for each piezometer in the Quaternary aquifer. After several calibration trials, the final zones were four with values varying between 0.2 and 0.35 (Figure 3-16). The same procedure was applied to the Tertiary aquifer; however, there was only one zone of specific storage whose final value after calibration was 0.005 (Figure 3-17).

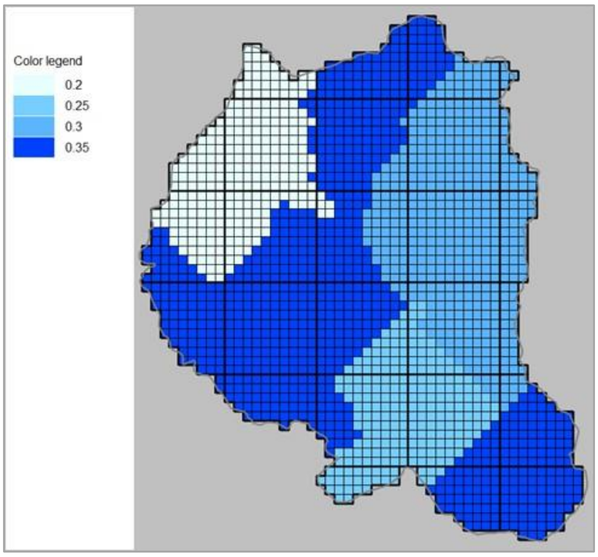

Figure 3-16: Specific yield of the Quaternary aquifer after transient calibration

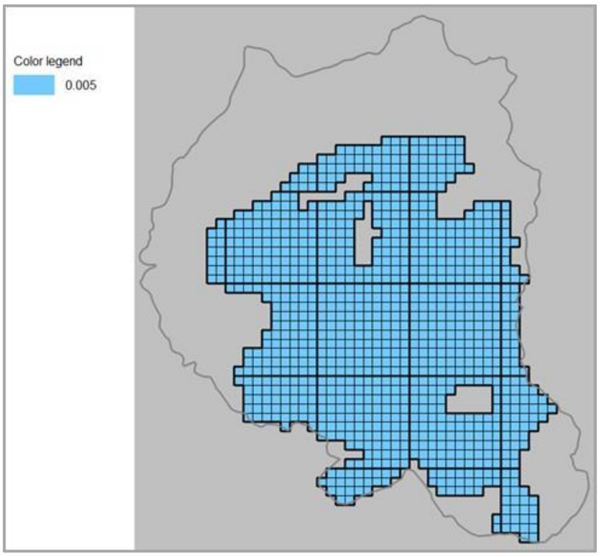

Figure 3-17: Specific storage of the Tertiary aquifer after transient calibration

3.3.2. Stream discharges

Calibration of stream discharges was done simultaneously with groundwater heads. Since there was only one stream gaging station, the task of stream calibration was not complicated despite the many parameters involved. The best matching between the observed and simulated stream discharges (Figure 3-18) was achieved with the volumetric efficiency (VE) of 0.94. The obtained value of VE was considered acceptable and indicated a good matching between the observed and simulated streamflow. Generally, the model reproduces the pattern of streamflow (Figure 3-19).

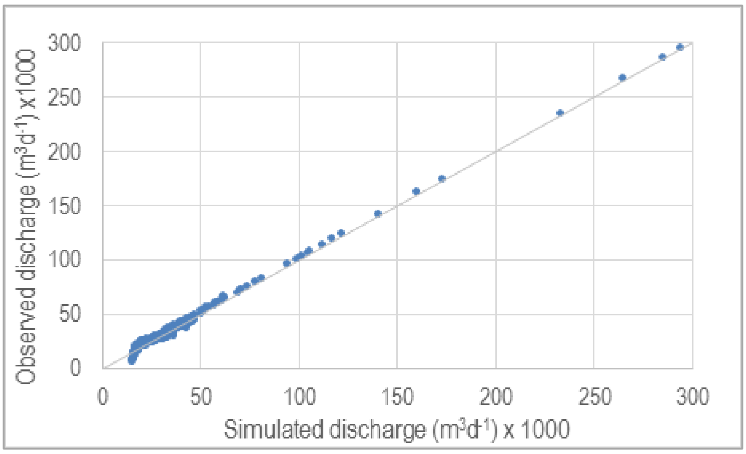

Figure 3-18: Comparison between observed and simulated stream flow

It is observed from Figure 3-19 that the stream has a continuous flow throughout a year as shown in the Figure as from the late March 2006 to the late May 2008. The stream gaging station had its minimum flow record of about 5227 m^{3}d^{-1} only during the late July 2007. The streamflow is contributed by precipitation runoff, snowmelt water and stream baseflow. It is evident that the persistence of flow in the stream is maintained by the stream baseflow. The precipitation runoff and snowmelt water are mostly responsible for the stream peaks which last for short duration in the Basin.

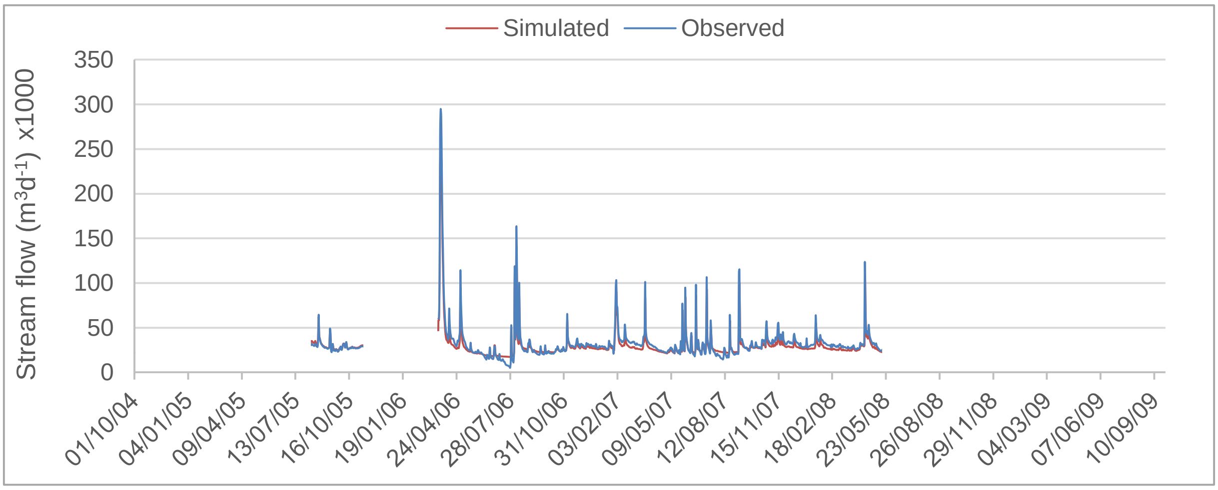

Figure 3-19: Comparison between stream flows after transient calibration

3.3.3. Groundwater heads

Calibration of groundwater heads involved seven monitoring wells of which six are in the Quaternary and one in the Tertiary aquifers as shown in Figure 1-1 and Figure 2-5. The plot of observed heads as a function of simulated heads is shown in Figure 3-20(a) through (g). The calculated ME and MAE of the heads measurements were -0.149 and 0.295 m, respectively and RMSE of 0.395 m. The obtained RMSE was about 0.3% and was considered good because it is within the acceptable limit of 10% of the maximum acceptable error of 13.085 m (Section 3.2.2).

The time series plots of groundwater head observations are shown in Figure 2-2(a) through (g) and Figure 3-20(a) through (g). Considering the fluctuations and the decline of piezometric levels, the monitoring wells are categorised into three groups. While the first and the second group are in the Quaternary, the last group is in the Tertiary aquifer. The first group, i.e. DL36521, DL36482 and Dl36483, showed moderate fluctuations with no trend of decline in piezometric level with time. The second group, i.e. DL36527, DL36525 and ADAS, showed high fluctuations with no trend of decline in piezometric level with time. The third group, i.e. DL36522, showed moderate fluctuation with considerable trend in the increase of the piezometric levels with time.

There are various factors that can cause different response properties of piezometric levels in the piezometers. These may include, but not limited to seasonal changes in rainfall recharge, effects of hydraulic conductivity and recharge occurring outside the neighbourhood of piezometer (Wang and Jiao, 2005). For instance, in the first group, i.e. with low fluctuations, points DL36482 has high hydraulic conductivity and is closer to the stream while DL36483 has low hydraulic conductivity and very close to the stream. High hydraulic conductivity allows for easy water replenishment into the piezometers and stabilises the piezometric level. The piezometric level fluctuations in DL36521 is also moderate and might be caused by low seasonal variability of rainfall recharge. For the case of the second group, i.e. with high water level fluctuations, they could be affected by high seasonal variability of rainfall recharge. Considering the last group, it is most likely that the gradual and smooth increase of the piezometric level at DL36522 might have been caused by dominantly clayey soils with low permeability on its surrounding environment.

The calibration results of piezometers in Figure 3-20(a) and (g) have shown a good pattern and trend between the observed and simulated groundwater heads. In Figures (c), (d) and (f), the model maintained the trend but did not capture the pattern. In Figure (b), the model captured the pattern at some parts and showed a declining trend of simulated heads. The possible reason for this is that the assigned infiltration rates might be high at the start of simulation and low at the last stress periods.

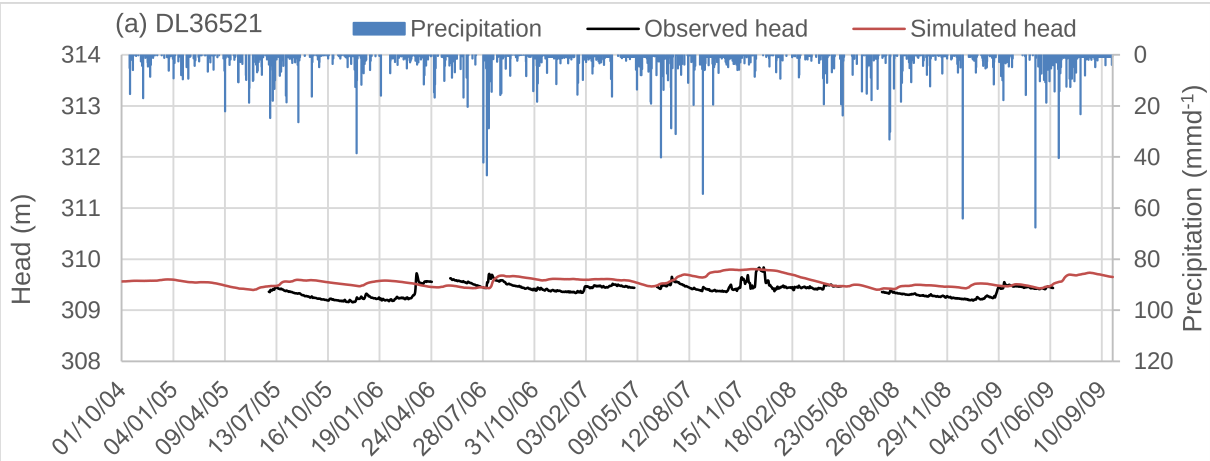

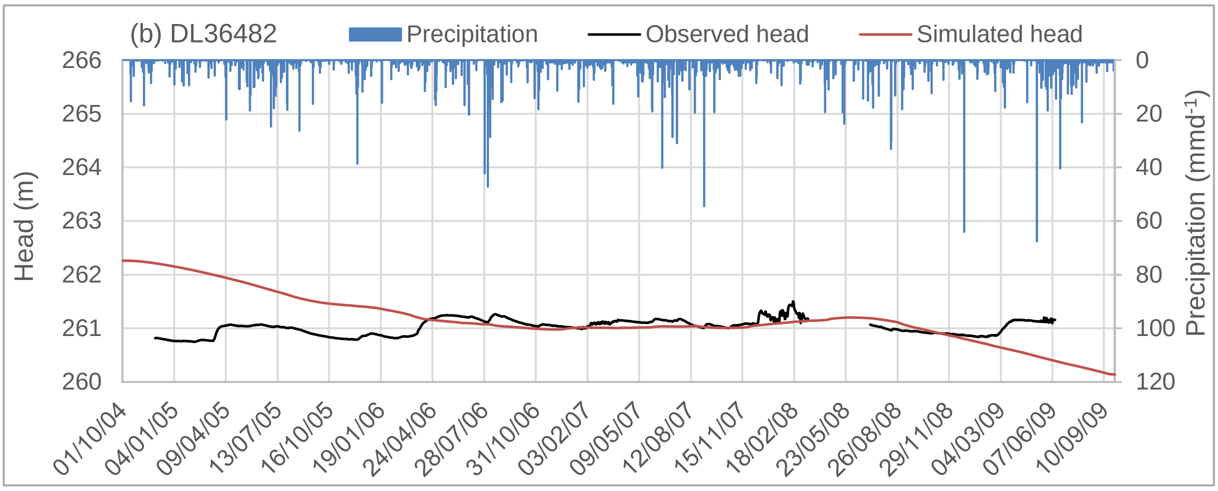
(b) DL36482
Precipitation
Observed head
Simulated head
Head (m)
Precipitation (mmd-1)
266
265
264
263
262
261
260
0
20
40
60
80
100
120
01/10/04
04/01/05
09/04/05
13/07/05
16/10/05
19/01/06
24/04/06
28/07/06
31/10/06
03/02/07
09/05/07
12/08/07
15/11/07
18/02/08
23/05/08
26/08/08
29/11/08
04/03/09
07/06/09
10/09/09

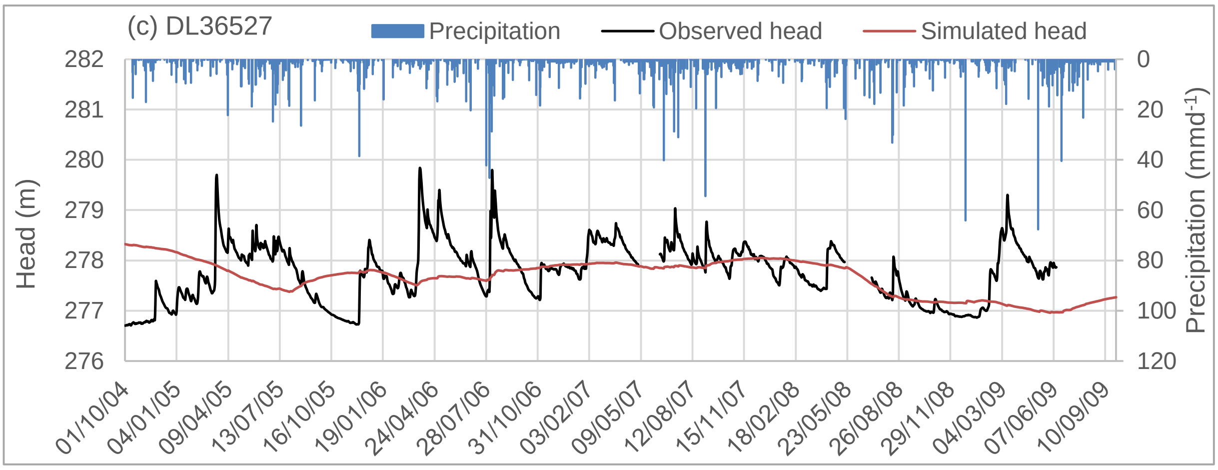
(c) DL36527
Precipitation
Observed head
Simulated head
Head (m)
Precipitation (mmd-1)
282
281
280
279
278
277
276
0
20
40
60
80
100
120
01/10/04
04/01/05
09/04/05
13/07/05
16/10/05
19/01/06
24/04/06
28/07/06
31/10/06
03/02/07
09/05/07
12/08/07
15/11/07
18/02/08
23/05/08
26/08/08
29/11/08
04/03/09
07/06/09
10/09/09

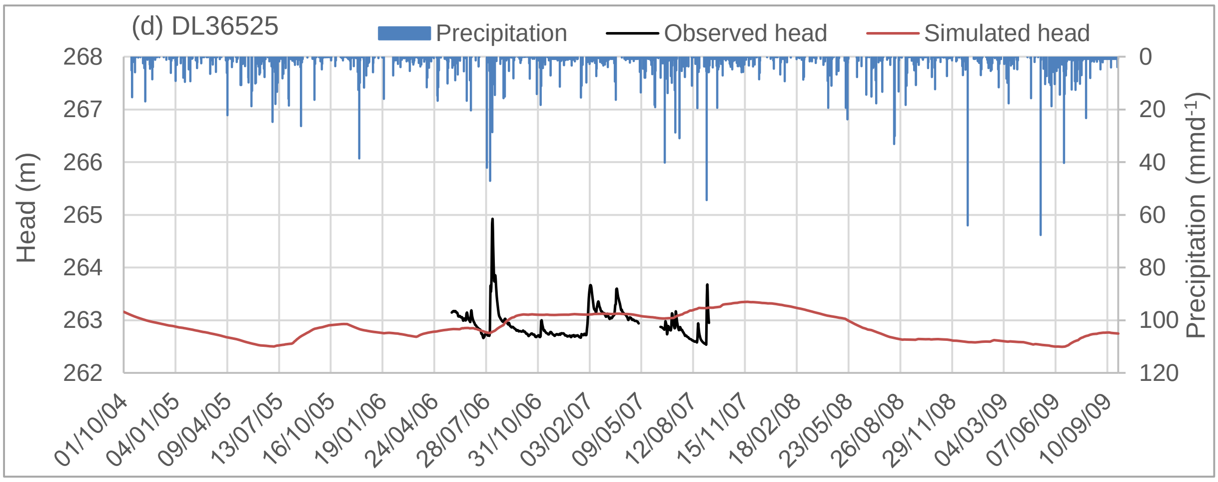
(d) DL36525
Precipitation
Observed head
Simulated head
Head (m)
Precipitation (mmd-1)
268
267
266
265
264
263
262
0
20
40
60
80
100
120
01/10/04
04/01/05
09/04/05
13/07/05
16/10/05
19/01/06
24/04/06
28/07/06
31/10/06
03/02/07
09/05/07
12/08/07
15/11/07
18/02/08
23/05/08
26/08/08
29/11/08
04/03/09
07/06/09
10/09/09

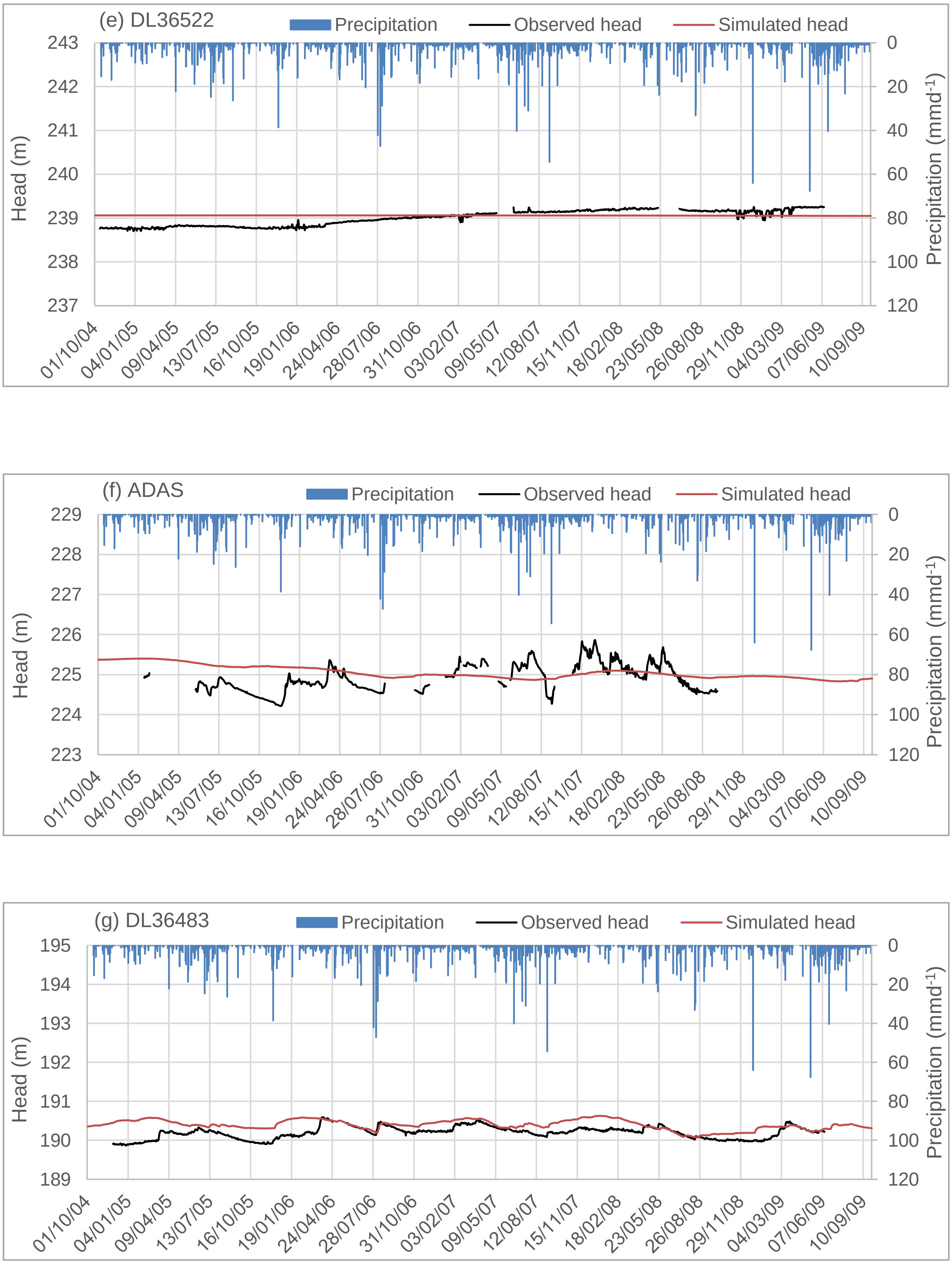

Figure 3-20: Observed and simulated heads after transient calibration

3.3.4. Error assessment and sensitivity analysis of the transient model results

3.3.4.1. Heads calibration

As in the case of steady-state calibration, the transient heads from the seven monitoring wells were used in model calibration (Figure 1-1 and Figure 2-2(a) through (g)). The calculated ME and MAE were, respectively, equal to -0.149 and 0.295 m and the comparison between the observed and simulated heads are shown in Figure 3-21. The RMSE, which estimates the errors in piezometric heads was 0.395 m. The ratio of RMSE to the total head loss was about 0.3%. The results were smaller when compared to the maximum acceptable error (10%) of 13.085 m and, thus, the calibration results were good and acceptable. The scatter plot (Figure 3-21) shows a good correlation between the observed and simulated heads with more or less good random distribution of points along the equal line.

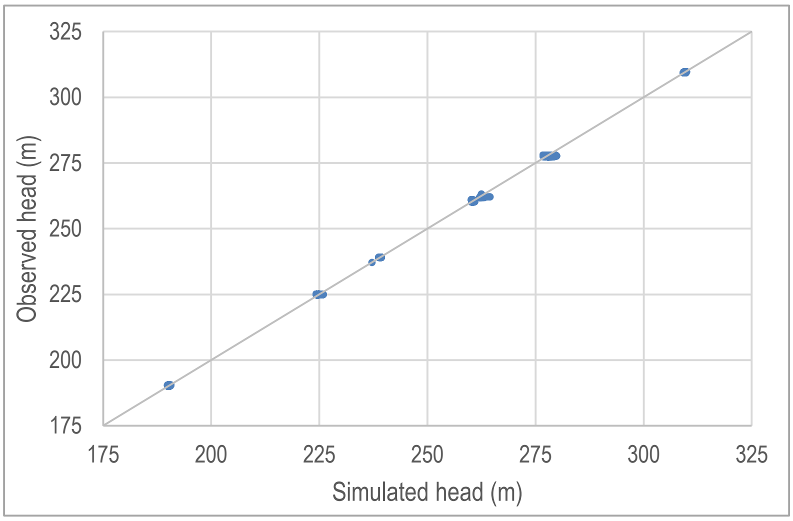

Figure 3-21: Scatter plot of observed and simulated heads after transient calibration

3.3.4.2. Sensitivity of model parameters

The response of the model hydraulic head was assessed by varying model parameters as shown in Figure 3-22. It was observed that the HK and VKCB parameters showed higher response to the model while the VK hardly showed any response. Moreover, the HK and VKCB showed a similar trend of model response to large and small values of the parameters, i.e. high response to decreasing and low response on increasing parameter values. However, when the two parameters were compared, the model response was higher to the variations in the HK parameters than the VKCB.

Considering the storage parameters, i.e. specific yield (Sy) and specific storage (Ss) parameters, the hydraulic heads hardly showed any response to the changes in Ss (Figure 3-23). The response of Sy parameter was increasing when decreasing values of the parameter and showed slight response when the parameter value was increased.

In general, the more sensitive parameters (HK, VKCB and Sy) may be considered of good quality and reliability and for the less sensitive parameters, its quality and reliability are objectionable. However, the very sensitive parameters may also be associated with high uncertainty. Therefore, more effort is needed to get quality and reliable information about the insensitive parameters and to reduce uncertainty of the sensitive parameters in order to improve calibration results and its prediction ability.

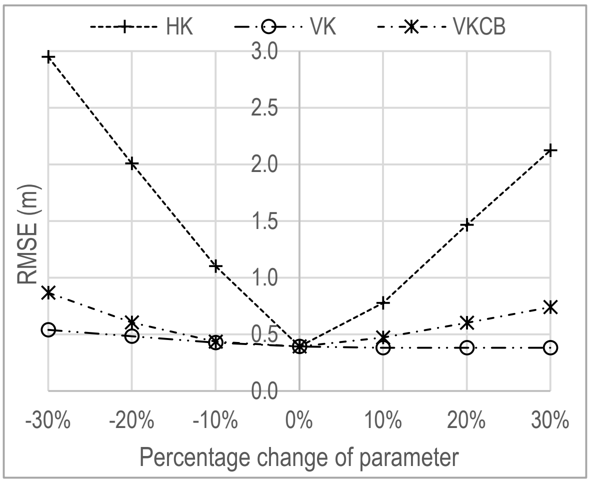

Figure 3-22: Sensitivity of model hydraulic conductivities under transient conditions

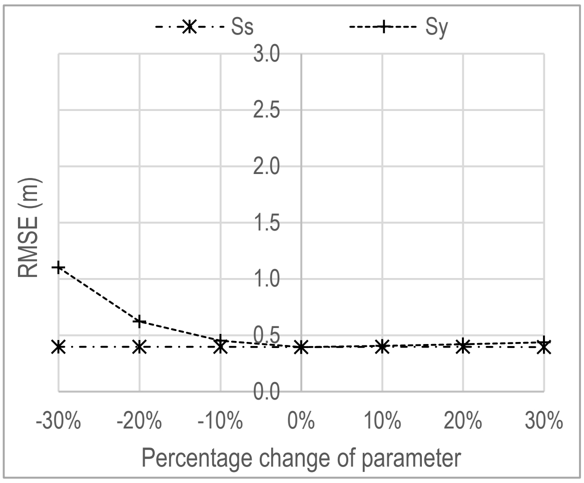

Figure 3-23: Sensitivity of specific yield and specific storage

3.3.4.3. Sensitivity of hydrologic stresses

Sensitivity of hydrologic stresses, i.e. infiltration, PET, streamflow and well abstraction was tested and the results are presented in Figure 3-24(a) and (b). It was observed that groundwater abstraction produced high response on groundwater heads on lower values and response diminishes with higher values (Figure 3-24(b)). The similar trend of response was also observed on streamflow. However, its response was smaller compared to the well abstraction. With regard to the PET and streamflow (Figure 3-24(a)), the model was highly sensitive to groundwater infiltration to both lower and higher values. The PET showed very small response on lower values and gradually decreased to higher values.

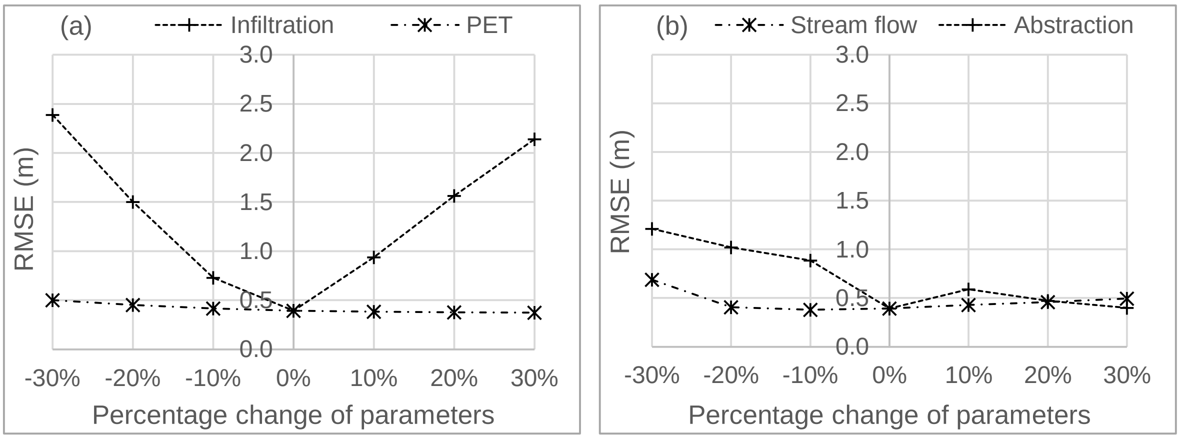

Figure 3-24: Sensitivity of hydrologic parameters

3.4. Water balance of the transient model

The compartmental water budget schema of the model is presented in Figure 3-26 and Figure 3-25 and the details of the budget components of the individual aquifers are summarised in Table 3-4 and Table 3-5, respectively. The budget refers to the average flow for the entire simulation period of the model (1st October 2004 to 30th September 2009). The inflow budget components of the Quaternary aquifer, as a percent of precipitation, are dominated by groundwater recharge which accounts for about 58%. The stream leakage into the aquifer accounts for about 18% and the inflow from the Tertiary to the Quaternary aquifer accounts for about 1%. The change of storage is about 3% of precipitation.

Table 3-4: Average water budget of the Quaternary and Tertiary aquifers after transient calibration for the period from 1st October 2004 to 30th September 2009

FLOW BUDGET COMPONENTS	QUATERNARY (m^3d^{-1})		TERTIARY (m^3d^{-1})	
	IN	OUT	IN	OUT
WELLS	0	2904	0	8225
DRAINS	0	6553		
STREAM LEAKAGE	73611	30669		
GW ET	0	114455		
UZF RECHARGE	232802	0		
SURFACE LEAKAGE	0	155160		
EXCHANGE BETWEEN AQUIFERS	2605	10511	10511	2605
STORAGE	68093	56805	384	65
Total	377112	377058	10895	10895
IN - OUT		54		0
Percent Discrepancy		0.00		0.00

The outflow budget is highly contributed by the surface leakage and the groundwater evapotranspiration from the Quaternary aquifer. The former accounts for about 35% while the latter accounts for 28%. The stream leakage out of the aquifer and the flow from the Quaternary to the Tertiary aquifer account for 8 and 3%, respectively. The groundwater abstraction and the lateral flow out of the drain boundary condition, respectively, account for about 1 and 2%. The inflow budget of the Tertiary aquifer is largely contributed by the flow from the Quaternary aquifer which accounts for about 3%. The outflow budget is dominated by groundwater abstraction accounting for about 2% while the flow into the Quaternary aquifer accounts about 1%. The change of storage was less than 1% of precipitation.

Table 3-5: Average water budget of the model composite after transient calibration for the period from 1st October 2004 to 30th September 2009

FLOW BUGET COMPONENTS	FLOW (m^3d^{-1})	
	IN	OUT
WELLS	0	11129
DRAINS	0	6553
STREAM LEAKAGE	73611	30669
GW ET	0	114455
UZF RECHARGE	232802	0
SURFACE LEAKAGE	0	155160
STORAGE	68476	56870
Total	374890	374837
IN - OUT		54
Percent Discrepancy		0.00

The flow budget of the model composite is summarised in Table 3-5. The groundwater recharge makes the largest contribution of about 58% of precipitation and stream leakage into the groundwater system accounts for about 20%. The outflow budget is comprised of many outflow budget components than the inflow budget. It is largely contributed by 39% of surface leakage and 28% of the groundwater evapotranspiration. The stream leakage out of the aquifer system contributes 8%. The least contribution to the outflow budget is 2% from each of the groundwater abstraction and lateral flow through the drain and the change of storage accounts for about 3%.

It can be concluded from the overall water budget that the groundwater system gained much water from the streams than what the streams received. Also, the inflow to the aquifer storage exceeds the outflow by about 17% which ensures sustainability of the groundwater system. From these observations, it is certainly that the groundwater system is dominantly influent and the streams are effluent.

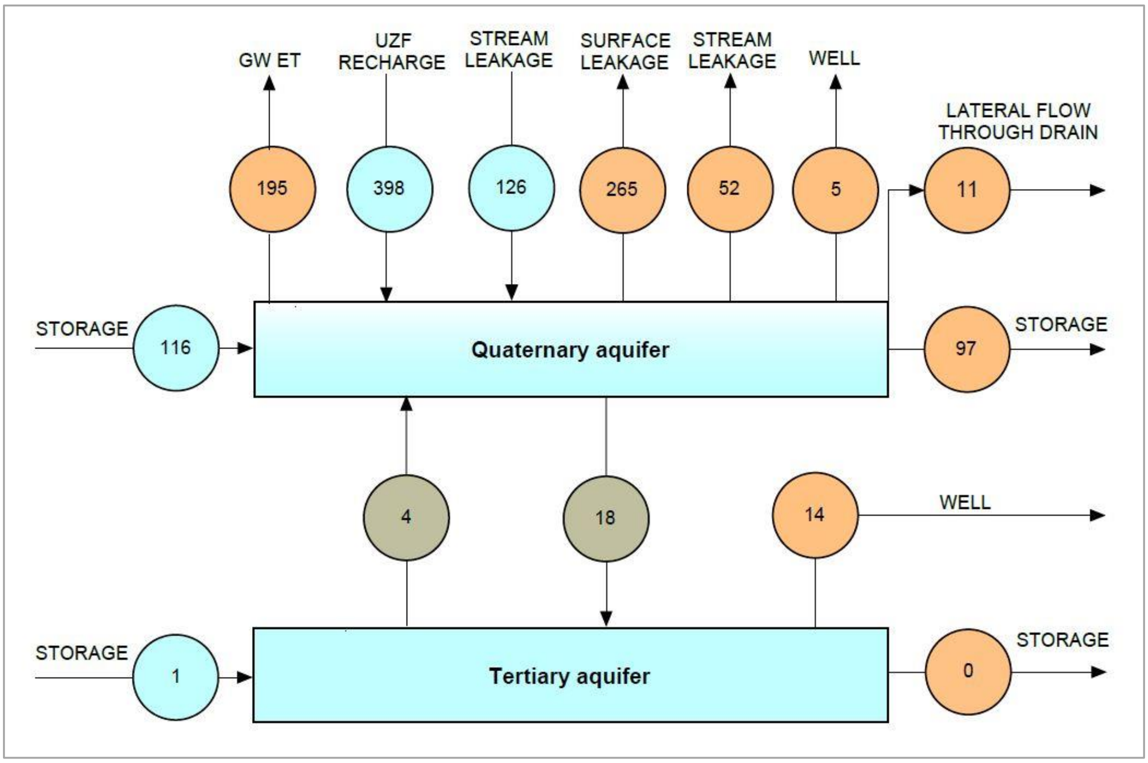

Figure 3-26: Average compartmental water budget of fluxes (mm.yr^{-1}) of the individual aquifers under transient conditions for the period from 1st October 2004 to 30th September 2009

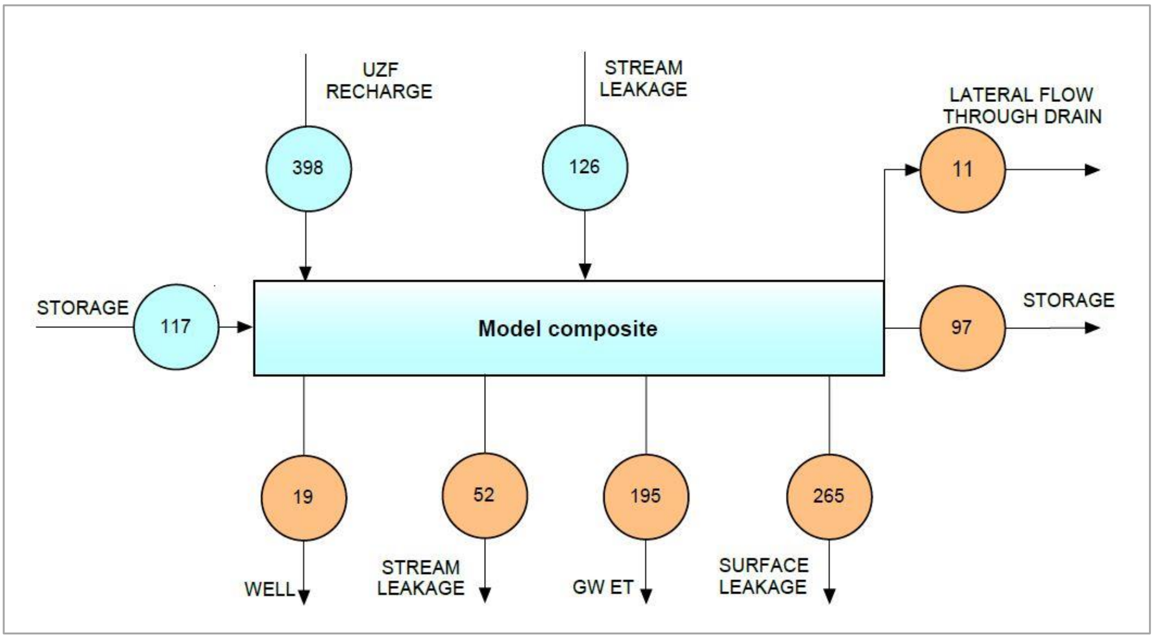

Figure 3-25: Average compartmental water budget of fluxes (mm.yr^{-1}) of the model composite under transient conditions for the period from 1st October 2004 to 30th September 2009

3.5. Comparison between the steady-state and transient model results

The calibration parameters of the steady-state model were further adjusted during the transient calibration to give the best match between the observed and simulated heads and stream discharges. The summary of the steady-state fluxes and the annual transient fluxes are presented in Table 3-6. The Table shows that the fluxes of the steady-state model do not differ significantly with the annual average fluxes of the transient model. For instance, the fluxes of the steady-state model varied between 0 and 967 mm.yr^{-1} while for the transient model varied between 11 and 1070 mm.yr^{-1}. In most cases, the steady-state fluxes were more or less closer to the maximum fluxes of the transient model results. This suggests that the solution of the calibrated steady-state model is very close to that of transient model and thus may be used to predict fluxes in Ziębice Basin.

3.6. Spatial and temporal variability of groundwater fluxes

3.6.1. Spatial variability of groundwater fluxes

Modflow-NWT under ModelMuse environment does not calculate fluxes, e.g. groundwater recharge (GW RECHARGE), groundwater evapotranspiration (GW ET), surface leakage and stream leakage, in the units of length per time (LT^{-1}), instead, it calculates flows in daily volumetric rates (L^{3}T^{-1}). Therefore, the calculated volumetric rates were converted into millimetres per year after performing some operations in the software based on the grid size. In order to facilitate the conversion, four new data sets were created, i.e. for GW RECHARGE, GW ET, surface leakage and stream leakage. The function *Grid or Mesh|BlockAreaTop*, which gives the cell area, was used. The data sets with calculated GW RECHARGE and GW ET values, surface leakage and stream leakage were then divided by the cell area to give the spatial distribution of fluxes in metres per day which was eventually converted into millimetres per year.

The spatial distribution of total GW RECHARGE, also called gross recharge, for the last model stress period (30th September 2009) is shown in Figure 3-27. It can be deduced from the Figure that the Basin has high spatial variability of GW RECHARGE fluxes. Also, the recharge covers almost the entire area of the Basin with the exception of few cells which might be due to high groundwater table and existence of deep streams. Moreover, the high spatial variability of recharge might be caused by different factors including, but not limited to, rainfall intensity and pattern, land cover type, depth to water table, vertical hydraulic conductivity and terrain slope. However, the effect of each parameter on recharge need special investigation. The major sources of recharge in the Basin are snow cover melting, which occurs in the summer period and precipitation which is maximum in July (Figure 1-2). In general, the gross recharge fluxes varied up to about 4 mmd^{-1}. In addition, the cells with gross recharge rate ranging between 0.4 and 1.8 mmd^{-1} appeared in large quantity in the model.

The spatial distribution of GW ET for the last model stress period (30th September 2009) is shown in Figure 3-28 and it varied up to about 1.98 mmd^{-1}. The GW ET seems to concentrate more on the central and western parts of the study area and dominantly along the main river stream. This might be due to shallow water table that interacts with the root depth and high soil moisture content around those areas. In the areas with no GW ET values, it implies that, both, the water table is far below the extinction depth (2 m) and the soil moisture is below the extinction water content(0.05 m^{3}m^{-3}). When these conditions prevail in the model, GW ET is not removed from the unsaturated zone (Niswonger et al., 2006).

The spatial distribution of stream leakage showed that the streams are influent in some segments and effluent in others (Figure 3-29). It can be observed from the figure that the number of influent reaches is much higher with fluxes up to about 16.9 mmd^{-1}. Moreover, the effluent reaches a very few with fluxes up to about 28 mmd^{-1}. Also, in some parts both types of interactions are observed within a segment. With regard to surface leakage fluxes (Figure 3-30), it has low spatial variability and occurs more at lower altitudes of the Basin and its values varied up to about 90.7 mmd^{-1}.

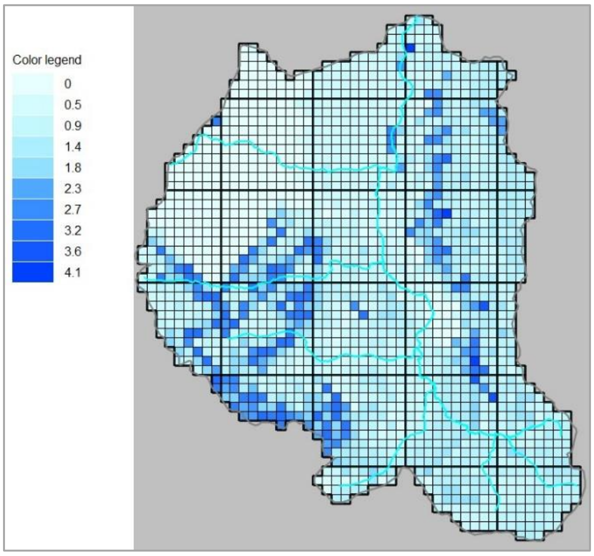

Figure 3-27: Total GW RECHARGE (mmd^{-1}) for 30th September 2009

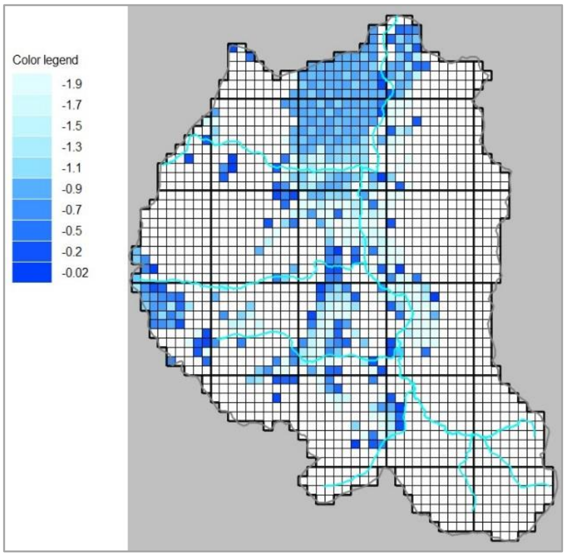

Figure 3-28: GW ET (mmd^{-1}) for 30th September 2009

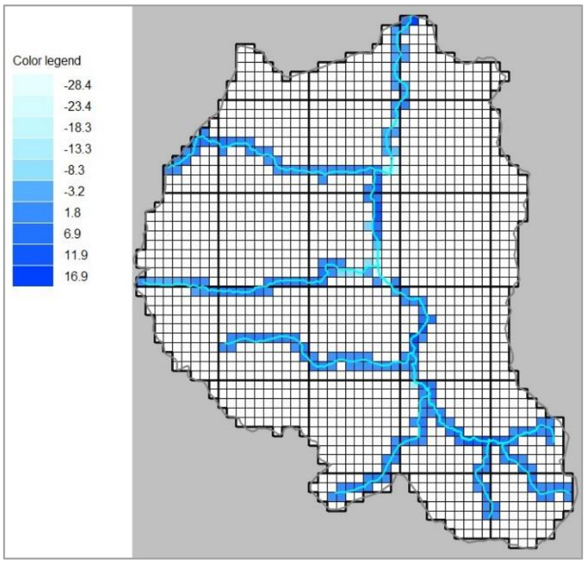

Figure 3-29: Stream leakage fluxes (mmd^{-1}) for 30th September 2009

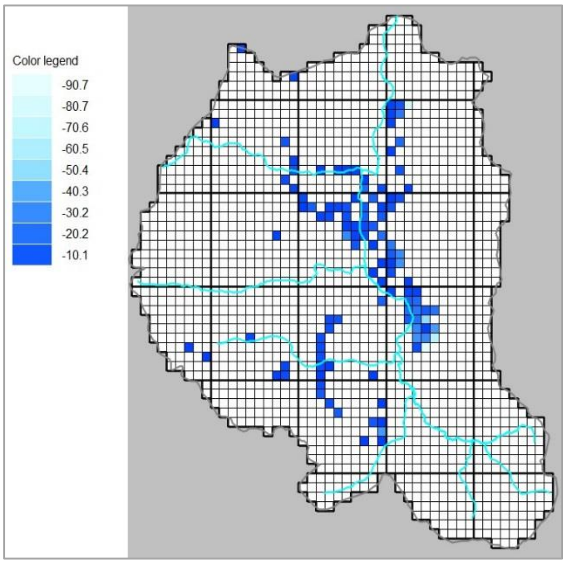

Figure 3-30: Surface leakage fluxes (mmd^{-1}) for 30th September 2009

3.6.2. Temporal variability of groundwater fluxes

In this study, the net recharge was estimated using Equation (2.18) and the results are presented in Figure 3-31 on daily basis, i.e. from 1st October 2004 to 30th September 2009, for better visualisation of trend and pattern of temporal variability of fluxes.

With regard to the gross recharge, the estimated maximum and minimum recharge fluxes were, respectively equal to 3.29 and 0.63 mmd^{-1} with an average of 1.04 mmd^{-1}. The gross recharge is highly responsive to precipitation and also depends on hydraulic conductivity and degree of saturation of the unsaturated zone. The GW ET had a maximum value of 1.07 mmd^{-1} and a minimum of 0.01 mmd^{-1} with an average of 0.45 mmd^{-1}. The effects of the GW ET is very noticeable on the estimated net recharge and showed a direct relationship. The surface leakage had a maximum value of 1.11 mmd^{-1} and a minimum of 0.53 mmd^{-1} with an average of 0.76 mmd^{-1}. It occurs when the groundwater head is above the ground surface. The net recharge, which is highly affected by GW ET (Figure 3-31), had a maximum value of about 3.3 mmd^{-1} and sometimes had negative values.

The annual temporal variability of fluxes of the transient model per hydrologic year is presented on an annual basis in Table 3-6. Considering the flux groups in the Table, i.e. surface, groundwater in, groundwater out and UZF fluxes, it can be deduced that the surface fluxes have high temporal variability compared to the rest of the mentioned flux groups. Their standard deviation is high ranging between 32 and 105 $mm.yr^{-1}$. For instance, within the surface fluxes group, precipitation has minimum and maximum fluxes of 565 and 809 $mm.yr^{-1}$, respectively with an average of 688 $mm.yr^{-1}$ and standard deviation of 105 $mm.yr^{-1}$. The high standard deviation of the fluxes implies a large difference from the mean which indicates high yearly flux variability. The UZF fluxes take the second position with the standard deviation varying between 13 and 70 $mm.yr^{-1}$. The fluxes into and from the groundwater system are moderate and the least with a standard deviation ranging between 0 and 32 $mm.yr^{-1}$. The fluxes due to well abstraction and lateral flow through the drain were always constant. In summary, the temporal variability of the surface and UZF fluxes is relatively high while the fluxes into and from the groundwater system are moderate.

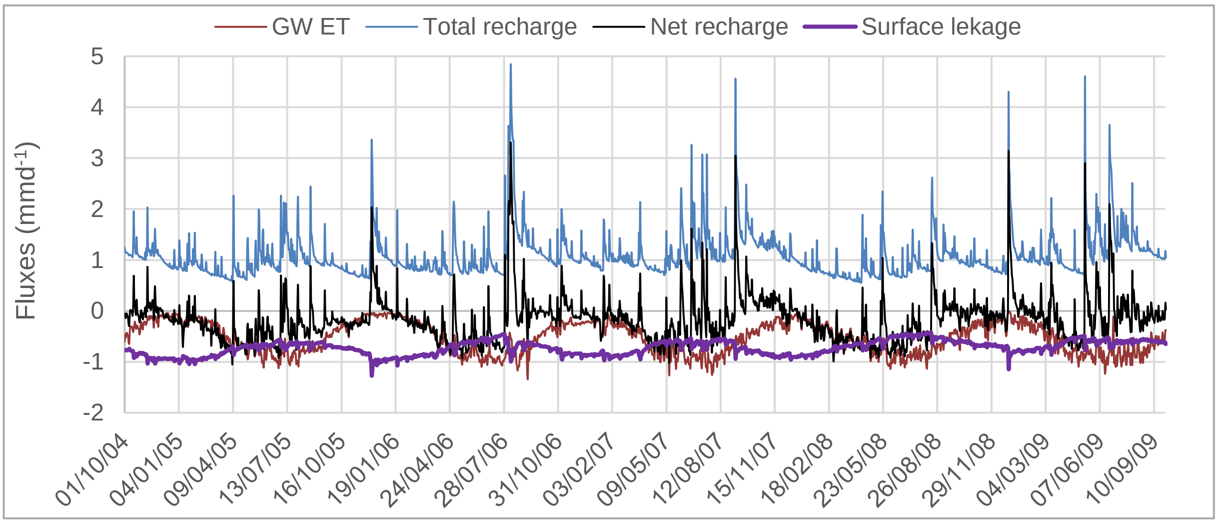

Figure 3-31: Daily variability of groundwater fluxes in Ziębice Basin from 1st October 2004 to 30th September 2009

3.6.3. Verification of water balance fluxes

Table 3-6 shows the annual variability of fluxes in the three compartments of the model, namely: surface, unsaturated zone and saturated zone. The fluxes in the Table must fulfil each of the Equations (2.10) for the whole model, Equation (2.13) for the surface and unsaturated zone and Equation (2.17) for the saturated zone. The closure error (percent discrepancy) of fluxes from each of the three equations must not exceed the allowable limit of ±1% as recommended by Anderson and Woessner (1992).

As an example, the fluxes for the hydrologic year October 2004 to September 2005 in Table 3-6 have been used to verify the calculated fluxes using Equations (2.10), (2.13) and (2.17) and the results are presented in Table 3-7. It can be seen from the Table that the fluxes fulfil the Equation (2.17) with a discrepancy of 0.2% which is inside the extremities of the closure error. However, the fluxes of Equations (2.10) and (2.13) closed the water balance with discrepancies of 2 and 20%, respectively which are beyond the allowable limits. The same trend of discrepancy was observed for the remaining years in all three Equations. It is most likely that the discrepancy was caused by flux tolerance error of 500 m^3d^{-1} set in the model.

Table 3-6: Annual temporal variability of surface and groundwater fluxes

HYDROLOGIC YEAR	FLUX PARAMETERS OF THE WATER BALANCE OF THE MODEL (mm.yr^{-1})																
	Precipitation (P)	PET	Interception (I)	Streamflow (Q_{out})	Infiltration	Stream Leakage (Q_{SLin})	Gross Recharge (R_g)	Stream leakage (Q_{SLout})	GW ET (ET_g)	Surface leakage (Slk_{gw})	Flow through Drain (Q_D)	Well Abstraction (Q_w)	Storage change (ΔS_a)	Net recharge (R_n)	Runoff (Ro)	Actual Infiltration (P_e)	Unsaturated zone ET (ET_{UZ})	UZF storage Change (ΔS_{UZ})
Steady-state	687	967	220	56	474	135	456	59	220	282	11	19	0	-46	377	459	122	0
2004/2005	610	852	189	55	420	134	369	56	183	288	11	19	-54	-102	322	407	75	-36
2005/2006	676	876	210	54	466	133	399	54	182	277	11	19	-12	-61	318	452	71	17
2006/2007	810	988	251	52	559	132	426	54	204	270	11	19	0	-48	327	541	101	41
2007/2008	563	1047	175	56	389	123	359	50	201	251	11	19	-49	-92	316	379	74	-43
2008/2009	780	1070	242	56	538	105	432	47	206	238	11	19	16	-12	296	521	95	14
Statistics																		
Minimum	565	853	175	52	390	105	360	47	182	238	11	19	-54	-102	296	379	72	-44
Average	688	966	213	55	474	126	397	52	195	265	11	19	-20	-63	316	460	83	-1
Maximum	809	1070	251	56	558	134	432	56	206	288	11	19	16	-12	327	542	100	42
Std. deviation	105	98	32	2	72	12	32	3	12	20	0	0	31	36	12	70	13	37

Table 3-7: Verification of the water balance equations for the hydrologic year 2004/2005

EQUATION	FLUX PARAMETERS OF THE WATER BALANCE EQUATIONS (mm.yr^{-1})														IN-OUT	PERCENT DESCREPANCY
	P	I	Q_{SLin}	R_g	Q_{SLout}	ET_g	Slk_{gw}	Q_D	Q_w	ΔS_g	Q_{out}	Ro	ET_{UZ}	ΔS_{UZ}		
2.10	610	-189				-183	-288	-11	-19	-(-54)	-55		-75	-(-36)	-120	20.0
2.13	610	-189		-369			288					-322	-75	-(-36)	-21	-2.0
2.17			134	369	-56	-183	-288	-11	-19	-(-54)					-1	0.2

3.7. Surface-groundwater interactions in the natural state

The spatial distribution of simulated groundwater heads of the calibrated model under natural conditions, i.e. no groundwater abstraction, is shown in Figure 3-32 and Figure 3-33 for the Quaternary and Tertiary aquifers for 30th September 2009. In Figure 3-32, the groundwater heads in the Quaternary aquifer depict that the flow converges towards the north with the general flow direction from the south to the north of the Basin. Moreover, the flow contribution is higher from the southern and the western sides of the Basin when compared to the eastern side. In the Tertiary aquifer, the groundwater flow from all directions of the Basin converge to the northern central part (Figure 3-33).

Figure 3-34 shows the behaviour of the streams in natural conditions. It can be seen from the Figure that, both, influent and effluent conditions take place in the streams. However, when the two conditions are compared, the spatial coverage of the influent stream segments and reaches dominate the effluent ones. The stream leakage fluxes into the aquifer varied up to about 17 mmd^{-1} for influent and up to about 30 mmd^{-1} for effluent conditions.

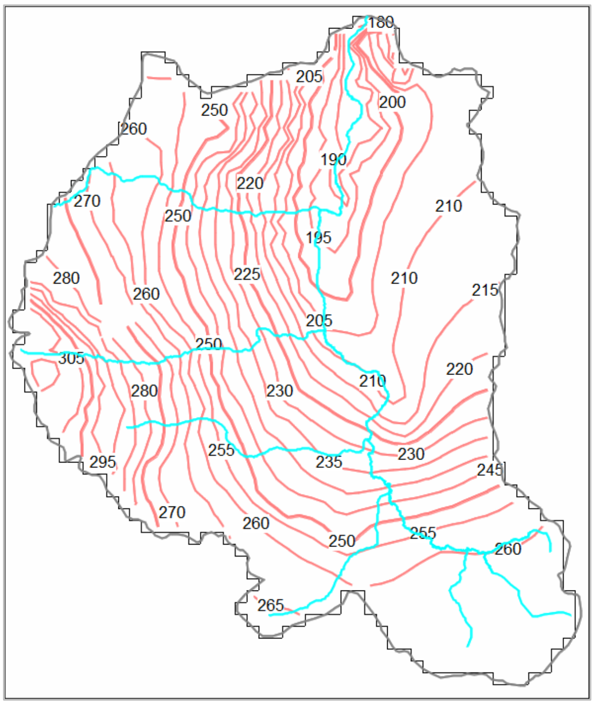

Figure 3-32: Groundwater heads (m-asl) in the Quaternary aquifer under the natural conditions for 30th September 2009

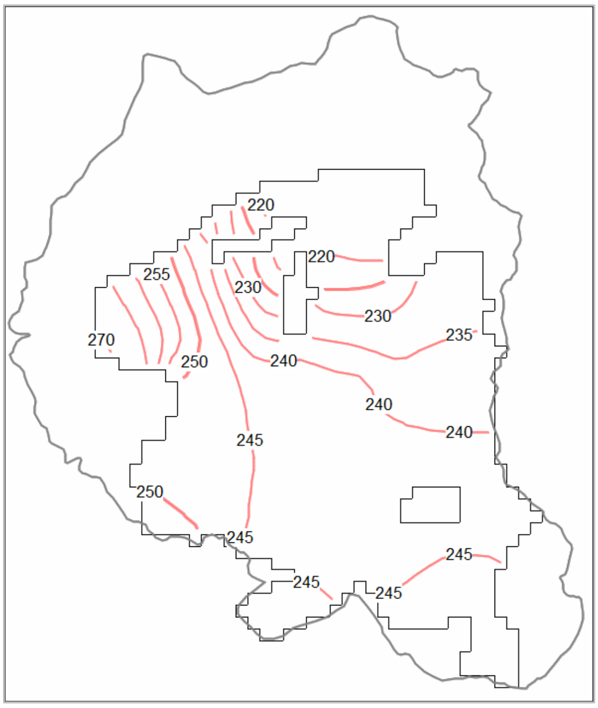

Figure 3-33: Groundwater heads (m-asl) in the Tertiary aquifer under the natural conditions for 30th September 2009

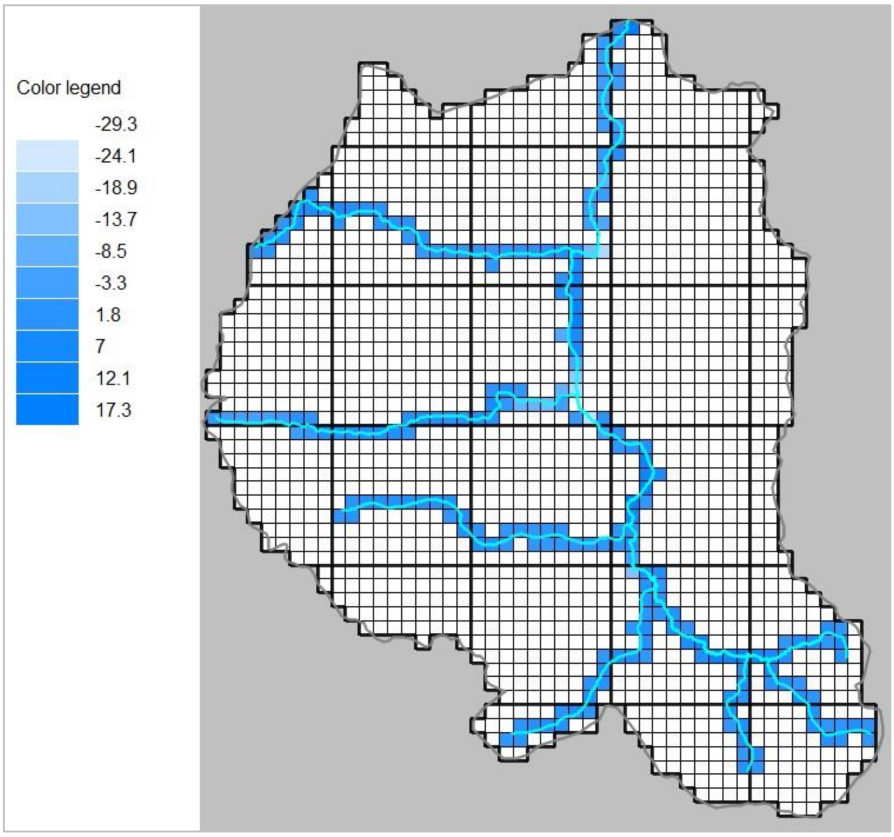

Figure 3-34: Stream leakage (mmd^{-1}) under natural conditions for 30th September 2009

3.8. Surface-groundwater interactions under groundwater abstraction

The groundwater model was calibrated with all ten abstraction wells being operational. In the Quaternary aquifer (Figure 3-35), one well at Henrykow wellfield was abstracting 336 m^{3}d^{-1} and the two wells at Starczowek wellfield were abstracting a total of 2376 m^{3}d^{-1}. Moreover, in the Tertiary aquifer, a total of 1008 and 7408.9 m^{3}d^{-1} were, respectively abstracted from the two wells at Henrykow and the five wells at Nieszkow wellfields (Figure 3-36).

The spatial distribution of the calibrated heads of the model under groundwater abstraction is shown in Figure 3-35 and Figure 3-36 by contour lines for 30th September 2009. Generally, there was no considerable changes of groundwater heads in the Quaternary aquifer. For instance, a closer look to Starczowek wellfield shows that the 260 m contour line moved closer to the wellfield (Figure 3-35). It is obvious that the heads lowering is due to groundwater abstraction conducted at the wellfield. However, the groundwater heads and its pattern at the downstream of the Basin remains similar to that of the natural state (Figure 3-32). In the Tertiary aquifer, the groundwater heads were generally lowered in the whole aquifer system by about 5 m which is observed by the shift of all contour lines when the Figure 3-33 and Figure 3-36 are compared. However, the flow pattern did not change. The lowering of groundwater heads might be a result of groundwater abstraction at Nieszkow wellfield. Also, there was almost small difference between stream leakage fluxes under the natural and groundwater induced conditions (Figure 3-34 and Figure 3-29). For instance, the flux to the Quaternary aquifer in the natural and groundwater induced conditions was almost similar (about 17 mmd^{-1}). In addition, the leakage fluxes into the streams from the aquifer system under natural condition was lower by 1 mmd^{-1} compared to the fluxes under groundwater abstraction.

It can be seen from the water budget of the model composite (Table 3-5) that the streams supplied 20% of its fluxes into the aquifer system and the aquifer supplied about 8% into the streams. The discharged amount of the fluxes into the aquifer system is most likely not only a natural phenomenon (Figure 3-32 and Figure 3-33) but also is induced by groundwater abstraction. Moreover, about 62% of inflow to the model is from groundwater recharge which ensures sustainable flow of about 18% into the storage of the aquifer system.

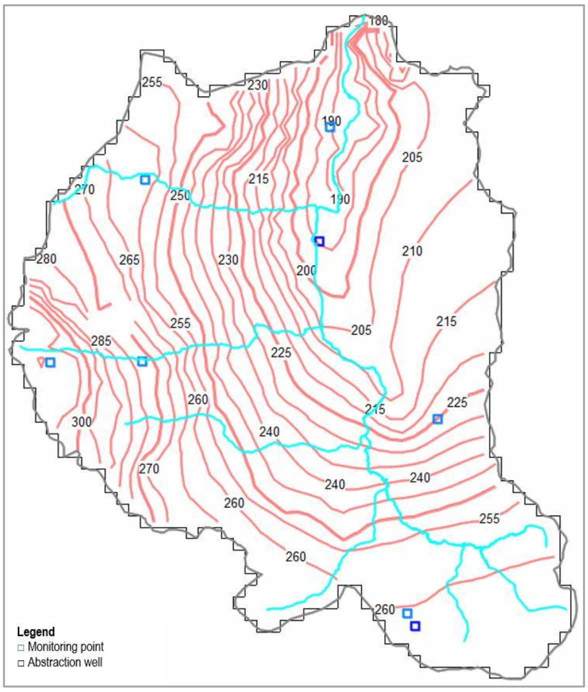

Figure 3-35: Heads (m-asl) in the Quaternary aquifer under groundwater abstraction for 30th September 2009; Location map Figure 1-1

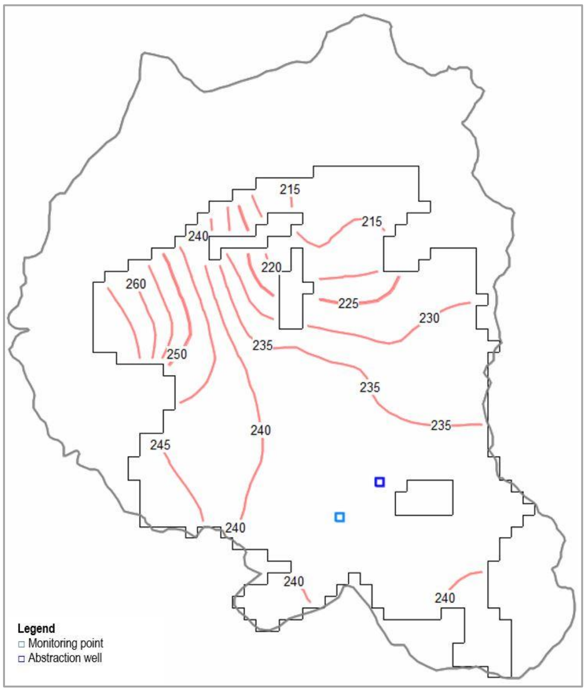

Figure 3-36: Heads (m-asl) in the Tertiary aquifer under groundwater abstraction for 30th September 2009; Location map Figure 1-1

3.9. Comparison with other studies

It has been mentioned earlier that there are different studies conducted in Ziębice Basin between 1990 and 2010. The documents are in Polish and some with a very shallow English abstract that could not give meaningful use for comparison. For comparison purposes, the document of Lubczynski (1991) and the most recent document, with a comprehensive English abstract, of Gurwin (2010) were selected.

The conductivity values did not differ very much with those of Koziol (2006) which varied between 16 to 88 md^{-1} and of (Shah, 1995) which varied between 0.5 to 7 md^{-1} and 100 md^{-1} in some areas of the Basin. The obtained calibrated values did not show much difference with those determined by Koziol (2006). For instance, at the Nieszkow wellfield (southern area) the determined hydraulic conductivities ranged between 10 and 25 md^{-1}. The high difference in hydraulic conductivity in some areas might be due to the fact that its determination concentrated only on a small area of the Basin which could not reflect complex heterogeneity of the aquifer system. For the case at Henrykow wellfield (northern part), the hydraulic conductivity was about 2 md^{-1} which was more or less closer to the value used in the calibration.

The model of Lubczynski (1991) showed more or less similar spatial distribution and the amount of heads (Figure 1-8(a) and (b)) when compared to this study in Figure 3-35 and Figure 3-36. However, the amount of heads in Gurwin (2010) model was relatively smaller despite the similar spatial distribution within the model. The possible reason for this difference might be due to the use of no-flow boundary in the model of the present study which was not the case in the study of Gurwin (2010).

The estimated values of ETo conformed with those determined by Gurwin (2010) at which the minimum and maximum values were, respectively equal to 0.1 and 7.0 mmd^{-1} with an average of 2.37 mmd^{-1}. However, the ETo estimates of Gurwin (2010) were only for the hydrologic year (224/2005) while for this study, the estimates were for a longer period of five hydrologic years (2004/2009). It is also worth to mention that, in some cases, the obtained recharge rates did not differ appreciably to those determined by Gurwin (2010). For instance, the recharge rates at Ziębice (central part) ranged between 3 to 6 mmd^{-1} and in Starczowek (southern part) 2 to 3.5 mmd^{-1}.

4. CONCLUSION AND RECOMMENDATIONS

4.1. Conclusion

The objective of this research was to assess the surface-groundwater interaction in Ziębice Basin. The interactions were modelled for a period of five hydrologic years from 1st October 2004 to 30th September 2009. The integrated hydrologic model (MODFLOW-NWT) was the main tool used for modelling the surface-groundwater interaction in Quasi-3D. The groundwater model was created and calibrated by the trial-and-error method in steady-state and transient conditions.

Calibration of the model was done with groundwater abstraction to determine the best parametric distribution that could optimally fulfil the model calibration. The calibration process in the steady-state model produced sufficient heads calibration results with ME and MAE of -0.341 and 0.697 m, respectively and RMSE of 0.829 m. The steady-state heads solution of the calibrated model was used as the initial hydraulic heads for transient calibration. The transient calibration produced the ME of -0.149 m and MAE of 0.295 m and RMSE of 0.395 m. Moreover, streamflow was simultaneously calibrated with groundwater heads and the volumetric efficiency associated with the flow calibration was about 0.9.

Sensitivity of the model was assessed basing on the calibration parameters and the hydrologic stresses. In the first case, both, steady-state and transient calibrations, the model showed high sensitivity to HK and VKCB parameters and low sensitivity to VK parameter. Similarly, the specific yield showed high sensitivity while specific storage was insensitive. In the second case, i.e. hydrologic stress, the model showed high response to groundwater infiltration and response to neither increase nor decrease of PET and streamflow.

The water budget of the model was assessed on the basis of the annual average flows for the entire period of the model simulation under transient conditions with groundwater abstraction. It was dominated by groundwater recharge which accounted for about 58% of precipitation. The stream leakage into the aquifer system accounted for about 20% of precipitation. The flow out of the aquifer was dominated by the surface leakage and groundwater evapotranspiration which accounted for 39 and 28%, respectively while the stream leakage out of the aquifer accounted for about 8% of precipitation. The lateral flow through the drain and groundwater abstraction were equal to 2% each. The change of storage accounted for about 3% of precipitation. The water budget revealed that the streams of shallow Quaternary aquifer were mostly influent. The streams supplied 20% of its flow into the groundwater system and the groundwater released only 8% of its flow into the streams.

The spatial and temporal variability of the fluxes on a daily basis of the entire simulation period showed that recharge varied between 0.63 and 3.29 mmd^{-1}. It showed moderate response to precipitation. The surface leakage, which occurs when the groundwater head is above the soil surface varied between 0.53 and 1.11 mmd^{-1}. The evapotranspiration was ranging between 0.01 and 1.07 mmd^{-1}. The net recharge had a maximum value of 1.98 mmd^{-1} and sometimes it was below zero. The negative net recharge indicates advantage of in-situ groundwater discharge (ETg + Slkgw) over gross recharge. Moreover, the temporal variability of the surface and UZF fluxes were relatively high while the fluxes into and from the groundwater were moderate. The annual variability of the fluxes in the steady-state model did not differ substantially from the average fluxes of the transient model simulation. The highest variability was observed within surface fluxes with the standard deviation ranging between 32 and 105 $mm.yr^{-1}$. The standard deviation of the UZF fluxes varied between 13 and 70 $mm.yr^{-1}$ and that of groundwater fluxes varied between 0 and 32 $mm.yr^{-1}$. The fluxes of the steady-state model did not substantially differ with the maximum fluxes of the transient model simulation. The annual maximum fluxes of the transient model varied between 11 and 1070 $mm.yr^{-1}$ with a standard deviation varying between 0 and 105 $mmyr^{-1}$.

The surface-groundwater interaction under natural state of the Basin was simulated by removing all groundwater abstraction wells from the model. The spatial distribution of heads in the model showed that, under natural state, the streams were in, both conditions, influent and effluent and groundwater flowed towards the north from all other remaining directions. However, the influent state dominated the effluent one. With regard to surface-groundwater interaction under groundwater abstraction, the groundwater heads declined to about 5 m in the Tertiary aquifer and in the Quaternary aquifer the decline was noticeable around Starczowek wellfield. The decline of heads was induced by groundwater abstraction taking place at Starczowek and Nieszkow wellfields. However, the groundwater flow direction and the pattern of groundwater heads were unchanged. It was further observed that the streams were influent in some reaches of segments and effluent in others and sometimes both influent and effluent cases were found in the same stream segment.

Comparison of the fluxes results between the steady-state and transient model showed that the fluxes of the steady-state model were above the annual average values of the fluxes of the transient model and closer to the maximum. On that basis, the transient model may also be used to predict fluxes in Ziębice Basin.

Finally, the integrated hydrologic model is a useful and effective tool for water resources management especially when the surface and groundwater systems are highly interconnected. It gives good results that may lead to proper planning and management of water resources.

4.2. Recommendations

The groundwater monitoring points are scarce in the study area. Thus, densification of monitoring points, especially along the main stream and on the eastern side of the study area, needs special attention in order to have an even distribution of monitoring points in the Basin. Moreover, densification of groundwater monitoring points may lead to improvement of model grid resolution and improve prediction capacity of the model.

Since it was revealed that the effects of groundwater abstraction started to emerge in the neighbourhood of Starczowek wellfield, it is a good idea to conduct localised study in the neighbourhood of the wellfield to ascertain the actual effects of groundwater abstraction. Moreover, installation of groundwater monitoring points in this wellfield is important to improve data quality for further groundwater assessment in the wellfield.

In the Basin, there was only one stream gaging station located at the downstream end of the main stream at Kazanow. It is better for the authority responsible for water resources management to install more streamflow-gaging stations in the tributaries in order to understand the exact flow contribution of each stream to the total streamflow. This will help to minimise biases and uncertainties of streamflow estimates in model calibration and improve calibration results.

The available land use map did not show enough information on the types of vegetation cover found in different places of the study area. As a result, the estimated canopy interception might have strongly affected the estimates of infiltration rates which is a very important parameter for recharge estimation. It is suggested to implement a classification of land covers to enable accurate estimates of canopy interception.

LIST OF REFERENCES

Allen, R.G., Pereira, L.S., Raes, D., Smith, M., 1998. Crop evapotranspiration - Guidelines for computing crop water requirements - FAO Irrigation and drainage paper 56 [WWW Document]. URL http://www.fao.org/docrep/x0490e/x0490e06.htm#TopOfPage (accessed 10.15.14).

Anderson, M.P., Woessner, W.W., 1992. Applied groundwater modeling: Simulation of flow and advective transport. Academic Press Inc.

Bear, J., Cheng, A.H.-D., 2010. Modeling Groundwater Flow and Contaminant Transport. Springer Netherlands, Dordrecht. doi:10.1007/978-1-4020-6682-5

Burba, G., 2010. Evapotranspiration [WWW Document]. URL http://www.eoearth.org/view/article/152693/ (accessed 12.27.14).

Ely, D.M., Kahle, S.C., 2012. Simulation of groundwater and surface-water resources and evaluation of water-management alternatives for the Chamokane Creek basin, Stevens County, Washington.

Fleming, M., Asce, M., Neary, V., 2004. Continuous Hydrologic Modeling Study with the Hydrologic Modeling System. J. Hydrol. Eng. 175–183.

Furman, A., 2008. Modeling Coupled Surface–Subsurface Flow Processes: A Review. Vadose Zo. J. 7, 741. doi:10.2136/vzj2007.0065

Guay, C., Nastev, M., Paniconi, C., Sulis, M., 2013. Comparison of two modeling approaches for groundwater-surface water interactions. Hydrol. Process. 27, 2258–2270. doi:10.1002/hyp.9323

Gupta, S.K., 2010. Modern Hydrology and Sustainable Water Development. Wiley, Hoboken.

Gurwin, J., 2010. Renewal Assessment of Water-bearing Structures within the Fore-Sudetic Block: Integration of Monitoring nad GIS/RS Data with Numerical Flow Models.

Gurwin, J., Lubczynski, M., 2004. Modeling of complex multi-aquifer systems for groundwater resources evaluation - Swidnica study case (Poland). Hydrogeol. J. 13, 627–639. doi:10.1007/s10040-004-0382-9

Hassan, S.M.T., Lubczynski, M.W., Niswonger, R.G., Su, Z., 2014. Surface–groundwater interactions in hard rocks in Sardon Catchment of western Spain: An integrated modeling approach. J. Hydrol. 517, 390–410. doi:10.1016/j.jhydrol.2014.05.026

Koziol, A., 2006. Pracaujec wod podziemnych kenozoicznych poziomow wodonosnych niecki Ziebice. Wroclaw University Faculty of Natural Sciences Institute of Geological Sciences, Wroclaw.

Krause, S., Bronstert, A., Zehe, E., 2007. Groundwater–surface water interactions in a North German lowland floodplain – Implications for the river discharge dynamics and riparian water balance. J. Hydrol. 347, 404–417. doi:10.1016/j.jhydrol.2007.09.028

Leuning, R., Condon, A., Dunin, F., 1994. Rainfall interception and evaporation from soil below a wheat canopy. Agric. For. … 67, 221–238.

Lubczynski, M., 1991. Flow Model of Ziebice Basin. PhD Thesis University of Wroclaw.

McCallum, A.M., Andersen, M.S., Giambastiani, B.M.S., Kelly, B.F.J., Ian Acworth, R., 2013. River-aquifer interactions in a semi-arid environment stressed by groundwater abstraction. Hydrol. Process. 27, 1072–1085. doi:10.1002/hyp.9229

Niswonger, R.G., Prudic, D.E., Regan, R.S., 2006. Documentation of the Unsaturated-Zone Flow (UZF1) Package for Modeling Unsaturated Flow Between the Land Surface and the Water Table with MODFLOW-2005: U.S. Geological Survey Techniques and Methods 6-A19 62 p.

Nossent, J., Bauwens, W., Pereira, F., Verwaest, T., Mostaert, F., Government, F., Engineering, H., Brussel, U., 2014. Are the driving forces of hydrological models really driving the model output ?

Palma, C.H., Bentley, L.R., 2007. A regional-scale groundwater flow model for the Leon-Chinandega aquifer, Nicaragua. Hydrogeol. J. 15, 1457–1472. doi:10.1007/s10040-007-0197-6

Pawalec, R., 2006. Analiza odplywu podziemnego w niecce Ziebice. Wroclaw University Faculty of Natural Sciences Institute of Geological Sciences, Wroclaw.

Prudic, D.E., Konikow, L.F., Banta, E.R., 2004. A New Streamflow-Routing (SFR1) Package to Simulate Stream-Aquifer Interaction with MODFLOW-2000.

Shah, F.M., 1995. Groundwater resources evaluation and GIS study as preprocessing for 3-D groundwater flow modelling of Olawa River basin. Twente.

Sophocleous, M., 2002. Interactions between groundwater and surface water: the state of the science. Hydrogeol. J. 10, 52–67. doi:10.1007/s10040-001-0170-8

Wang, D., Wang, G., Anagnostou, E.N., 2007. Evaluation of canopy interception schemes in land surface models. J. Hydrol. 347, 308–318. doi:10.1016/j.jhydrol.2007.09.041

Wang, F., Jiao, J., 2005. Preliminary numerical study on groundwater system at the Hong Kong International Airport. Environ. Hydraul. Sustain. Water Manag. 2047–2052.

Wu, J., Zeng, X., 2013. Review of the uncertainty analysis of groundwater numerical simulation. Chinese Sci. Bull. 58, 3044–3052. doi:10.1007/s11434-013-5950-8

APPENDICES

APPENDIX 1: CALCULATION PROCEDURE OF FAO PENMAN-MONTEITH METHOD

The general equation of the FAO Penman-Monteith Method is shown in equation (2.1).

$$ETo = \frac{0.408\Delta(R_n - G) + \gamma \frac{900}{T_{mean}+273} u_2(e_s - e_a)}{\Delta + \gamma(1 + 0.34u_2)} \tag{2.1}$$

where:

ETo is the reference evapotranspiration (mmday^{-1}), Δ is the slope of the saturation vapour pressure curve (kPa°C^{-1}), R_n is the net radiation at the crop surface (MJm^{-2}day^{-1}), G is the soil heat flux density (MJm^{-2}day^{-1}), γ is the psychrometric constant (kPa°C^{-1}), T_{mean} is the mean daily air temperature at a height of 2m (°C), u_2 is the wind speed at a height of 2m (ms^{-1}), e_s is the mean saturation vapour pressure (kPa), and e_a is the actual vapour pressure (kPa).

The slope of the saturation vapour pressure curve (Δ) at T_{mean} is calculated in equation (2.2).

$$\Delta = \frac{4098\left(0.6108 \exp\left(\frac{17.27 T_{mean}}{T_{mean}+273.3}\right)\right)}{(T_{mean}+237.3)^2} \tag{2.2}$$

The T_{mean} is calculated as an average of the daily maximum and minimum temperature (°C) in equation (2.3).

$$T_{mean} = \frac{(T_{max} + T_{\min})}{2} \tag{2.3}$$

The net radiation (R_n) at the reference crop surface is calculated from equation (2.4).

$$R_n = R_{ns} - R_{nl} \tag{2.4}$$

where:

R_{ns} and R_{nl} are the net incoming shortwave and net outgoing long-wave radiations all in MJm^{-2}day^{-1} as shown in equations (2.5) and (2.6), respectively.

$$R_{ns} = (1 - \alpha)R_s \tag{2.5}$$

where:

α is the albedo of the grass reference crop equal to 0.23 and Rs is the global solar exposure (MJm^{-2}day^{-1}).

$$R_{nl} = \sigma(0.34 - 0.139\sqrt{e}_a)(1.35\frac{R_s}{R_{so}} - 0.35)(\frac{T_{max,K}^4 + T_{min,K}^4}{2}) \tag{2.6}$$

where:

σ is the Stefan-Boltzmann constant = 4.903x10^{-9} (MJK^{-4}m^{-2}day^{-1}), $T_{max,K}$ is the maximum absolute temperature in the 24-hour period (K = °C + 273.16), $T_{min,K}$ is the minimum absolute temperature in the 24-hour period (K = °C + 273.16), e_a is the actual vapour pressure (kPa), R_s/R_{so} is the relative shortwave radiation (limited to $\leq$ 1.0), R_s is the global solar exposure (MJm^{-2}day^{-1}) and R_{so} is the clear-sky solar radiation (MJm^{-2}day^{-1}).

The clear-sky solar radiation (R_{so}) is computed using equation (2.7).

$$R_{so} = (0.75 + 2 \times 10^{-5} z_e)R_a \tag{2.7}$$

where:

z_e is the station elevation above mean sea level (m) and R_a is the extra-terrestrial radiation ($MJm^{-2}day^{-1}$).

Estimation of the extra-terrestrial radiation is made using the solar constant, the solar declination and the time of the year as shown in equation (2.8).

$$R_{so} = \frac{24\times60}{\pi} G_{sc} d_r [\omega_s \sin(\varphi)\sin(\delta) + \cos(\varphi)\cos(\delta)\sin(\omega_s)] \tag{2.8}$$

where:

G_{sc} is the solar constant = 0.0820 $MJm^{-2}min^{-1}$, d_r is the inverse relative distance Earth-Sun, ω_s is the sunset hour angle, φ is the latitude in radians, and δ is the solar declination, which is the latitude at which the Sun is directly overhead (Ladson, 2008).

The inverse relative distance Earth-Sun is calculated using equation (2.9).

$$d_r = 1 + 0.033\cos\left(\frac{2\pi}{365}J\right) \tag{2.9}$$

where:

J is the Julian day, which is the number of the day in the year between 1 (January 1st) and 365 or 366 (December 31st).

The sun-set hour angle is calculated using equation (2.10).

$$\omega_s = \arccos[-\tan(\varphi)\tan(\delta)] \tag{2.10}$$

where:

φ is the latitude in radians (which must be negative for the southern hemisphere) = π/180 (latitude in decimal degrees) and δ is the solar declination.

Computation of solar declination is done using equation (2.11).

$$d_r = 0.409\sin\left(\frac{2\pi}{365}J - 1.39\right) \tag{2.11}$$

where:

J is the Julian day explained under equation (2.9).

The relative humidity data are used to calculate actual vapour pressure (ea) as shown in equation (2.12).

$$e_a = \frac{e_o(T_{min})\frac{RH_{max}}{100} - e_o(T_{max})\frac{RH_{min}}{100}}{2} \tag{2.12}$$

where:

e_a is the actual vapour pressure (kPa), RH_{max} and RH_{min} are the daily maximum and minimum relative humidities (%) and e_o is the saturation vapour pressure (kPa).

The e_o is calculated using equation (2.12).

$$e_o(T) = 0.6108\exp\left[\frac{17.27T}{T+237.3}\right] \tag{2.13}$$

The calculation of the mean daily saturation vapour pressure (e_s) is done using equation (2.14).

$$e_a = \frac{e_o(T_{min}) - e_o(T_{max})}{2} \tag{2.14}$$

where:

e_o is calculated using equation (2.13) mentioned earlier.

The calculation of the soil heat flux (G) is ignored for time periods between one and ten days. This is due to the fact that the energy stored in the soil will be about the same at the start and the end of the period and the net energy flux is close to zero (Allen et al., 1998).

The psychrometric constant defined in equation (2.1) is calculated using equation (2.15).

$$\gamma = 0.665 \times 10^{-3} P \tag{2.15}$$

where P is in kPa and is calculated using equation (2.16) and z_e is explained in equation (2.7).

$$P = 101.3 \left(\frac{293 - 0.0065 z_e}{293}\right)^{5.26} \tag{2.16}$$

The calculation of the average daily wind speed (u_2) for 24-hour period beginning at midnight at a height of 2 m (ms^{-1}) is done using equation (2.17)

$$u_2 = u_z \frac{4.87}{\ln(67.8 \times z - 5.42)} \tag{2.17}$$

where

u_z is the average daily wind speed (ms^{-1}) at a height z where z is the height of original wind measurement (m).

APPENDIX 2: WELLFIELD DATA

Well name	Wellfield	Aquifer	Well depth (m)	Discharge (m^3h^{-1})	Drawdown (m)	Hydraulic conductivity (md^{-1})
st. 1	Henrykow	Tr	46	14	12.8	2.2
st. 2		Tr	45	20	13	2.2
st. r-1		Q	16.5	22	5.8	16
st. II	Nieszkowie	Tr	52	90	12	11.7
st. III		Tr	57/44	18.5	16.4	11.8
st, IIIz		Tr	50	87	19.3	10.8
st. IV		Tr	62.2	68.2	15	24.7
st. V		Tr	59	45	11	14.9
st. 1	Starczowku	Q	47	48	2.8	85.7
st. 2		Q	52	51	2.1	88.1